

DISSIPATION AND
AMPLIFICATION IN
QUANTUM OPTICS.

by

Sam Tarzi

A thesis presented for the degree of Doctor of
Philosophy of the University of London and for
the Diploma of Membership of Imperial College.

Blackett Laboratory

Imperial College

London SW7 2BZ

England.

June 1988.

To

My Parents

Reem & Sheila

Aunty Nazhat

and Family.

ABSTRACT

In this thesis, we consider response problems in Multiphoton Physics and Quantum Optics, partitioning the work into two main sections. Firstly, in chapters one to four, we study aspects of the photoexcitation of both a quasicontinuum (QC) of atomic or molecular levels and a structured continuum. Chapter five comprises the second section, and deals with quantum amplification.

In chapter one we review previous studies of the Bixon-Jortner model of a quasicontinuum, by way of setting the scene for the following three chapters.

Chapter two examines the interaction dynamics of a system in which a ground state is coupled to a QC of energy levels and to a true continuum, as a generalisation of the work in the previous chapter.

Chapter three is concerned with the photoexcitation of a structured continuum of states from a single ground state. We compare and contrast the results obtained with this model, with those of QC excitation.

In chapter four, we consider a system in which a ground state is coupled to a general QC of levels and to a true continuum. In the long-time limit the true continuum spectrum can exhibit zeros, the positions of which depend only on the energies of the QC levels. The initial conditions determine the existence of these zeros. We describe this phenomenon by studying dressed states for the complete system and in particular derive dressed states which are ground-state independent. We use these to explain the locations of the zeros and

their dependence on the initial conditions.

Chapter five considers the derivation of some quantum statistical results for the 'inverted' harmonic oscillator, (one with negative kinetic and potential energies), which are equivalent to ones that exist for the more familiar simple harmonic oscillator. It is an object that is frequently employed in modelling amplifiers in Quantum Optics, but also arises in statistical and quantum mechanics and is of interest in its own right.

We summarise and discuss our findings in chapter six.

CONTENTS

	Page
ABSTRACT	3
CONTENTS	5
LIST OF FIGURES	7
CHAPTER 1: INTRODUCTION	9
CHAPTER 2: THE EXTENDED BIXON–JORTNER MODEL	15
2.1 Introduction	
2.2 The Model	
2.3 Ground–State Population	
2.4 Further Discussion	
2.5 Quasicontinuum Population	
2.6 Summary.	
CHAPTER 3: PHOTO–EXCITATION OF A STRUCTURED CONTINUUM: A SOLUBLE MODEL.	53
3.1 Introduction	
3.2 A Soluble Model	
3.3 Ground–State Population	
3.4 Final State Spectrum	
3.5 Summary.	
CHAPTER 4: DRESSED STATES & SPECTRA IN QUASICONTINUUM EXCITATION.	72
4.1 Introduction	
4.2 Basic Equations	
4.3 Specific Quasicontinua	
4.4 Dressed States	
4.5 Conclusions.	

CHAPTER 5: THE INVERTED HARMONIC OSCILLATOR:	94
SOME STATISTICAL PROPERTIES.	
5.1 Introduction	
5.2 The Fluctuation–Amplification Theorem	
5.3 The Einstein Relation & Spectra.	
5.4 Relevance of the Quantum Regression Theorem & the Kubo Formula.	
5.5 Discussion	
5.6 Conclusions.	
CHAPTER 6: DISCUSSION & CONCLUSIONS	119
APPENDIX I	123
APPENDIX II	125
APPENDIX III	128
APPENDIX IV	129
APPENDIX V	133
REFERENCES	142
ACKNOWLEDGMENTS.	148

LIST OF FIGURES

	Page	
1.1	The Bixon-Jortner Model.	10
2.1	The Extended Bixon-Jortner Model.	16
2.2-2.8	Evolution of initial state population for various values of γ , V , Δ , & Δ_0 .	33 - 38
3.1	Excitation of a single discrete state to a structured continuum.	54
3.2-3.8	Evolution of ground-state population for various values of γ & φ .	59 - 64
3.9-3.13	Final-state spectrum for various values of γ , φ , & x .	66 - 69
4.1	The level scheme with the ground state coupled to an arbitrary QC & to a true continuum.	73
4.2-4.3	The spectrum $S_1(x)$ for Bixon-Jortner QC for various values of V_0 , V_1 , γ , & Δ .	77 - 78
4.4-4.6	The spectrum $S_2(x)$ for Bixon-Jortner QC for various values of V_0 , V_1 , γ , Δ , & N .	80 - 81
4.7-4.8	The spectrum $S_1(y)$ for Rydberg QC for various values of P , Q , R & N .	83
4.9	The spectrum $S_2(y)$ for Rydberg QC.	84
4.10	The spectrum $S_1(y)$ for Rydberg-like QC.	85
5.1	Harmonic & inverted oscillator potentials & stationary states.	96
5.2	Harmonic oscillator coupled to a heat	96

bath of oscillators.

5.3

Inverted oscillator coupled to a heat

97

bath of oscillators.

CHAPTER ONE**INTRODUCTION**

We present below a study of the photoexcitation of a dense set or 'quasicontinuum' of states, by a pulse which is suddenly turned on, concentrating on population dynamics. The practical use of such physics [Zewail & Letokhov, 1980] relates to an understanding of problems in laser-induced chemical processes, such as the infrared laser-driven dissociation of polyatomic molecules in photochemistry which may have implications for laser isotope separation, laser purification of substances, as well as photobiochemistry and photomedicine. Physical chemists employ quasicontinua in their modelling of vibrational levels in small polyatomic molecules.

The decay of a single excited quantum state into a background of states is a recurring theme in nature. Thus we now give a brief overview of the more important contributions to this field, relevant to our particular investigations.

The initial studies of the decay of an isolated, unstable initially populated energy level into an initially unoccupied background of energy levels, were undertaken by M. Bixon and J. Jortner [Bixon & Jortner, 1968]. They employed the model of O. K. Rice [Rice, 1933] in their study of 'Radiationless Transitions', the reduction in the radiative lifetime of excited levels in a manifold of densely-spaced indistinguishable levels, caused by interference effects and the subsequent reduction in the emission yield per typical

intramolecular recurrence time [Bixon et al., 1969b]. The Bixon-Jortner model (see Fig. 1.1) adopts the assumptions of equidistant quasicontinuum (QC) level spacing and equal strength coupling of the ground state to each QC level.

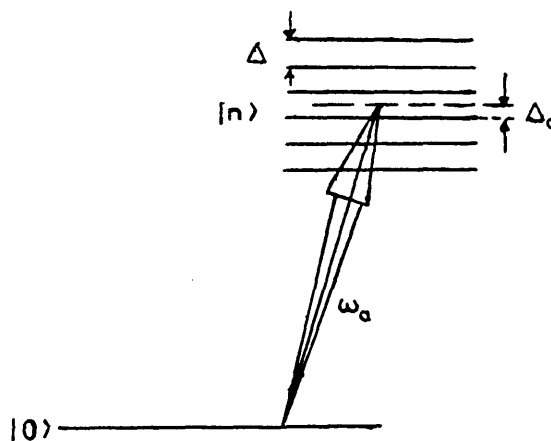


Figure 1.1. The Bixon-Jortner Model

Although there are inherent difficulties in the mathematical modeling of any physical situation, and simplifications of the extraordinarily complex energy-level configurations of polyatomic molecules must be made, there do arise in polyatomic molecules relatively isolated discrete states coupled with sets of relatively densely packed yet nevertheless discrete states. In turn, the ground state/QC system is assumed to form an isolated group of molecular states, well separated from other molecular states. Moreover, the dipole selection rules often allow access to only a small fraction of the available states.

Yet this situation appears elsewhere, particularly in the limit

of a continuum of background states. For example, the spontaneous emission of a photon [Ackerhalt et al., 1973; Loudon, 1985], by say, an excited atom, where the initial state corresponds to the excited atoms and no photons, and the final state is the de-excited atom and photons of differing direction, polarization and energy. Then there is 'Autoionisation' [Knight, 1984] and ref. therein, of great importance in Quantum Optics where the electrostatic interaction of several excited electrons in an atom, whose total energy is larger than the ionization limit of the atom, cause the formation of an ion and an electron.

If we imagine an initially unstable energy level coupled to each of the energy levels comprising the QC, we have the Bixon- Jortner model. Davies employed this model in his study of the apparent 'asymmetry of time', [Davies, 1977]. For although the laws at the quantum level are time reversal invariant (with the exception of neutral K-meson decay), processes are seen to be asymmetric in time or with respect to time because of the boundary conditions involved; initial conditions introduce the concept of a 'memory' into the evolution of the system.

Stey and Gibberd [1972] employed it, among other models, in studying the decay of the initial state in the limit of a background continuum of states. They noted the occurrence of quasi-periodicities in the time-evolution of the ground state. Lefebvre and Savolainen [1974] solved this and a generalised model, whereby the states in the QC are coupled to a true continuum, in addition to the couplings of the Bixon-Jortner model. Eberly et al. [1982], and Yeh et al. [1982] have given an 'interrupted coarse-grained theory' of QC

photoexcitation. Their perturbative analysis displayed recurrences, quasiperiodicities, and piecewise exponential decay for the ground state evolution. Galbraith et al. [1983] among others applied the model to problems of interest in multiphoton dynamics.

Milonni et al. [1982] in their pedagogic account, discussed how quantum-mechanical spreading of probability over the QC states of the system is mainly restricted to those closest in energy to the initial state in the Bixon-Jortner model. They prove numerically that the population never gets very far from the initial state. They also showed how under certain (slowly varying envelope) assumptions, the model has a classical analogue of a harmonic oscillator coupled equally to a large set of background harmonic oscillators. (Any vibrational state in a molecule may be written in terms of harmonic oscillator energy eigenstates $|n_1, \dots, n_N\rangle$, N being the number of vibrational degrees freedom.)

A further analogy is the retarded interaction of two dipole oscillators as derived by Milonni and Knight [1976]. There is remarkable similarity between the final solutions of this and the Bixon-Jortner model. In this respect, we note that the $N+1$ level Bixon-Jortner system is actually solved, essentially by considering only one of the QC levels explicitly, that is a two-level system.

Makarov et al., [1978] provided solutions for the coherent-excitation dynamics of a ground state linked by dipole transitions into a set of equispaced levels whose oscillator strengths follow a Lorentzian contour. They found a non-exponential, segmented time dependence.

Kyrölä [1984] has used a perturbative approach to show that in the weak-field limit, where the coupling constant is much smaller than the QC level spacing, that the recurrence dynamics in the Bixon-Jortner model resembles few-level dynamics. Kyrölä and Eberly [1985] give a detailed study of a model wherein two discrete levels are coupled to a QC.

Javanainen and Kyrölä [1985] show that for the long-time averages of populations in a discrete state/(flat) QC system, regardless of whether the QC is truncated or otherwise, the long-time and continuum limits are equivalent, if the coupling strength is much greater in magnitude than the level spacing. This is not surprising, since for very small level spacing, the QC 'looks' like a true continuum.

Throughout this work, we assume a suddenly switched-on interaction. Kyrölä has given [1986a] an adiabatic approximation treatment of certain QC interactions. For a slower turn-on, the initial state population undergoes periodic oscillations. As field strength is increased, the population recurrences of the sudden approximation disappear, and eventually adiabatic population inversion becomes possible. More recently, Kyrölä and Lindberg [1987] have shown how a unitary transformation can recast an arbitrary N-level Hamiltonian matrix in serial or parallel form. These latter are simpler in that the number of possible couplings is the smallest, and that their properties are relatively well-known. A supplementary historical survey is given in a paper by Shore [1983].

Several of the above studies have shown that the ground state population, instead of decreasing monotonically has reversals, during which part of the excited population returns to the ground level, i.e.

'recurrence of ground state probability.' Moreover, in the limit as the level spacing tends to zero, the recurrence period, or Poincaré Cycle [Davies, 1977; Gibbs, 1960; Wax, 1954] associated with the population dynamics gets ever larger, and becomes infinite when the QC becomes a true continuum, whence we obtain irreversible decay. Strictly we can only speak of a Poincare Cycle for a system, if the number of levels is finite.

Our model, to be solved below, the 'Extended Bixon-Jortner model' provides an extension of previous work on the subject [Radmore et al., 1987], in that we include the effects of decay in our model. The irreversible loss corresponds to photoionisation. Here, the initially occupied energy-level is connected not only to a QC of states but also to a true continuum. The discreteness of the distribution of energy levels is a hallmark of a quantal system. At the same time, classical physics presupposes a continuous energy spectrum for a system, possibly bounded only by extreme values peculiar to a specific model. Using our scheme we can study the transition between the two domains in a particular context. We thereby hope to examine the competition for population between the QC and the true continuum. After producing a closed form expression for the time evolution of the ground (initially occupied) level, we discuss the solutions using graphical output and limiting cases.

CHAPTER TWO

THE EXTENDED BIXON-JORTNER MODEL2.1 Introduction

In this chapter, we extend the traditional Bixon-Jortner model by the inclusion of a genuine continuum, whose states are labelled $|f\rangle$, coupled only to state $|0\rangle$ by a second electromagnetic field. We anticipate that the irreversible loss to the true continuum will damp out at rate γ all QC coherences and modify the regular revivals and related features noted previously. We will analyze the dynamics of this model paying particular attention to the population in the initial state as a function of coupling strength, decay rate and detunings. We employ Schrodinger equations of motion for each state, working in the Interaction Picture, and use a Markov approximation for the decay channel.

2.2 The Model.

The scheme employed is pictured in Figure 2.1. Initially, at time $t = 0$, all of the population lies in the ground level, or initial state $|0\rangle$, with associated probability amplitude $c_0(t)$. The background states of the QC are all coupled to a single, initially excited quantum state, but not directly to each other. There is an incoherent loss which takes the form of an induced 'decay' rate γ , due to photoionisation or dissociation to a true continuum. Note that we

require a real continuum in order to use Markov Theory.

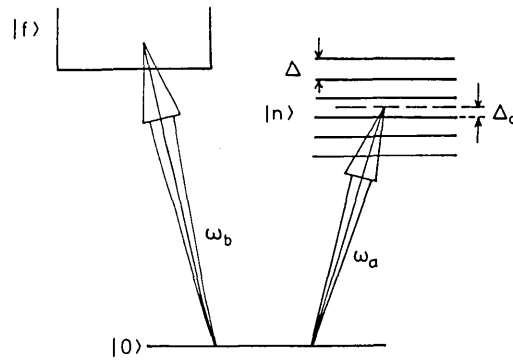


Figure 2.1. The Extended Bixon-Jortner Model.

Our primary task is to derive the population dynamics by finding an evolution equation for the the probability amplitude, and hence probability, of being in state $|0\rangle$. The Interaction Picture is employed.

As noted above, we have an element of competition in our model, in that both the QC and the true continuum are vying for the population that was initially in the isolated discrete state $|0\rangle$. A coherent electromagnetic field of frequency ω_a drives the $|0\rangle \rightarrow$ QC transition, while a laser field of frequency ω_b drives the $|0\rangle \rightarrow$ continuum, ($|f\rangle$) transition.

The explicit form of the interaction Hamiltonian \hat{V} is

$$\hat{V} = \frac{-e}{m} \mathbf{p} \cdot \mathbf{A}$$

where the vector potential is $\underline{A} = \underline{A}_a + \underline{A}_b$, with

$$\underline{A}_a(\underline{r}) = \sqrt{\frac{1}{2 \omega_{\underline{k}} V}} \left[a_a \hat{\epsilon}(\underline{k}_\lambda) e^{i \underline{k} \cdot \underline{r}} + \text{hermitian conjugate} \right]$$

and similarly for \underline{A}_b . Here V is the quantisation volume, $\hat{\epsilon}(\underline{k}_\lambda)$ is a polarization unit vector, $\underline{k} \cdot \hat{\epsilon}(\underline{k}_\lambda) = 0$ ($\lambda = 1, 2$), and $\hat{\epsilon} = 1 - \epsilon_0$.

We take the laser radiation fields to be quantised in number states $|n\rangle$. If the initial population is all in $|0\rangle$, and if we permit only energy-conserving transitions, we have that the essential states for the problem are

$$\begin{aligned} |0\rangle &= |E_0\rangle |n_a, n_b\rangle \\ |f\rangle &= |E_f\rangle |n_a, n_b - 1\rangle \\ |n_{QC}\rangle &= |E_{QC}\rangle |n_a - 1, n_b\rangle \end{aligned}$$

where the suffix 'QC' labels the quasicontinuum of states. If the detunings are small, then these are almost degenerate.

The laser fields, $E_i = \epsilon_i (\hat{a} - \hat{a}^\dagger)$ ($i = a, b$), assumed monochromatic have constant amplitudes ϵ_i detuned from resonance frequencies $\omega_n - \omega_0$ ($n = 1, \dots, N$) by detunings $\Delta_n = \omega_{n0} - \omega_a$, for an N -level QC.

The wavefunction for the system is, in the Interaction Picture,

$$\Psi(\underline{r}, t) = c_o(t) e^{-iE_o t/\hbar} \psi_o(\underline{r}) + \sum_f c_f(t) e^{-iE_f t/\hbar} \psi_f(\underline{r}) + \sum_{n=1}^N c_n(t) e^{-iE_n t/\hbar} \psi_n(\underline{r})$$

where $\psi_o = |0\rangle$, $\psi_f = |f\rangle$, $\psi_n = |n\rangle$.

We have also adopted the rotating-wave approximation (R. W. A) for the time-dependent couplings, by ignoring all terms containing

$$e^{-i(\omega_{of} + \omega_b)t} \quad \text{and} \quad e^{-i(\omega_{on} + \omega_a)t}.$$

This is equivalent to requiring energy conservation. For near resonant excitation $\omega_{on} \approx \omega_a$ and these terms oscillate at approximately twice ω_a . This gives rise to a small shift [Bloch & Siegert, 1940], and may be thought of as a small amplitude modulation superimposed on the more slowly oscillating term $e^{i(\omega_{on} - \omega_a)t}$.

We employ the Extended Bixon-Jortner Model with the following assumptions:-

- (a) The QC states are equally spaced in energy, (uniform QC), with the level spacing given by $\Delta = (\rho)^{-1}$, where ρ is the density of QC states.
- (b) The QC states have constant and equal coupling (matrix elements) to the initially occupied state, (flat QC), where the coupling constants and widths are independent of the QC level index. Thus, for example, $V_{on} \equiv \langle 0|V|n\rangle \equiv V \equiv V_{no}$, for all n .
- (c) The QC states are doubly infinite in number. Thus by extending

the states to positive and negative detunings, we can obtain closed form analytic expressions for $c_0(t)$ and $c_n(t)$.

Throughout, the laser field excitation, between the discrete levels is assumed coherent, (phase-preserving), and the field turn-on is assumed sudden. We could also assume, for simplicity of computation, that all matrix elements are real. These features of preservation of coherence and reality (and positivity) of transition dipole moments have been proved in the not dissimilar model of Shore [1983], who has the ground state coupled by a different laser interaction with each QC level. Furthermore, we define Δ_0 to be an energy-level detuning of the initial state from the closest background state above the initial state. So, when $\Delta_0 = 0$, one of the closest QC levels is exactly resonant with $|0\rangle$. This has the effect of producing a detuning of $\Delta_n = \Delta_0 + n\Delta$ for the n^{th} QC state.

2.3 Ground-State Population

Our method of solution will be to use Laplace Transforms. We may suppose that there exists a ' β ' such that,

$$\bar{c}(s) = \int_0^{\infty} e^{-st} c(t) dt$$

is defined (that is exists), with $\text{Re}(s) > \beta$, where β is real.

More precisely, $\bar{c}(s)$ is holomorphic in this region if $c(t)$ is piecewise continuous, and $c(t) e^{-\beta t}$ is bounded as $t \rightarrow \infty$. Also, $s = u + iv$, $u > \beta$.

In Appendix I, we outline a derivation of the general equations

of motion, from which we arrive at the following dynamical equations for our problem:-

$$i \dot{c}_o(t) = \sum_n v_{on} e^{-i(\omega_{no} - \omega_a)t} c_n(t) + \int d\omega_f v_{of} e^{-i(\omega_{fo} - \omega_b)t} c_f(t) \quad (2.3.1)$$

$$i \dot{c}_f(t) = v_{fo} e^{i(\omega_{fo} - \omega_b)t} c_o(t) \quad (2.3.2)$$

$$i \dot{c}_n(t) = v_{no} e^{i(\omega_{no} - \omega_a)t} c_o(t) \quad (2.3.3)$$

We solve these equations by first eliminating the true continuum by writing the second of the equations in integral form as

$$c_f(t) = c_f(0) - i \int_0^t v_{fo} c_o(t') e^{i\Delta_f t'} dt' \quad (2.3.4)$$

where the continuum detuning $\Delta_f = \omega_{fo} - \omega_b$. We will take for our initial conditions

$$c_o(t=0) = 1, \quad c_n(t=0) = 0 = c_f(t=0). \quad (2.3.5)$$

This formal expression for the continuum amplitude $c_f(t)$ is then substituted into equation (2.3.1), to give

$$i \dot{c}_0 = V \sum_n c_n(t) e^{-i\Delta_n t} - i \int d\omega_f |V_{of}|^2 \int_0^t e^{-i\Delta_f(t-t')} c_0(t') dt' \quad (2.3.6)$$

where the QC detuning $\Delta_n \equiv \omega_{no} - \omega_a$.

Next we assume that the continuum states $\{|f\rangle\}$ are dense, and have matrix elements V_{of} which vary sufficiently slowly with ω_f so that we may invoke the Markov approximation. This process is dealt with in appendix II. We find as a result, that

$$i \dot{c}_0 = V \sum_n c_n(t) e^{-i\Delta_n t} - i \Gamma c_0(t) \quad (2.3.7)$$

where the complex decay rate Γ is given by

$$\Gamma = \int d\omega_f |V_{of}|^2 \left[\pi \delta(\omega_{fo} - \omega_b) - i \mathcal{P} \frac{1}{\omega_{fo} - \omega_b} \right] \\ \equiv \gamma + i \Delta\omega_0. \quad (2.3.8)$$

The first term γ represents the photoexcitation rate from $|0\rangle$ to the continuum; the second (principal part) $\Delta\omega_0$, a Stark shift of the initial state due to the electromagnetic field. The coupled set of equations of motion for the amplitudes of the discrete states $|0\rangle$ and $|n\rangle$ become, on using the substitution, $b_n = c_n e^{-i\Delta_n t}$,

$$i \dot{c}_0 = V \sum_n b_n - i \Gamma c_0 \quad (2.3.9)$$

$$i \dot{b}_n = \Delta_n b_n + V c_0 \quad (2.3.10)$$

Solving these by Laplace Transforms, gives for the Laplace transform of the initial state amplitude,

$$\tilde{c}_0(s) = \left[s + \Gamma + V^2 \sum_n \frac{1}{s + i \Delta_n} \right]^{-1} \quad (2.3.11)$$

Following Davies [1977], we take the eigenenergy of the n^{th} QC state to lie in the range

$$E_0 - L < E_n < E_0 + L \quad (2.3.12)$$

where,

$$V_{on} \ll L \ll E_0. \quad (2.3.13)$$

The last inequalities mean that we may ignore contributions from E_n for which $|E_n - E_0| \gtrsim L$.

(In all of these inequalities, we can absorb ω_a into E_0 .)

We conveniently divide the energy range from $E_0 - L$ to $E_0 + L$ into $2N + 1$ levels with equal spacing Δ , so as to use the equally-spaced level property of the Bixon-Jortner QC. Let us, for the present, take the form of the detuning to be

$$\Delta_n = n \Delta \quad (2.3.14)$$

where $n = -N, -N+1, \dots, 0, \dots, N-1, N$.

So there are $2N+1 = \frac{2L}{\Delta}$ states in this truncated QC.

Later, we rectify this to include a non-vanishing Δ_0 , as in Figures 1.1, and 2.1, but for now, we assume the initial state $|0\rangle$ to be on resonance with the QC level $|n=0\rangle$.

$1/\Delta$ represents the density of states, for as N increases, Δ decreases. Condition (2.3.13) causes us to extend the range to infinity, to a good approximation.

Then,

$$\begin{aligned} \sum_{n=-\infty}^{\infty} (s + in\Delta)^{-1} &= \lim_{N \rightarrow \infty} \sum_{n=-N}^N (s + in\Delta)^{-1} \\ &= \frac{\pi}{\Delta} \coth \left[\frac{\pi s}{\Delta} \right]. \end{aligned} \quad (2.3.15)$$

This is proved in Appendix Three.

Therefore,

$$\tilde{c}_0(s) = \left[s + \Gamma + \frac{\pi V^2}{\Delta} \coth \left[\frac{\pi s}{\Delta} \right] \right]^{-1}. \quad (2.3.16)$$

It can be shown [Bocchieri & Loinger, 1957] for a closed system of bound states with discrete energy eigenvalues, for example the

ordinary N-level Bixon-Jortner Model with finite N, that the amplitude will display Poincare Cycles [Gibbs, 1960].

Hogg and Huberman [1983] have shown that a bounded quantal system with a time-periodic Hamiltonian, will reassemble itself infinitely often in the course of time. For a periodically kicked rotator, quantum interference effects suppress diffusive flow through phase space, leaving primarily quasiperiodic (regular) motion. Peres [1982] concludes that the recurrence argument against quantum chaos is of no practical concern unless there are a small number of incommensurate energy levels, and that recurrence times may simply be exceedingly large.

Indeed, this may be seen explicitly in the simple case of just two identical coupled systems ($|0\rangle$ and $|n=0\rangle$, say) the behaviour of which is recovered from (2.3.16) by taking the limit $\Delta \rightarrow \infty$, if we ignore the effect of the continuum $|f\rangle$.

In this limit,

$$\tilde{c}_0(s) = \left[s + \Gamma + \frac{V^2}{s} \right]^{-1}$$

$$= \frac{s}{(s - A)(s - B)}$$

where,

$$A, B = \frac{1}{2} \left[-\Gamma \pm (\Gamma^2 - 4V^2)^{1/2} \right].$$

Therefore,

$$c_o(t) = \frac{A e^{At} - B e^{Bt}}{(A - B)}$$

that is

$$c_o(t) = \frac{e^{-\Gamma t/2}}{\Omega} \left[\Omega \cos \left[\frac{\Omega t}{2} \right] - \Gamma \sin \left[\frac{\Omega t}{2} \right] \right].$$

Hence we obtain the familiar Rabi Oscillations between two levels, with Rabi Frequency Ω given by $\Omega = (\Gamma^2 - 4V^2)^{1/2}$. In the absence of the true continuum, $c_o(t) = \cos(|V_{on}|t)$. As more and more states are added, the density of states ($1/\Delta$) increases and the Poincare cycles become larger. The opposite limit $\Delta \rightarrow 0$, corresponds to $N \rightarrow \infty$, that is an open system. In that case,

$$\tilde{c}_o(s) = \left[s + \Gamma + \frac{\pi V^2}{\Delta} \right]^{-1}$$

from which it follows that the probability of occupation of level $|0\rangle$ is

$$\begin{aligned} |c_o(t)|^2 &= \left| e^{-(\Gamma + \pi V^2/\Delta)t} \right|^2 \\ &= e^{-(2\Gamma + 2\pi V^2/\Delta)t} \end{aligned}$$

This result is the usual time asymmetric exponential decay of an excited state, with the half-life $(2\Gamma + 2\pi V^2/\Delta)^{-1}$. In this limit of an open system, the probability of the excitation returning to $|0\rangle$ in a Poincaré fluctuation tends to zero. The Poincaré cycles are just

the Rabi nutational oscillations. Hence, the Poincaré cycles die away too.

The problem remains to invert the Laplace Transform of equation (2.3.16). Let us redefine certain terms, for ease of manipulation

$$r^2 = \frac{\pi |V_{\text{on}}|^2}{\Delta}, \quad g = \frac{\pi}{\Delta}.$$

Therefore,

$$\begin{aligned} \tilde{c}_0(s) &= \left[s + \Gamma + r^2 \left[\frac{1 + e^{-2gs}}{1 - e^{-2gs}} \right] \right]^{-1} \\ &= (1 - e^{-2gs}) \frac{1}{(s + \Gamma)(1 - e^{-2gs}) + r^2(1 + e^{-2gs})} \\ &= \frac{(1 - e^{-2gs})}{(s + \Gamma + r^2)} \left[1 - \left[\frac{s + \Gamma - r^2}{s + \Gamma + r^2} \right] e^{-2gs} \right]^{-1}. \end{aligned}$$

Given that we may take the real part of the Bromwich contour,

$$c_0(t) = \frac{1}{2\pi i} \int_{\text{Br}} e^{st} c_0(s) ds,$$

to be as large (that is, as positive) as we wish, we choose it so that

$$\left| \frac{(s + \Gamma - r^2) e^{-2gs}}{(s + \Gamma + r^2)} \right| < 1$$

which in fact holds if $\text{Re}(s) > 0$.

We can then legitimately use the expression

$$(1 - x)^{-1} = \sum_{m=0}^{\infty} x^m \quad (-1 < x < 1)$$

on the contour. Thus,

Thus,

$$\begin{aligned} \tilde{c}_0(s) &= \frac{(1 - e^{-2gs})}{(s + \Gamma + r^2)} \sum_{m=0}^{\infty} \frac{(s + \Gamma - r^2)^m}{(s + \Gamma + r^2)^m} e^{-2mgs} \\ &= (1 - e^{-2gs}) \left[\frac{1}{(s + \Gamma + r^2)} + \sum_{m=1}^{\infty} \frac{(s + \Gamma - r^2)^m}{(s + \Gamma + r^2)^{m+1}} e^{-2mgs} \right]. \end{aligned}$$

Evaluating further,

$$\begin{aligned} \tilde{c}_0(s) &= \frac{(1 - e^{-2gs})}{(s + \Gamma + r^2)} + \sum_{m=1}^{\infty} \frac{(s + \Gamma - r^2)^m}{(s + \Gamma + r^2)^{m+1}} e^{-2mgs} \\ &\quad + e^{-2gs} \sum_{m=1}^{\infty} \frac{(s + \Gamma - r^2)^m}{(s + \Gamma + r^2)^{m+1}} e^{-2mgs} \end{aligned}$$

$$\begin{aligned}
& - \frac{(1 - e^{-2gs})}{(s + \Gamma + r^2)} + (s + \Gamma - r^2) \sum_{m=1}^{\infty} \frac{(s + \Gamma - r^2)^{m-1}}{(s + \Gamma + r^2)^{m+1}} e^{-2mgs} \\
& - (s + \Gamma + r^2) \sum_{m=2}^{\infty} \frac{(s + \Gamma - r^2)^{m-1}}{(s + \Gamma + r^2)^{m+1}} e^{-2mgs} \\
& - \frac{(1 - e^{-2gs})}{(s + \Gamma + r^2)} + (s + \Gamma - r^2) \sum_{m=1}^{\infty} \frac{(s + \Gamma - r^2)^{m-1}}{(s + \Gamma + r^2)^{m+1}} e^{-2mgs} \\
& - (s + \Gamma + r^2) \sum_{m=1}^{\infty} \frac{(s + \Gamma - r^2)^{m-1}}{(s + \Gamma + r^2)^{m+1}} e^{-2mgs} + \frac{e^{-2gs}}{(s + \Gamma + r^2)} \\
& - \frac{(1 - e^{-2gs})}{(s + \Gamma + r^2)} + \frac{e^{-2gs}}{(s + \Gamma + r^2)} \\
& - 2r^2 \sum_{m=1}^{\infty} \frac{(s + \Gamma - r^2)^{m-1}}{(s + \Gamma + r^2)^{m+1}} e^{-2mgs} \\
& - \left[\frac{1}{(s + \Gamma + r^2)} - 2r^2 \sum_{m=1}^{\infty} \frac{(s + \Gamma - r^2)^{m-1}}{(s + \Gamma + r^2)^{m+1}} e^{-2mgs} \right].
\end{aligned}$$

Now we invert this expression.

$$\text{Using } L. T.^{-1} \left[\frac{1}{(s + \delta)^{n+1}} \right] = \frac{t^n}{n!} e^{-\delta t}, \text{ we find that the first}$$

term is $e^{-(\Gamma + r^2)t}$. Then, using the formula [Magnus et al., 1949]

$$L. T. \left[e^{\lambda t} t^{2\mu} L_n^{(2\mu)}(at) \right] = \frac{\Gamma(2\mu + n + 1)}{n!} \frac{(s - \lambda - a)^n}{(s - \lambda)^{n+2\mu+1}},$$

where $\text{Re}(2\mu + 1) > 0$, and $L_n^{(2\mu)}$ is a Generalised Laguerre Polynomial.

Taking $n = m - 1$, $\mu = 1/2$, $\lambda = -(\Gamma + r^2)$, $a = 2r^2$, we have

$$L. T. \left[\frac{(s + \Gamma - r^2)^{m-1}}{(s + \Gamma + r^2)^{m+1}} \right] = \frac{(m-1)!}{\Gamma(m+1)!} \left[t e^{-(\Gamma + r^2)t} L_{n-1}^{(1)}(2r^2 t) \right]$$

Therefore,

$$c_0(t) = e^{-(\Gamma + r^2)t} - \sum_{n=1}^{\infty} \frac{2r^2}{n} T_n L_{n-1}^{(1)} \left[2r^2 T_n \right] e^{-(\Gamma + r^2)T_n} \theta(T_n)$$

where $T_n = t - 2ng$, θ is the Heaviside Step Function, and use has been made of the shifting property,

$$L \{ f(t - a) \theta(t - a) \} = e^{-as} L \{ f(t) \}$$

where $a > 0$.

This expression was previously derived in a different context, by Stey & Gibberd [1972], who were interested in general decay models. However whereas the Γ term in our model corresponds to the Markov approximated effect of the true continuum, they view it as simply a 'complex energy', of the initial-state, with no physical interpretation beyond that. Lefebvre and Savolainen [1974], have used

an iterative method, instead of transforms to obtain a very similar result; (not having used a Markov-type approximation they do not have level-shifts.) But like Stey & Gibberd, they do not examine the continuum coupling.

We now include the effect of an initial level detuning Δ_0 into our solution for $c_0(t)$, but using

$$\Delta_n = \Delta_0 + n\Delta \quad (2.3.17)$$

for the detuning from resonance with $|0\rangle$ of the n^{th} QC state, as in Figures 1.1 and 2.1. Equation (2.3.11) becomes modified to

$$\tilde{c}_0(s) = \left[s + \Gamma + V^2 \sum_{n=-\infty}^{\infty} \frac{1}{s + i(\Delta_0 + n\Delta)} \right]^{-1} \quad (2.3.18)$$

The Laplace Inversion is taken over a suitable Bromwich Contour of this equation. With the definition $s' = s + i\Delta_0$, $\tilde{c}_0(s)$ may be written as,

$$\tilde{c}_0(s') = \left[s' + \Gamma - i\Delta_0 + \frac{\pi V^2}{\Delta} \text{Coth} \left[\frac{\pi s'}{\Delta} \right] \right]^{-1}.$$

Note that on shifting the complex s -plane parallel to the $\text{Im}(s)$ axis by a distance Δ_0 , we need shift our Bromwich contour accordingly. We can legitimately do this to obtain a new contour Br' , so long as the new contour encloses all the poles of the integrand, enabling us to use Cauchy's Residue Theorem. Then,

$$c_o(t) = \frac{e^{-i\Delta_o t}}{2\pi i} \int_{Br'} \tilde{c}_o(s') e^{s't} ds'.$$

The argument now goes through, with the replacement $\Gamma \rightarrow \Gamma - i\Delta_o$, and the extra factor $e^{-i\Delta_o t}$.

Therefore, we arrive at

$$c_o(t) = e^{-(\Gamma+r^2)t} - \sum_{n=1}^{\infty} \frac{2r^2}{n} T_n e^{-in\Delta_o 2g} \times L_{n-1}^{(1)} [2r^2 T_n] e^{-(\Gamma+r^2)T_n} \theta(T_n) \quad (2.3.19)$$

$$\left[r^2 = \frac{\pi |V_{on}|^2}{\Delta}, \quad g = \frac{\pi}{\Delta}, \quad T_n = t - 2ng \right]$$

which is the requisite, modified solution, in close analogy, mutatis mutandis, with expressions obtained previously [Stey et al., 1972; Lefebvre et al., 1974].

In turn, the $\Delta \rightarrow \infty$ limit of $c_o(t)$ is altered to

$$c_o(t) = \frac{e^{-(\Gamma + i\Delta_o)t/2}}{\Omega} \left[\Omega \cos \left[\frac{\Omega t}{2} \right] - (\Gamma - i\Delta_o) \sin \left[\frac{\Omega t}{2} \right] \right],$$

with modified Rabi Frequency, $\Omega = \sqrt{(\Gamma - i\Delta_o)^2 - 4V^2}$.

This is analogous to the two-level Rabi model result, equation (2.23) of Knight and Milonni [1980]. Also, since $2n_1 \geq 0$, the step function vanishes initially, since then $\theta(t - 2n_1)$ has a negative argument. So the initial condition $c_0(0) = 1$ is satisfied by our solution, equation (2.3.19).

We note that the Extended Bixon-Jortner model including a true continuum produces an initial state evolution closely resembling that of the original model but with the addition of damping and Stark shifts to the original detuning Δ_0 . We illustrate these additions by plotting the time-evolution of initial-state population, $P_0(t) = |c_0(t)|^2$, for various choices of the coupling V , the detuning Δ_0 and the decay rate γ and shift $\Delta\omega_0$.

When the coupling to the true continuum is turned off, the complex damping Γ is zero and the usual Bixon-Jortner results are recovered. In Figure 2.2 we show the time-evolution of the initial state population $|c_0(t)|^2$ for the case $V/\Delta = 1/3$, with one state exactly on resonance with $|0\rangle$, as a function of scaled time Vt . The general features of this evolution are first, an exponential decay at a rate given by the Weisskopf-Wigner approximation $2\pi|V|^2/\Delta$ [Louisell, 1973] in the first interval, from $t = 0$ to $t = 2\pi/\Delta$, at the end of which the initial state sees the QC of state density proportional to $1/\Delta$. Second, there is a recurrence of initial state population at $t = 2\pi/\Delta$ at which time the discrete nature of the QC is resolved. Thereafter, the dressed eigenfrequencies of the coupled QC beat to generate a complicated irregular time-evolution. When the decay rate Γ is turned on for the same resonant system (incorporating the shift $\Delta\omega_0$ into the transition frequency), the recurrences are damped out.

In Figure 2.3 we illustrate this with the choice of weak damping $\gamma = V/10$, all other parameters being the same as Figure 2.2.

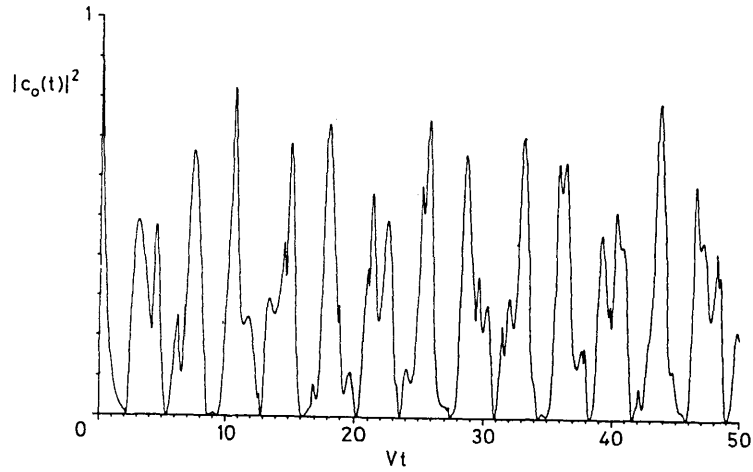


Figure 2.2. Initial state population evolution for $\Gamma=0$, $V/\Delta=1/3$, $\Delta_0=0$.

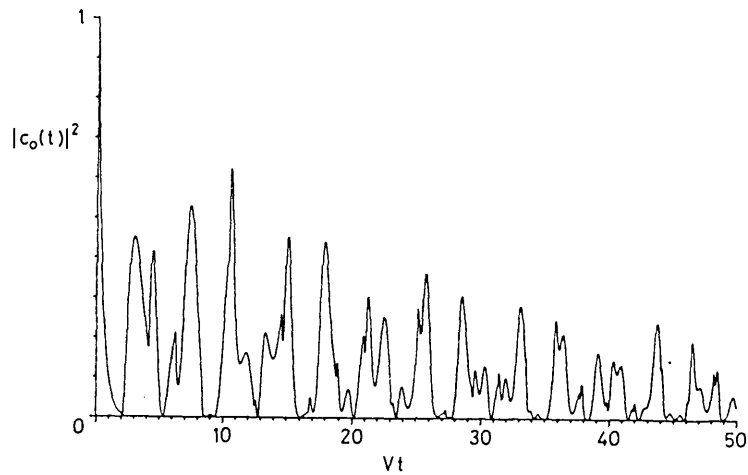


Figure 2.3. Initial state population evolution for $\gamma = V/10$,

$$V/\Delta = 1/3, \Delta_0 = 0.$$

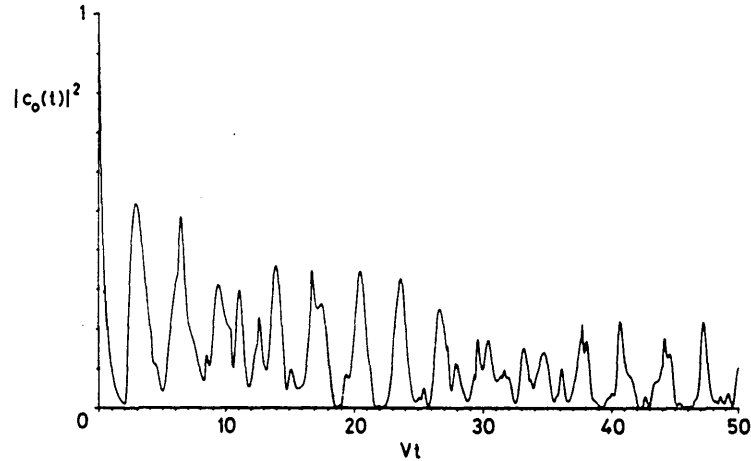


Figure 2.4. Initial state population evolution for $\gamma = V/10$,

$$V/\Delta = 1/3, \Delta_0 = 1/3.$$

In Figure 2.4 we relax the resonance condition and allow a detuning $\Delta_0 = V/3$ and decay rate $\gamma = V/10$. Note that the initial state population does not collapse entirely to zero in this case (just as a two-level Rabi model cannot be completely inverted by an off-resonance pulse.) The effect of a non-zero initial state detuning Δ_0 , is to ensure that destructive interference in the contribution to $c_0(t)$ from previous time intervals is now ⁱⁿ⁻complete; in turn $P_0(t) = |c_0(t)|^2$ does not reach zero. In Figure 2.5 we demonstrate how strong damping rapidly dissipates recurrences.

Many of the dynamical features result from the interplay between the coupling and decay rate. For example, a ratio of $V/\gamma = 0.1$ gives a marked exponential decay to zero for $P_0(t)$. At the same time $\Delta\omega_0$ has no perceptible effect on the time-evolution of $|c_0(t)|^2$.

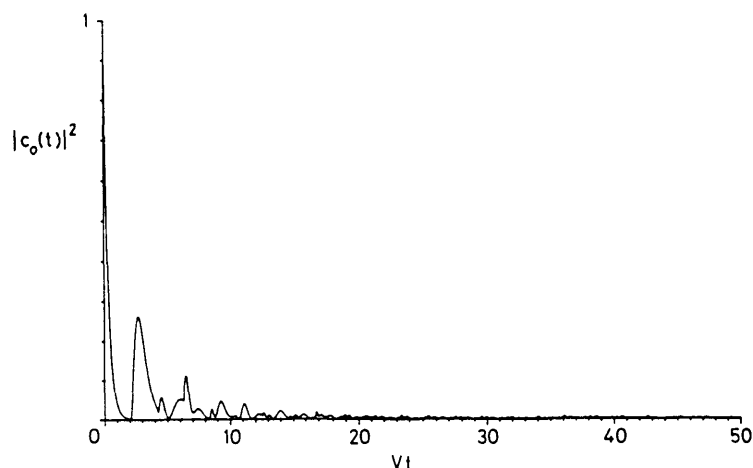


Figure 2.5. Initial state population evolution for $\gamma = V$,
 $V/\Delta = 1/3$, $\Delta_0 = V/3$.

For very weak excitation, the evolution is entirely perturbative: in Figure 2.6a we plot initial state population versus Vt for $V/\Delta = 0.1$ weak damping $\gamma = V/10$ and exact resonance $\Delta_0 = 0$ and observe a periodically interrupted damped two-state Rabi evolution. In Figure 2.6b we expand the time-scale and display the short-time evolution. We note that the evolution consists of a sequence of arcs: had we ignored the decay, the corresponding evolution would consist of a sequence of steepening straight lines attributed [Eberly et al., 1982; Yeh et al., 1982] to the interrupted coarse-graining. The regular interruptions are caused by periodic reconstructions of background state amplitudes. The 'arc' feature corresponds to a Fermi Golden Rule approximation of pure exponential decay $e^{-\gamma t}$ by the zeroth and first order terms to give $P_0(t) \approx 1 - \gamma t$ [Cohen-Tannoudji et al., 1977, p.1352].

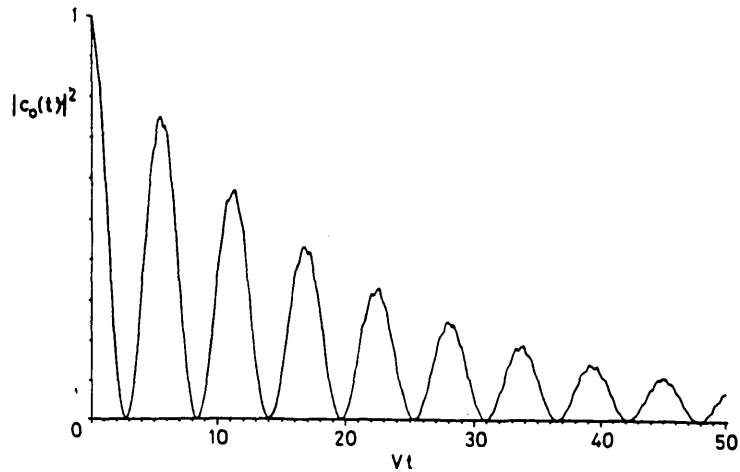


Figure 2.6(a). Initial state population evolution for $\gamma = V/10$,
 $V/\Delta = 1/10$, $\Delta_0 = 0$.

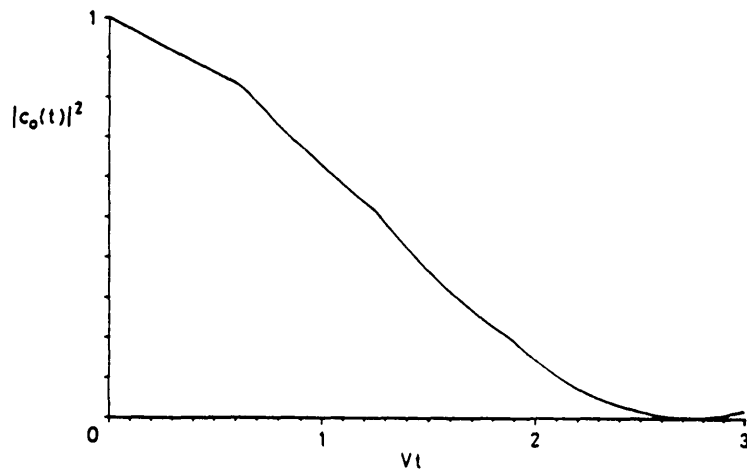


Figure 2.6(b). As in Figure 2.6(a), but on an extended scale.

When the detuning Δ_0 is chosen to be $\Delta/2$, that is maximum detuning, exactly midway between two states, the irregular recurrences are replaced by a zig-zag (or sawtooth) evolution [Kyrölä and Eberly, 1985]. In Figure 2.7 we display such an evolution when $V/\Delta = 1/200$ and $\gamma = 0$. The collapsing initial state population slightly deviates from exact straight lines. The saw-tooth behaviour arises because in the weak-field limit it is the discreteness of the QC rather than its continuum-like nature that is

significant to the dynamics. In particular, if the field is detuned to be precisely midway between two QC levels, the population will attempt to emulate few-level behaviour, that is two-level dynamics, because on being transferred from $|0\rangle$ to the QC, it cannot decide which of the two (equally) closest levels to occupy. Although these appear to be straight line rates, they are in fact curves; this becomes apparent if we wait for a sufficiently long time. This is more clearly visible in Figure 2.8a where $V/\Delta = 1/\pi$, $\Delta_0 = \Delta/2$ and $\gamma = 0$. When damping is added to this case (Figure 2.8b) this evolution is unchanged apart from a decaying envelope function.

Also, even if we are tuned midway between two QC levels, by increasing the laser from a weak field to a strong field, (increasing the ratio V/Δ), we regain recurrences. The explanation for this is that the zig-zags are purely a weak-field feature.

When the perturbation V increases, the power-broadening is sufficient to compensate for the detuning Δ_0 and we recover the appearance of the resonant evolution.

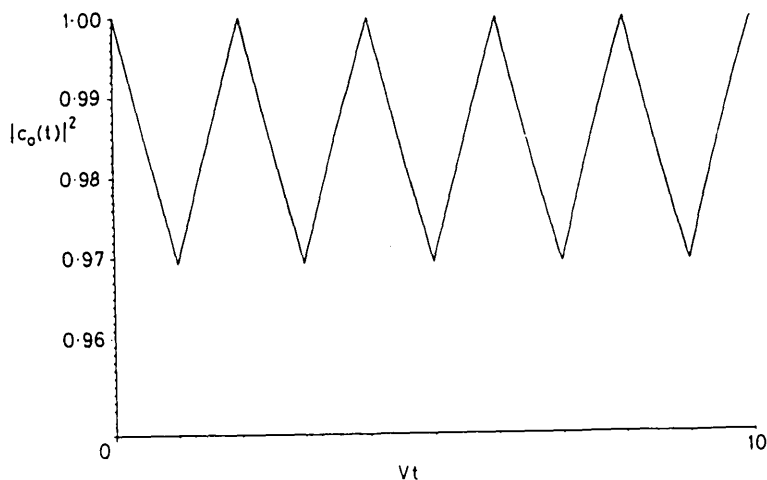


Figure 2.7. Initial state population evolution for $\Gamma = 0$,

$$V/\Delta = 1/200, \Delta_0 = \Delta/2.$$

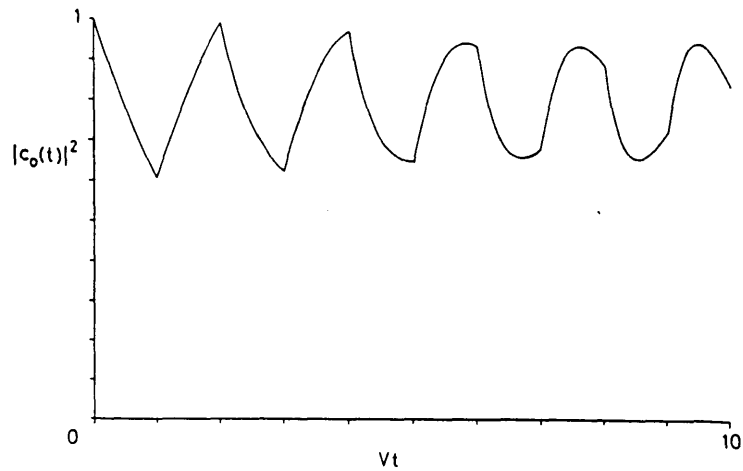


Figure 2.8(a). Initial state population evolution for $\Gamma = 0$,
 $V/\Delta = 1/\pi$, $\Delta_0 = \Delta/2$.

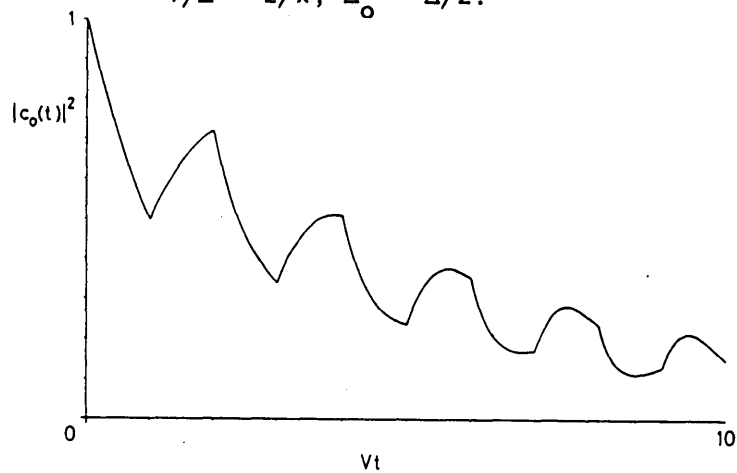


Figure 2.8(b). Initial state population evolution for $\gamma = V/5$,
 $V/\Delta = 1/\pi$, $\Delta_0 = \Delta/2$

In general, then, we have noted the important effect that Δ_0 has on $c_0(t)$. However, this assumes that the power broadening associated with the couplings do not exceed the level spacing of the QC. For a finite QC when the power broadening from the QC levels exceeds the QC's spectral width, the QC is effectively a single level, and the dynamics is essentially that of a two-level system. Similarly, for strong fields, the QC width is smaller than the induced width, so there is a Rabi oscillation between $|0\rangle$ and the whole QC.

2.4 Further Discussion

Below, we analyse our model in greater depth.

(A) Limiting Cases.

As $\Delta \rightarrow 0$, $r^2 g \rightarrow \infty$ given that $|V_{on}|^2$ remains constant. Then, the $e^{-r^2 t}$ factor present in all terms in the solution for $c_o(t)$ decays to zero. Accordingly $P_o(t)$ decays away exponentially. Alternatively, since $2ng \rightarrow \infty$, it becomes increasingly unlikely that $t - 2ng > 0$ (that is, that $\theta(t - 2ng) = 1$.) Effectively then, the terms including the step functions do not contribute to $c_o(t)$. Quite equivalently, even without the true continuum, because we considered the number of QC levels in a narrow energy range $(-L, L)$ as we increase the number of QC levels we approach an open system, and it is this that results in the time-asymmetric exponential decay of an excited state, with half-life $\Delta/\pi|V_{on}|^2$.

Our predictions that as $\Delta \rightarrow \infty$, the evolution of $P_o(t)$ resembles ever more closely the Rabi nutational oscillations reminiscent of few-level, (that is two-level), dynamics were confirmed with computer plots.

(B) Recurrences of Initial-State Probability

For a finite QC level spacing, Δ , we expect recurrences of $P_o(t)$. The retarded time functions $\theta(t - 2ng)$, ensure that for any given time t , only a finite number of terms in the infinite summations will contribute. In particular, for $0 < t < 2g$, the decay is strictly exponential.

The '2g' represents a 'delay', which retards the interactions. There is successive additive dipole dephasing and rephasing of the QC states, which leads to population transfer from $|0\rangle$ to states $\{|n\rangle\}$, back again to $|0\rangle$, and so on. This phenomenon is referred to as 'recurrence' of probability. At each cycle, that is at each integral multiple of $2g$, a further contribution is made to the overall dynamics, from the next term in the summation over n .

From our solution for $c_0(t)$, we see that all the terms contain exponentials damped in a time of the order of $[\Gamma + (\pi V^2/\Delta)]^{-1}$. Alongside this, the evolution of $c_0(t)$ will be ever increasing in complexity, with each time interval $2g$, because of the monomial terms $(t - 2ng)^P$, which increase in order, as more terms in the 'n' and Laguerre polynomial sums are included. So it is to be expected when n is large enough, that successive recurrences will interfere.

As the recurrence time is increased, there is for a given interval, less contribution from previous intervals. Also, $P_0(t)$ becomes smaller with successive cycles, but will remain non-zero if we turn-off the true continuum and there is no longer as irreversible loss mechanism.

Note that $(t - 2ng)$ is always non-negative, for otherwise $\theta(t - 2ng)$ will ensure that the whole expression in the n^{th} interval and subsequent intervals, in the summand, vanishes so does not need to be considered. Therefore, the factor $e^{-\Gamma(t - 2ng)}$ in the n^{th} retarded term has the expected attenuation effect, regardless of the relative magnitude of γ and Δ .

The Bixon-Jortner model may describe polyatomic molecules, where relatively isolated states are coupled to a manifold of vibronic (electronic and vibrational) states. Because bound states cause the relaxation mechanism there is a 'period' of $2g$ associated with the dynamics.

The 'kicking', which repopulates $|0\rangle$ is due to phased dipole interactions. This δ -function kicking is more apparent in the model of Milonni et al. [1982] where taking QC detunings as $\Delta_n = \Delta_0 + n\Delta$ enables use of the Poisson Sum Rule,

$$\sum_{n=-\infty}^{\infty} e^{-2\pi i n x} = \sum_{n=-\infty}^{\infty} \delta(x - n).$$

As has been previously argued, [Grenpel et al., 1984], the recurrence of probability $P_0(t)$ could be said to be quantum-mechanical localization of the relevant wavefunction. This is not at variance with the studies of Casati et al. [1979] which show that a periodic " δ -kicked rotator" leads to quantum mechanical localization in regions where the classically analogous model is chaotic.

Ackerhalt et al. [1986], and ref. therein, have considered a classical model for multiple photon excitation (M. P. E.) of molecular vibrations by infra-red laser fields. There, a pumped mode is coupled to a background of harmonic modes. They explain the dependence of the M. P. E. process on the laser fluence (that is, the time integral of intensity) in terms of decaying correlations associated with chaotic time-evolution of the pumped-mode amplitude. It is not yet

known whether chaos will likewise be displayed in the analogous quantal system.

It has also been discovered, for two-state systems [Pomeau et al., 1986; Milonni et al., 1987] that when there are two incommensurate irrational kicking frequencies assumed for the quasiperiodic force, chaotic evolution, in a precisely defined sense, is observed for the erratically driven probability amplitudes. Here, quantum chaos is defined by

(a)decaying autocorrelation function of the state vector,

(b)broadband power spectrum of the state vector,

and (c)ergodic motion on the Bloch sphere, (see Appendix V.)

More recently, Cerdeira & Huberman [1987] examined the time-evolution of observables for bounded quantum systems subjected to time-periodic fields, and for which the number of energy-levels N is finite. They showed that in spite of their recurrent, almost periodic behaviour, the distribution of values produced by the evolution of the observables becomes Gaussian in the large- N limit. The process remains nondiffusive even though the observable may appear to be random. Thus, since the energy does not grow in time, the dynamics does not remain chaotic. They suggest that only a Fourier transform would display the non-random behaviour.

(C) Interpretation

In our model, the laser field induces a dipole moment, that couples the system to the field. The polarization density is the dipole moment per unit volume of the molecules comprising "Bixon-Jortner" type subsystems among their energy levels. The

polarization will include terms in the molecular or atomic density, (which can be set to unity if we are only considering one molecule, say), $c_n^*(t)$, $c_o(t)$, and the component of the dipole operator parallel to the electric field. The largest coupling (square of the relevant off-diagonal Hamiltonian matrix element) is that between $|0\rangle$ and the centermost QC level. The strength drops off as we approach the edges of the manifold. Now the dissipative mechanism will alter the time evolution of the amplitudes c_n^* and c_o , and hence could be said to give rise to the dephasing effect of the true continuum, through the term $e^{-\Gamma t}$. A quite similar situation arises in the classical theory of Resonance Optics, [Allen & Eberly, 1975].

H. A. Lorentz imagined an electron-ion pair to act like a simple harmonic oscillator, its electric dipole moment coupling it to the electromagnetic field. (The electron is at the end of a spring, attached to the nucleus, which is the equilibrium position, and is driven to oscillate by the electric field of the wave.) It is Inhomogeneous Broadening which causes dipole dephasing. An electric pulse transfers energy to the dipoles, which then oscillate in phase at the field frequency. When the pulse is switched-off, the dipoles return to oscillate at their natural frequencies. For the collection of dipoles, with inhomogeneous spectral line halfwidth $\delta\omega_I$, there is a decay factor $e^{-\delta\omega_I t}$ in the expression for the macroscopic polarization density, $P(t)$, associated with the dipoles. (Note that from the Maxwell Equation

$$\left[\frac{\partial^2}{\partial z^2} - \frac{1}{c^2} \frac{\partial^2}{\partial t^2} \right] E(t, z) = \frac{4\pi}{c^2} \frac{\partial^2}{\partial t^2} P(t, z)$$

for wave propagation, that $P(t)$ causes the radiation.) The factor $e^{-\delta\omega_I t}$ represents the interference of all of the dipoles, whose frequencies comprise the inhomogeneous line. By the time that the inhomogeneous lifetime is reached, the dipoles are completely mutually out of phase and $P(t)$ is damped away, almost to zero.

In conclusion, then, each dipole moment monochromatically damps in amplitude, at the same time that it is dephasing and rephasing along with the other dipoles. The magnitude of the total dipole moment decreases to zero, whence all of the population is lost to the true continuum. This compares favourably with, for example, the analogous situation which arises in the theory of 'photon echoes', [Allen & Eberly, 1975, p.215].

(D) Finite Number of Background States

For greater physical accuracy, we would require a finite QC, but this rules out the possibility of a closed analytic solution. As we increase the number of QC levels, (to an infinite number,) the precise time-evolution of $c_0(t)$ diminishes rapidly with detuning from the "center" of the QC. Energy non-conserving states (large detuning with $\omega_0 - \omega_n$), then, are weakly non-perturbative. It has been previously noted [Milonni et al., 1982] that the $n = 15$ state QC is already in excellent agreement with the infinite state QC, in the ordinary Bixon-Jortner model. This relates to the finding [Milonni et al., 1982] that population never gets very far from the initial state.

Even with a relatively small number of QC levels, if their density is large, exponential decay is an excellent approximation, crudely because with a large density of QC states, the "lifetime" of

the decaying state is shorter, and so contributions from different intervals do not appreciably overlap. That is, a densely spaced QC approximates a true continuum very well.

(E) Deviations from Exponential Decay

Robiscoe & Hermanson [1972, 1973] developed a model of exponential decay with a memory, which yields pure exponential decay in the limit of zero memory time. They suggest that finite memory times may yield non-Lorentzian lineshapes [Winter, 1979]. Pietenpol [1967] has discussed the decay of a discrete state to a continuum via a Lorentzian coupling. A weak coupling to the continuum corresponds to a short memory time in the model of Robiscoe & Hermanson.

For pure exponential decay, we require a decay energy spectrum that is continuous and unbounded from both above and below. The latter condition is a consequence of the Paley-Wiener Theorem [Fonda & Ghirardi, 1972]. Thus in realistic physical models, which require a lower bound in the energy spectrum of the unstable quantum system on physical grounds, exact decay is merely an approximation, and there are deviations at very short times, just after the formation of the unstable state, and at very large times, after many mean lives have elapsed [Winter, 1979]. Nevertheless, because these extreme domains are so difficult to access in practice, no deviation from exponential decay has been reported for quantum systems.

Fonda & Ghirardi interpreted the deviations from exponential decay as being due to the already-decayed states, which because of the evolution of the system, can partially reconstruct the initial unstable state; hence a regenerative process.

(F)Energy-Level Degeneracy

If the QC energy levels are degenerate [Lefebvre et al., 1974, p.2515; Bixon et al., 1969, p.3284], with degeneracy d , all other factors remaining constant, we can derive the modified form of $c_0(t)$.

In our previous analysis, we were led to

$$\tilde{c}_0(s) = \left[s + \Gamma + V^2 \sum_{n=-\infty}^{\infty} \frac{1}{s + i\Delta_n} \right]^{-1} \quad (2.3.11)$$

(which for our model reduced to

$$- \frac{\pi}{\Delta} \text{Coth} \left[\frac{\pi s}{\Delta} \right].)$$

It follows for the case in hand, that the only change will be that V^2 becomes dV^2 . Hence the coupling r^2 is in turn modified and we arrive at

$$c_o(t) = e^{-(\Gamma + \bar{r}^2)t} - \sum_{n=1}^{\infty} \frac{2\bar{r}^2}{n} (t - 2n1) e^{-in\Delta_o 21}$$

$$L_{n-1}^{(1)}[2\bar{r}^2 (t - 2n1)] e^{-(\Gamma + \bar{r}^2)(t - 2n1)} \theta(t - 2n1)$$

where,

$$1 = \frac{\pi}{\Delta}$$

$$\bar{r}^2 = d r^2 = \frac{\pi |V_{on}|^2}{\Delta}$$

d is the degree of degeneracy.

These modifications are physically reasonable; the degeneracy ought not to affect the delay (or interval or fundamental period) of the evolution, whereas the initial decay constant, $\{\text{Re}(\Gamma + \bar{r}^2)\}^{-1}$ ought to be affected through a decrease in the recurrence period; in other words, recurrence effects affect the dynamics.

This phenomenon is important, where an appropriate substitution would destroy the symmetry in a highly symmetrical small molecule thereby lengthening the initial rate, while retaining the same recurrence period.

In what Bixon and Jortner call the "Resonance Limit" in their theory of electronic relaxation in polyatomic molecules for the study of unusually long radiative lifetimes of small molecules, they state

[Bixon & Jortner, 1969a] that "when the energy levels are coarsely spaced, a small number of degenerate or quasidegenerate zero-order levels may be split by the intrinsic or by external perturbations."

The degenerate, equidistant QC may be employed in producing a reasonable model of Landau levels [Blakemore, 1974; Ziman, 1972] although modifications would be required, such as truncating the QC because of the cut-off in Landau levels. The connection is particularly clear, if we follow Ziman's derivation [Ziman, 1972 p.319] of Landau levels, which uses the Poisson summation formula.

2.5 Quasicontinuum Properties

In order to derive the probability amplitude $c_p(t)$, for a typical QC level $|p\rangle$, great care must be exercised to ensure that the effect of the true continuum is properly accounted for in the Interaction Picture. We follow the method of Radmore and Knight [1982, appendix], employing the equations,

$$i \dot{c}_0(t) = V \sum_n c_n(t) e^{-i\Delta_n t} - i \Gamma c_0(t) \quad (2.5.1)$$

$$i \dot{c}_n(t) = V_{no} e^{-i\Delta_n t} c_0(t) \quad (2.5.2)$$

Letting $b_0(t) = c_0(t) e^{\Gamma t}$, with $\Gamma = \gamma + i \Delta\omega_0$ as before, gives,

$$i \dot{b}_0(t) = \sum_n V_{on} e^{(i\Delta_n + \Gamma)t} c_n(t) \quad (2.5.3)$$

Rather than proceed naively with equation (2.5.2), equation (2.5.3) indicates, on comparison with the continuum-free version of (2.5.1), that the dynamics is altered by the continuum so as to require the replacement $c_n(t) \rightarrow c_n(t) e^{\Gamma t}$, for all n .

So equation (2.5.2) becomes, for a specific QC level p ,

$$\frac{d}{dt} \left[c_p(t) e^{\Gamma t} \right] = -i v_{po} e^{i\Delta_p t} c_o(t).$$

That is,

$$c_p(t) = e^{-\Gamma t} (-i v_{po}) \int_0^t e^{i\Delta_p \tau} c_o(\tau) d\tau \quad (2.5.4)$$

as compared to (2.5.2).

We defer the calculation to Appendix IV, merely quoting our answer as

$$\begin{aligned} c_p(t) = & -i v_{po} \left[\frac{e^{(i\Delta_p - \Gamma - r^2)t} - 1}{(i\Delta_p - \Gamma - r^2)} \right] e^{-\Gamma t} \\ & - e^{-(\Gamma + r^2)T_n} \sum_{n=1}^{\infty} \frac{2r^2}{n} \sum_{k=0}^{n-1} \binom{n}{n-1-k} \frac{(-2r^2)^k}{k!} e^{-in\Delta_o 2g} \\ & \times e^{(i\Delta_p - \Gamma)t} \sum_{q=0}^{k+1} \frac{(T_n)^{k+1-q} (-1)^q (k+1)!}{(i\Delta_p - \Gamma - r^2)^{q+1} (k+1-q)!} \theta(T_n) \quad (2.5.5) \end{aligned}$$

The population in QC level $|p\rangle$, at time t , is given by $\bar{P}_p(t) = |c_p(t)|^2$. Note that the ground-state is shifted due to its coupling to the true continuum. In turn each QC level is shifted. Hence in equation (2.5.5) each detuning Δ_p comes attached to a ' Γ '. Clearly, the initial condition $c_p(0) = 0$ is satisfied. Also, $c_p(t \rightarrow \infty) \rightarrow 0$, because of the presence of the $e^{-\Gamma t}$ term, which together with $c_o(t \rightarrow \infty) \rightarrow 0$, gives

$$P_f(t \rightarrow \infty) \sim 1 - P_o(t \rightarrow \infty) - \sum_n P_n(t \rightarrow \infty)$$

$\rightarrow 1$.

Hence with our choice of initial conditions, there is no population trapping between the discrete states $|0\rangle$ and $|n\rangle$ in our Extended Bixon-Jortner model.

Radmore [1982] has studied a similar system, but with the ground state in the Extended Bixon-Jortner model being coupled to an extra discrete level, and with arbitrary QC level spacings. He found that if population was initially placed in this extra level, instead of $|0\rangle$, then in the long time limit, some population is trapped in a noninteracting superposition state, comprising this initially populated level and that QC level with which it is two-photon resonant. This arises because dipole cancellations are such that this 'dressed' superposition state decouples itself from the system dynamics, and retains its initial population.

2.6 Summary

The work in this chapter uncovered aspects of the dynamical behaviour in the Extended Bixon-Jortner model. Primarily, and as predicted, the continuum was found to modulate the recurrences, that were predicted by previous studies of the ordinary Bixon-Jortner scheme, by causing transient behaviour. This latter arose in much the same way that multiplying $\sin(x)$ by e^{-x} , causes the former to die away inside an envelope created by e^{-x} , as x approaches infinity, whilst retaining its sinusoidal feature.

Our examinations included studying the effects of limiting cases, and strong and weak-field approximations. We noted that when the population was initially carried by one of the QC levels, there was trapping of population within the discrete levels, in the long-time limit, and not all of the population decayed into the true continuum.

By way of an addendum, we draw special attention to the semi-perturbative theory for general QC, proposed by Radmore et al. [1987]; see also Kyrölä [1984].

Radmore ignored the true continuum and resonantly coupled the initially populated state to a particular QC level. These two states were treated as an exact two-level system. The other QC levels, each detuned from resonance with $|0\rangle$, were treated perturbative using a weak-field approximation; these act to perturb the two-state evolution.

When applied to the Bixon-Jortner model, the weak-field results of the non-perturbative model were reproduced; for example, straight-line 'rates' were found to be superimposed on an underlying oscillatory evolution of $P_0(t)$, i.e., the Rabi oscillations were

periodically interrupted by the background states. The theoretical method was further applied to a Rydberg series QC.

CHAPTER THREE

PHOTO-EXCITATION OF A STRUCTURED CONTINUUM:A SOLUBLE MODEL3.1 Introduction

In chapter two we studied the excitation of a single ground-state to a QC of levels [Radmore et al., 1987 and ref. therein]. In particular the Bixon-Jortner model [Bixon and Jortner, 1968], consisting of the excitation from the ground-state to an equally-spaced QC, has received much attention [Radmore et al., 1987 and ref. therein]. The dynamics of the population of the ground-state exhibits an initial Weisskopf-Wigner exponential decay, followed by a revival and a complicated time-evolution which receives periodic interruptions or 'kicks'.

In the present chapter, we consider the excitation of the initially-occupied state to a structured continuum having dipole matrix elements which vary periodically between zero and a maximum value [Radmore and Tarzi, 1987]. Such a continuum could result from the embedding of a QC in a true continuum [Kyrölä, 1986b] and a full diagonalisation of this in the manner of the 'dressed resonance representation' of Agassi and Eberly [1986]. Our idealised model has the advantage of being analytically soluble allowing straightforward calculation of the ground-state occupation probability. We consider the ground-state to be coupled to an arbitrary position in the structured continuum, thus allowing tuning from a position of maximum coupling, where an evolution of the Bixon-Jortner type is seen in certain cases, to a position of zero coupling where population

trapping is observed. The evolution possesses kicks due to the periodic nature of the structured continuum, although these are damped out significantly. The final-state spectrum exhibits splitting of the main resonance peak for sufficiently strong coupling and subsequent narrowing of resonance peaks as they approach zeros in the spectrum.

3.2 A Soluble Model

We consider a ground-state $|0\rangle$ coupled to a structured continuum of states ($|f\rangle$) by a monochromatic field detuned by a particular continuum state $|f\rangle$. The continuum is taken to be infinite in extent and to have dipole matrix elements V_{of} between states $|0\rangle$ and $|f\rangle$ such that $|V_{of}|^2$ varies periodically (Figure 3.1).

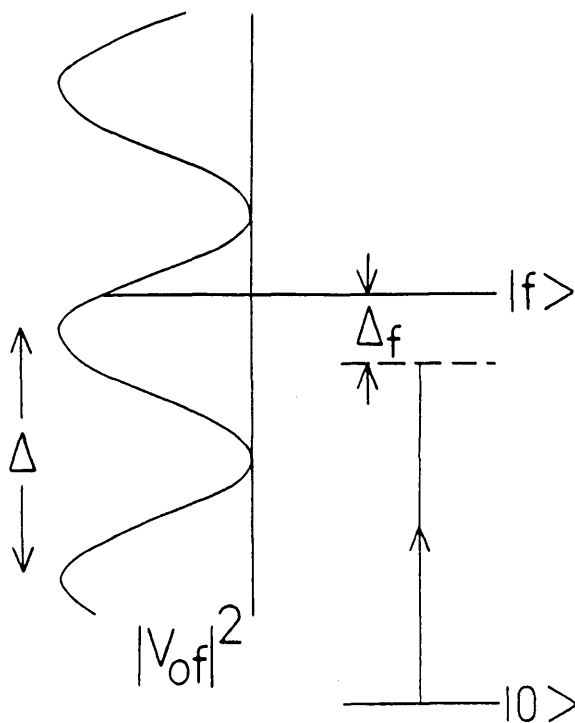


Figure 3.1. Excitation of a single discrete state to a structured continuum.

The equations of motion for the state amplitudes are then

$$\dot{c}_o = -i \int_f V_{of} e^{-i\Delta_f t} c_f \quad (3.2.1a)$$

$$\dot{c}_f = -i V_{fo} e^{i\Delta_f t} c_o \quad (3.2.1b)$$

Putting $b_f = c_f \exp(-i\Delta_f t)$ transforms these to

$$\dot{c}_o = -i \int_f V_{of} b_f \quad (3.2.2a)$$

$$\dot{b}_f = -i\Delta_f b_f - i V_{fo} c_o \quad (3.2.2b)$$

We now take the Laplace transform of equations (3.2.2) with initial conditions $c_o(t) = 1$, $b_f(0) = 0$, giving

$$s\tilde{c}_o - 1 = -i \int_f V_{of} \tilde{b}_f \quad (3.2.3a)$$

$$s\tilde{b}_f = -i\Delta_f \tilde{b}_f - iV_{fo} \tilde{c}_o \quad (3.2.3b)$$

where the tilde denotes Laplace transform with variable s . Solving equations (3.2.3) for \tilde{c}_o gives the familiar result

$$\tilde{c}_o = [s + I(s)]^{-1} \quad (3.2.4)$$

where

$$I(s) = \int_{\mathbf{f}} \frac{|V_{\text{of}}|^2}{s + i\Delta_{\mathbf{f}}} \quad (3.2.5)$$

We now take the following model of the structured continuum:

$I(s)$ in equation (3.2.5) is evaluated by choosing

$$|V_{\text{of}}|^2 \propto \cos^2 \left[\frac{\pi \Delta_{\mathbf{f}}}{\Delta} + \varphi \right] \quad (3.2.6)$$

so that the matrix elements have a periodic structure with separation Δ between peaks. We have chosen to use $\Delta_{\mathbf{f}}$ as the dummy variable of integration in what follows and use the 'phase' φ to allow tuning of the laser field: choosing $\varphi = 0$ makes $|0\rangle$ resonant with the position of maximum coupling while choosing $\varphi = \pi/2$ makes $|0\rangle$ resonant with a position of zero coupling. This is therefore related to the Bixon-Jortner model [Bixon & Jortner, 1968] where the QC levels have constant separation Δ . Then

$$I(s) = \frac{2V^2}{\Delta} \int_{-\infty}^{\infty} \frac{\cos^2(\pi\Delta_{\mathbf{f}}/\Delta + \varphi)}{s + i\Delta_{\mathbf{f}}} d\Delta_{\mathbf{f}} \quad (3.2.7)$$

where we have chosen the proportionality constant to give the familiar Weisskopf-Wigner result when Δ becomes small (the cosine squared averaging to 1/2.) We then find that $I(s)$ can be evaluated, for example by contour integration, to give

$$I(s) = \frac{\pi V^2}{\Delta} \left[1 + e^{2i\varphi} e^{-2\pi s/\Delta} \right]. \quad (3.2.8)$$

If we formally let Δ become small, we obtain the Weisskopf-Wigner result, $I(s) \sim \pi V^2/\Delta$.

To find $c_o(t)$, we use equations (3.2.4) and (3.2.8), writing the inversion as

$$c_o(t) = \frac{1}{2\pi i} \int_{Br} \frac{e^{st}}{s + \frac{\pi V^2 (1 + e^{2i\varphi} e^{-2\pi s/\Delta})}{\Delta}} ds. \quad (3.2.9)$$

This expression can be simplified somewhat by the substitutions $T = \Delta t/2\pi$, $z = (s + \pi V^2/\Delta) 2\pi/\Delta$ and

$$\gamma = 2\pi^2 V^2/\Delta^2, \quad a = \gamma e^\gamma e^{2i\varphi} \quad (3.2.10)$$

giving

$$c_o(T) = e^{-\gamma T} L_T^{-1} \left[(z + a e^{-z})^{-1} \right] \quad (3.2.11)$$

where L_T^{-1} denotes the Laplace inversion with variable T . Before inverting this we note that in the case $\varphi = \pi/2$, then $a = -\gamma e^{-\gamma}$ and we see from equation (3.2.11) that the function of z to be inverted has a pole at $z = \gamma$. This generates a term proportional to $e^{\gamma T}$ in the inversion and the cancelling of this with the factor $e^{-\gamma T}$ leads to population trapping. The residue at this pole is $(1 + \gamma)^{-1}$ and hence we expect population in the state $|0\rangle$ equal to $(1 + \gamma)^{-2}$. It is not

difficult to show that, as expected, all the other roots of $z + ae^{-z}$ lie in the left-hand half-plane.

To invert equation (3.2.11), we express $(z + ae^{-z})^{-1}$ as a sum and proceed in a similar way to the method used for Bixon-Jortner studies [Milonni et al., 1982; Radmore et al., 1987]:

$$\begin{aligned} L_T^{-1} \left[(z + ae^{-z})^{-1} \right] &= L_T^{-1} \left[\sum_{n=0}^{\infty} (-a)^n e^{-nz} / z^{n+1} \right] \\ &= \sum_{n=0}^{\infty} \frac{(-a)^n (T - n)^n H(T - n)}{n!} \end{aligned} \quad (3.2.12)$$

(see [Abramowitz & Stegun, 1972] for example) where H is the unit step-function. Hence $c_o(T)$ can be written

$$c_o(T) = e^{-\gamma T} \sum_{n=0}^{\infty} \frac{(-a)^n (T - n)^n H(T - n)}{n!} \quad (3.2.13)$$

Note that in the early stages of the evolution ($0 \leq T \leq 1$), $c_o(T) = e^{-\gamma T}$ in agreement with the Weisskopf-Wigner result and the time-development will possess 'kicks' at each integer value of T as in the Bixon-Jortner model. We argued in chapter two that this feature is due to the periodicity of the continuum; in QC excitation it is absent when the Bixon-Jortner QC is replaced by a Rydberg series [Radmore et al., 1987].

of γ is increased then, although the decay rate is increased, so is the coupling between the ground-state and the continuum. We might expect therefore to see evidence of oscillatory behaviour in $P_0(T)$ for sufficiently large γ . We illustrate that this is the case in Figures 3.3, 3.4 and 3.5. For the same three values of φ as in Figure 3.2, we plot $P_0(T)$ against T with $\gamma = 2$.

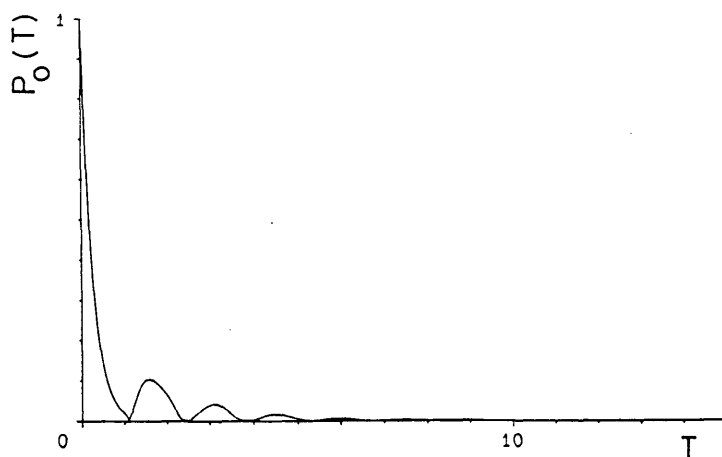


Figure 3.3. The ground-state population as a function of T with $\gamma = 2$ and $\varphi = 0$.

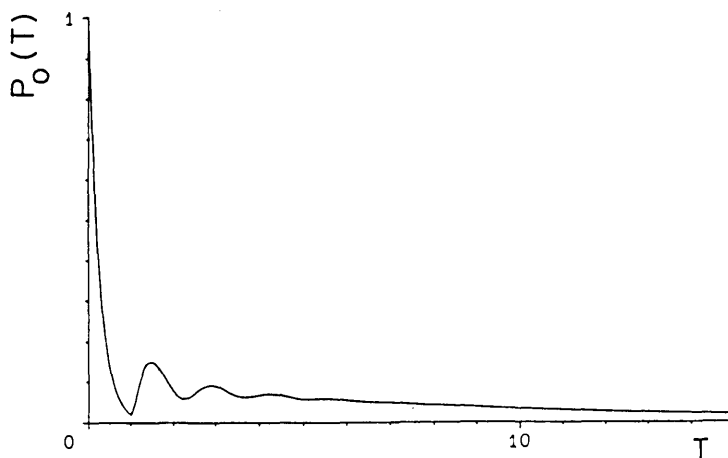


Figure 3.4. As in Figure 3.3 but with $\varphi = 0.3\pi$.

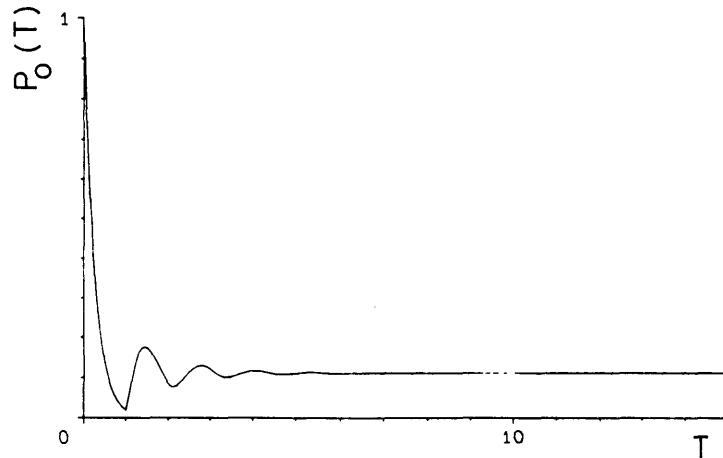


Figure 3.5. As in Figure 3.3 but with $\varphi = \pi/2$.

After the initial decay, the oscillations are clearly visible. For $\varphi = \pi/2$ the trapped value is now 0.111.

To obtain some indication of the value of γ for which we may expect oscillations, we concentrate on the case $\varphi = 0$ for which $a = \gamma e^\gamma$. The behaviour of the solution for $c_0(T)$ is governed by the complex roots of the equation $F(z) = z + ae^{-z} = 0$ (see equation (3.2.11)), the dominant behaviour after the initial decay being due to those roots with the smallest negative real parts (and hence the smallest decay rates). Putting $z = x + iy$ and taking real and imaginary parts in $F(z) = 0$ leads to

$$x + a e^{-x} \cos(y) = 0 \quad (3.3.14a)$$

$$y - a e^{-x} \sin(y) = 0 \quad (3.3.14b)$$

Hence it is possible to have a root with $y = 0$ provided there is an $x (<0)$ for which $-x e^x/a = 1$. The curve of $-x e^x/a$ is highly peaked for $x < 0$ with maximum value $M = (ae)^{-1} = \gamma^{-1} e^{-(\gamma + 1)}$. If $M > 1$, then there are two real negative roots of $F(z) = 0$ (in addition to an infinite number of complex roots) and these roots are those with the smallest negative real parts (a plot of equations (3.3.14) will show this). The dominant behaviour is then exponential decay. If however $M < 1$, then there are no real roots and the dominant behaviour will exhibit oscillations due to the imaginary parts of the dominant roots. The limiting case is therefore $M = 1$ for which $\gamma \approx 0.279$. To further demonstrate this we plot $|c_0(T)|^2$ against T for $\varphi = 0$ with $\gamma = 0.02$ (Figure 3.6) and $\gamma = 5$ (figure 3.7). Note the absence of oscillations in the first and the greater number of oscillations in the second when compared with the case $\gamma = 2$ (Figure 3.3).

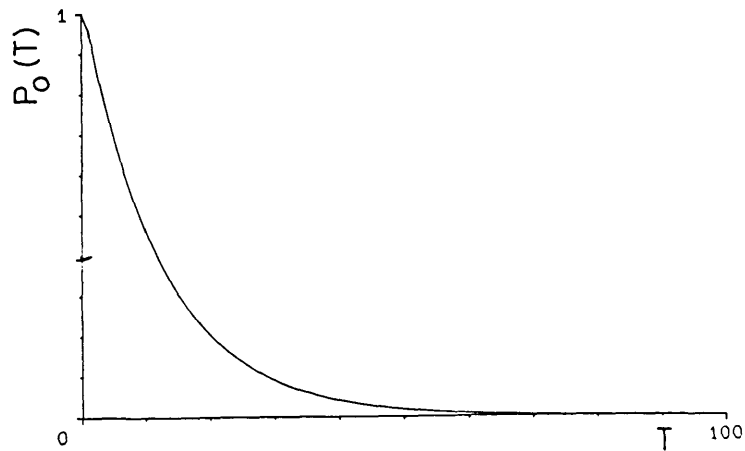


Figure 3.6. The ground-state population as a function of T with $\varphi = 0$ and $\gamma = 0.02$

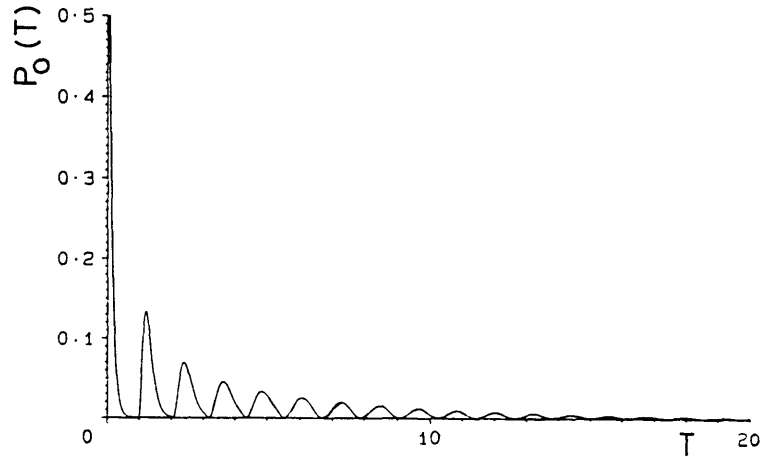


Figure 3.7. As Figure 3.6 but with $\gamma = 5$. For clarity we have expanded the vertical scale. The evolution in the interval $0 \leq T \leq 1$ begins at unity and follows the usual Weisskopf-Wigner decay.

In order to compare the above results with those for a Bixon-Jortner model, we consider the corresponding ground-state occupation amplitude for that case. From eqn.(2.3.19) of chapter two, and Radmore et al. [1987] this amplitude can be written

$$c_o^{BJ}(T) = e^{-(\sigma + \lambda)T} \left(1 - \sum_{n=1}^{\infty} 2\lambda (T - n) L_{n-1}^{(1)}[2\lambda (T-n)] \right) e^{n(\sigma + \lambda)} H(T - n) / n \quad (3.3.15)$$

where $L_{\beta}^{(\alpha)}$ is the generalized Laguerre Polynomial. Here the ground-state is coupled (with constant matrix elements K) to each of the levels of the QC of spacing Δ and is resonant with one of them.

Additionally it is coupled to a true continuum giving a decay rate Γ . In equation (3.2.5) $\lambda = 2\pi^2 \kappa^2 / \Delta^2$ and $\sigma = 2\pi \Gamma / \Delta$. The most obvious comparison between the models can be made if we choose $\sigma = \lambda = \gamma/2$ so that equation (3.3.15) becomes

$$c_o^{BJ}(T) = e^{-\gamma T} \left[1 - \sum_{n=1}^{\infty} \gamma e^{n\gamma} (T-n) L_{n-1}^{(1)}[\gamma(T-n)] H(T-n)/n \right] \quad (3.3.16)$$

In fact this expression is identical to the corresponding result for the structured continuum (equation (3.3.13) with $\varphi = 0$) not only in the initial interval, $0 \leq T \leq 1$, but also in the interval $1 \leq T \leq 2$. This can be seen in Figure 3.8 where we plot $|c_o^{BJ}(T)|^2$ from equation (3.3.16) against T for $\gamma = 5$.

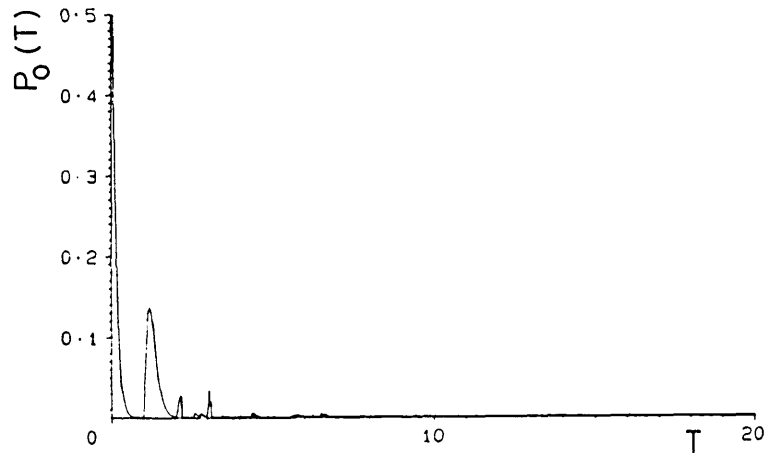


Figure 3.8. The ground-state population as a function of T for the Bixon-Jortner model with decay from the ground-state. We use (3.3.16) with $\gamma = 5$ and plot as in Fig.3.7.

This evolution is to be compared with Figure 3.7: the initial decay and first oscillation are identical after which the difference in the structures of the continua is apparent in the evolution. For the Bixon-Jortner case the oscillations rapidly dephase. The essential difference between the two models is the nature of the irreversible decay. In our Bixon-Jortner model this is simply loss from the ground-state (see the previous chapter and [Radmore et al., 1987]). For the structured continuum, viewed as equally-spaced levels embedded in a true continuum, the decay is indirect.

3.4 Final-State Spectrum

From equations (3.2.3b) and (3.2.4) we have that

$$\tilde{b}_f = \frac{-iV_{f0}}{(s + i\Delta_f)(s + I(s))}. \quad (3.4.17)$$

For all values of φ except $\pi/2$ (the population trapping case), all the zeros of the denominator of this expression, apart from $s = -i\Delta_f$, have negative real parts. Hence the only term on the inversion of \tilde{b}_f which is not exponentially small at large times is that arising from the pole at $s = -i\Delta_f$, giving

$$b_f(\infty) \sim \left. \frac{-iV_{f0} e^{st}}{(s + I(s))} \right|_{s=-i\Delta_f} \quad (3.4.18)$$

Alternatively one could derive this from use of the final-value theorem for Laplace transforms. The Δ_f -dependence of $|b_f(\infty)|^2$ is

therefore, using equations (3.2.6) and (3.2.8),

$$S(x) \propto \frac{\cos^2(x + \varphi)}{\left[x - \frac{\gamma}{2} \sin 2(x + \varphi) \right]^2 + \left[\frac{\gamma}{2} + \frac{\gamma}{2} \cos 2(x + \varphi) \right]^2} \quad (3.4.19)$$

where $x = \pi \Delta_f / \Delta$. We now plot $S(x)$ from equation (3.4.19) against x , ignoring any x -independent multiplicative factor so that the vertical scale is arbitrary. In Figure 3.9, we have chosen $\varphi = 0$ and $\gamma = 0.3$. The symmetric spectrum has a major central peak (where resonance with the ground-state occurs), that accompanies a smooth monotonic leakage of population from $|0\rangle$ to the structured continuum, and has zeros where the dipole matrix elements vanish.

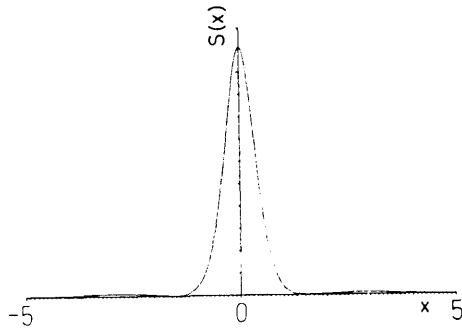


Figure 3.9. The dependence of the final-state spectrum on $x = \pi \Delta_f / \Delta$ for $\varphi = 0$ and $\gamma = 0.3$.

In Figure 3.10, we put $\varphi = 0$ and $\gamma = 2$. The increased coupling has caused the Autler-Townes splitting (see Appendix V) of the central peak, due to the creation of a coherent superposition of ground-state and continuum peak resonance [Makarov et al., 1978]. Note that a "continuum peak resonance" [i.e. a bump, here] is equivalent to a discrete state. For this case of $\varphi = 0$, it is straightforward to calculate the value of γ above which splitting of the central peak occurs, as follows. From equation (3.4.19) we evaluate $W = d^2S/dx^2 \Big|_{x=0}$. If W is negative then $x = 0$ is a maximum and we have a single central peak, whereas if W is positive then $x = 0$ is a minimum between two peaks which have split on either side of $x = 0$. We find that $W = 2(2\gamma - 1) \gamma^{-4}$ so that if $\gamma < 0.5$, we have a single peak and if $\gamma > 0.5$ we have splitting. As γ is increased, the two central peaks are pushed apart and move towards the first positions of zero matrix element. Subsidiary peaks move towards successive zeros.

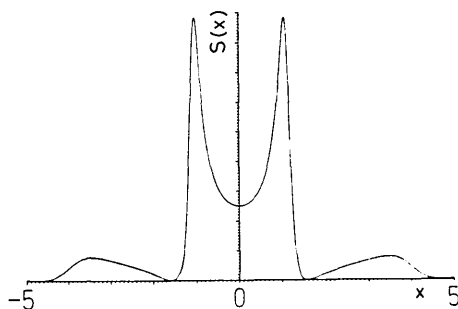


Figure 3.10. As Figure 3.9 but with $\gamma = 2$.

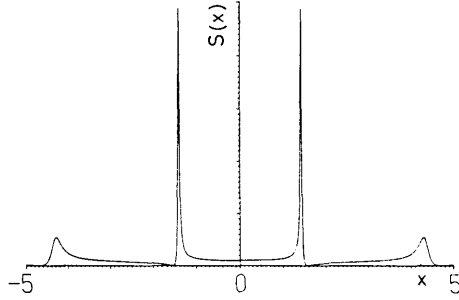


Figure 3.11. As Figure 3.9 but with $\gamma = 10$.

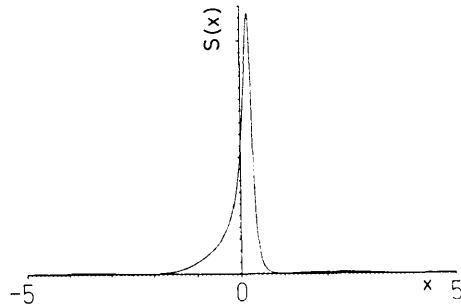


Figure 3.12. The dependence of the final-state spectrum on

$$x = \pi \Delta_f / \Delta \text{ for } \varphi = 0.2\pi \text{ and } \gamma = 0.3.$$

The peaks become narrower and their coincidence with the zeros in the manner of a multiple 'confluence' [Rzazewski & Eberly, 1981; *ibid*, 1983; Deng & Eberly, 1984b] (see also Appendix V), is asymptotic as $\gamma \rightarrow \infty$: by expanding $S(x)$ in equation (3.4.19) with $\varphi = 0$ about, say $x = \pi/2$ (the first zero), we find that a maximum of $S(x)$ occurs less than and within $O(\gamma^{-1})$ of $\pi/2$. We illustrate this by plotting

$S(x)$ for $\varphi = 0$ and $\gamma = 10$ in Figure 3.11. For large enough γ , the second peak of $S(x)$ near $x = 3\pi/2$ is found to be higher than the first peak; increasing γ still further causes the highest peak to occur near successive zeros of $S(x)$.

In Figures 3.12 and 3.13, we plot $S(x)$ for $\gamma = 0.3$ and 2 respectively with $\varphi = 0.2\pi$ to show similar behaviour for an asymmetrical case. Our Figure 3.13 closely resembles the final-state spectrum obtained recently for a double Fano system [Leonski et al. 1987] in which two states are embedded in a flat continuum leading, on diagonalisation, to a structured continuum with two peaks and two zeros.

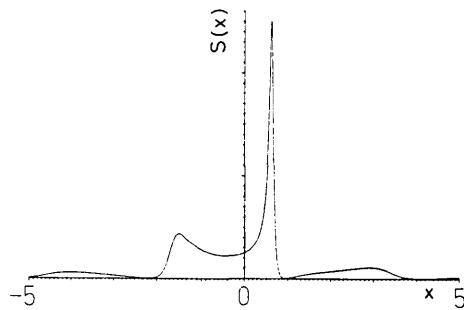


Figure 3.13. As Figure 3.12 but with $\gamma = 2$.

This would be expected since for modest field strengths only the structured continuum states in our model close to the position of resonance are appreciably populated and contribute significantly to the final-state spectrum. In the double Fano system, narrowing of the right-hand Autler-Townes peak occurs as confluence is approached but the left-hand peak is relatively unaltered. This is reflected in our

model also: the left-hand peak moves more slowly towards confluence than does the right-hand peak. The q-reversal effect discovered by Connerade and others [Connerade et al., 1985; Connerade and Lane, 1987] (see also Appendix V), is also observed in our spectra.

In the case $\varphi = \pi/2$, for which population trapping occurs, the expression for \bar{b}_f in equation (3.4.17) has two poles with zero real parts. One is at $s = -i\Delta_f$ as before and in addition there is the pole at $s = 0$ which gives rise to the trapping ($I(0) = 0$ for $\varphi = \pi/2$). Hence we cannot use a straightforward application of the final value theorem which would involve calculating the limit of $(s + i\Delta_f)\bar{b}_f$ as $s \rightarrow -i\Delta_f$. Instead

$$b_f(\infty) \sim -iV_{f0} \left[\frac{e^{-i\Delta_f t}}{-i\Delta_f + I(-i\Delta_f)} + \frac{1}{i\Delta_f (1 + \gamma)} \right] \quad (3.4.20)$$

the first term arising from the residue at $s = -i\Delta_f$, the second from that at $s = 0$ (we have used $dI/ds \Big|_{s=0} = \gamma$.) In this case there is no time-independent limit of $|b_f|^2$ as $t \rightarrow \infty$, its dependence on x and T being

$$S(x, T) \propto \sin^2 x \left| \frac{e^{-2ixT}}{x + i\gamma (1 - e^{2ix})/2} - \frac{1}{x (1 + \gamma)} \right| \quad (3.4.21)$$

For large T , the population at a general position x in the structured continuum will exhibit rapid oscillations with T as population is continually redistributed amongst the continuum states via the ground-state, although the integral of $|b_f(\infty)|^2$ over all continuum

states yields the value $1 - |c_0(\infty)|^2$, the 'untrapped' population. Oscillations with T are observed in

$$f_L(T) = \int_{-L}^L S(x,T) dx$$

for finite L and these decrease in amplitude as L is increased, $f_L(T)$ tending to a constant as $L \rightarrow \infty$.

3.5 Summary

We have studied a simple analytically soluble model of a periodically structured continuum. The population dynamics has a number of features in common with the Bixon-Jortner model, for example the interruptions caused by the strictly periodic nature of the continuum in question. We emphasize the use of such simple models to investigate the origin of properties which may be apparent in more complicated systems. In particular, the behaviour of confluences of coherence in the final-state spectrum and the corresponding dressed states for the system are of current interest.

CHAPTER FOUR

DRESSED STATES AND SPECTRAIN QUASICONTINUUM EXCITATION4.1 Introduction

In this chapter, the system we consider consists of a ground state coupled to a general QC of levels and to a true continuum. We examine the spectrum of final states in the true continuum. This spectrum can exhibit zeros, the positions of which are determined by the energies of the QC levels and the existence of which is determined by initial conditions. We obtain a general expression (for any QC) of the true continuum spectrum and consider the special cases of first a Bixon-Jortner QC and second, a Rydberg series. We then study the dressed states [Agassi & Eberly, 1986; Fano, 1961; Coleman & Knight, 1982] for the whole system and derive 'sparse' dressed states which contain few continuum levels and, more importantly, no contribution from the ground state. We show that the initial population in one of these sparse dressed states determines the existence of the corresponding zero in the spectrum. This is a similar mechanism to population trapping in certain systems [Radmore, 1982; Radmore & Knight, 1982] where population initially in a dressed state is immune to photoionisation. In section 4.2 we derive a general expression for the spectrum. Section 4.3 discusses the special cases with particular reference to the initial conditions. The two-photon ionisation

problem discussed by Knight [1979] is also seen as a special case of our general treatment. In section 4.4 we discuss the total dressed states and explain the observed features using the sparse dressed states.

4.2 Basic Equations

The system under consideration is that shown in Figure 4.1 where a single discrete state $|0\rangle$ is coupled to both a true continuum of discrete states ($|f\rangle$) and a quasicontinuum of discrete states ($|b\rangle$).

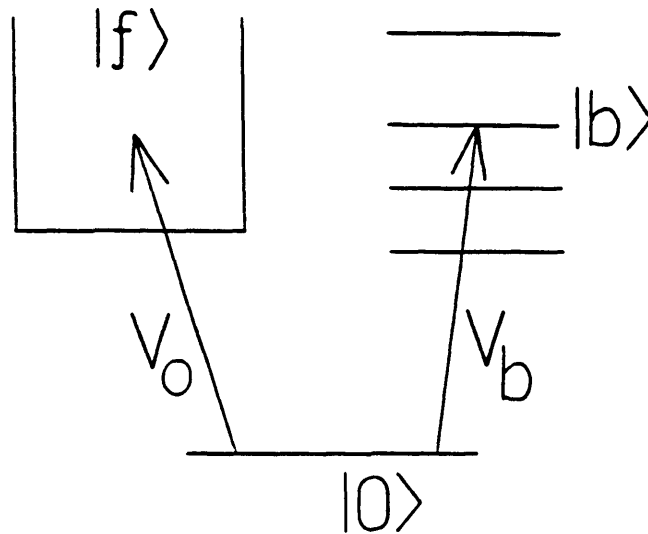


Figure 4.1. The level scheme with the ground state coupled to an arbitrary QC and to a true continuum.

For simplicity we take the matrix element between $|0\rangle$ and any state $|f\rangle$ to be V_0 (independent of f); that between $|0\rangle$ and state $|b\rangle$ is denoted V_b . A special case is the extended Bixon-Jortner model which we have studied in chapter two [Radmore et al., 1987]. The equations of motion for the probability amplitudes $c_0(t)$, $c_f(t)$ and $c_b(t)$

corresponding to states $|0\rangle$, $|f\rangle$ and $|b\rangle$ are, in R. W. A.

$$\dot{c}_o = -i \sum_b V_b c_b e^{-i\Delta_{ob}t} - i \int_f V_o c_f e^{-i\Delta_{of}t} \quad (4.2.1)$$

$$\dot{c}_b = -iV_b c_o e^{i\Delta_{ob}t} \quad (4.2.2)$$

$$\dot{c}_f = -iV_o c_o e^{i\Delta_{of}t} \quad (4.2.3)$$

where Δ_{ob} and Δ_{of} are the detunings between $|0\rangle$ and $|b\rangle$ and between $|0\rangle$ and $|f\rangle$ respectively. We now put

$$c_b e^{-i\Delta_{ob}t} = a_b \quad , \quad c_f e^{-i\Delta_{of}t} = a_f \quad (4.2.4)$$

so that (4.2.1)-(4.2.3) become

$$\dot{c}_o = -i \sum_b V_b a_b - i V_o \int_f a_f \quad (4.2.5)$$

$$\dot{a}_b = -i\Delta_{ob} a_b - iV_b c_o \quad (4.2.6)$$

$$\dot{a}_f = -i\Delta_{of} a_f - iV_f c_o \quad (4.2.7)$$

To solve these equations, we Laplace transform (with variable s) and take general initial conditions for the discrete states:

$$c_o(0) = A \quad , \quad a_b(0) = B_b \quad , \quad a_f(0) = 0. \quad (4.2.8)$$

Equations (4.2.5)-(4.2.7) become

$$s\tilde{c}_o - A = -i\Sigma_b V_b \tilde{a}_b - iV_o \int_f \tilde{a}_f \quad (4.2.9)$$

$$(s + i\Delta_{ob}) \tilde{a}_b - B_b = -iV_o \tilde{c}_o \quad (4.2.10)$$

$$(s + i\Delta_{of}) \tilde{a}_f = -iV_o \tilde{c}_o \quad (4.2.11)$$

where tilde denotes the Laplace transform. Using the final-value theorem in (4.2.11) gives

$$a_f(\infty) = -iV_o \tilde{c}_o(s - -i\Delta_{of}) \quad (4.2.12)$$

so that we require \tilde{c}_o to find the final-state spectrum. Substituting for \tilde{a}_b and \tilde{a}_f in (4.2.9) using (4.2.10) and (4.2.11) gives

$$s\tilde{c}_o - A = -i\Sigma_b V_b (B_b - iV_b \tilde{c}_o) / (s + i\Delta_{ob}) - V_o^2 \tilde{c}_o \int_f (s + i\Delta_{of})^{-1} \quad (4.2.13)$$

Assuming the states $(|f\rangle)$ form a true infinite continuum of density $1/\delta$, then

$$\int_f (s + i\Delta_{of})^{-1} = \pi/\delta \quad (4.3.14)$$

Using (4.2.14) and rearranging in (4.2.13) to find \tilde{c}_o , we have

$$\tilde{c}_0 = \frac{A - i \sum_b V_b B_b / (s + i\Delta_{ob})}{s + \gamma + \sum_b V_b^2 / (s + i\Delta_{ob})} \quad (4.2.15)$$

where $\gamma = \pi V_0^2 / \delta$. From (4.2.15) the final-value theorem result (4.2.12) can be written

$$a_f^{(\infty)} = \frac{-i V_0 \left[A + \sum_b V_b B_b / (\Delta_{of} - \Delta_{ob}) \right]}{-i \Delta_{of} + \gamma + i \sum_b V_b^2 / (\Delta_{of} - \Delta_{ob})} \quad (4.2.16)$$

so that the spectrum of true continuum final states is

$$|a_f^{(\infty)}|^2 = \frac{V_0^2 \left[A + \sum_b V_b B_b / (\Delta_{of} - \Delta_{ob}) \right]^2}{\gamma^2 + \left[\Delta_{of} - \sum_b V_b^2 / (\Delta_{of} - \Delta_{ob}) \right]^2} \quad (4.2.17)$$

In the next section we shall examine particular quasicontinua and their associated spectra using the general result above.

4.3 Specific Quasicontinua

(a) The Bixon-Jortner Quasicontinuum

In this case we assume that one of the levels $|b\rangle$ is resonantly coupled to $|0\rangle$ and that $\Delta_{ob} = b \Delta$ where b is an integer [Bixon & Jortner, 1968], $-\infty < b < \infty$ and $V_b = V_1$ (constant). Then

$$\sum_b (\Delta_{of} - \Delta_{ob})^{-1} = \frac{\pi}{\Delta} \cot \left[\frac{\pi \Delta_{of}}{\Delta} \right] \quad (4.3.18)$$

initial conditions:

(i) $C_o(0) = 1$, $c_b(0) = 0$ (so that $A = 1$, $B_b = 0$).

From (4.2.17) we have

$$|a_f(\omega)|^2 = \frac{V_o^2}{\gamma^2 + \left[\Delta_{of} - \frac{\pi}{\Delta} V_1^2 \cot \left[\frac{\pi}{\Delta} \Delta_{of} \right] \right]^2} \quad (4.3.19)$$

and for convenience put

$$F = \pi^2 V_o^2 / \Delta^2, \quad G = \pi^2 \gamma^2 / \Delta^2, \quad H = \pi^2 V_1^2 / \Delta^2 \quad (4.3.20)$$

and $x = \pi \Delta_{of} / \Delta$. The resulting spectrum is

$$S_1(x) = \frac{F \sin^2(x)}{(x \sin(x) - H \cos(x))^2 + G \sin^2(x)} \quad (4.3.21)$$

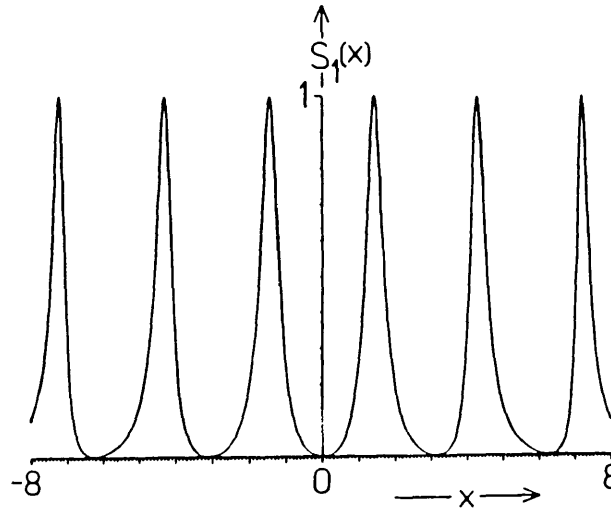


Figure 4.2. The spectrum $S_1(x)$ from equation (4.3.21) for

$$V_o = V_1 = \gamma = \Delta = 1 \text{ (Bixon-Jortner QC.)}$$

In Figure 4.2 we plot this spectrum as a function of x for $V_0 = V_1 = \gamma = \Delta = 1$. The spectrum has zeros corresponding to the positions of the energies of the Bixon-Jortner levels. This may be thought of as a 'multiple hole' in the same manner as that studied by Knight [1979] in two-photon ionisation. His results can, of course, be retrieved by replacing the QC by a single level. The origin of these zeros (or holes) can be described by reference to dressed states for the whole system which we discuss in section 4.4.

In Figure 4.3 we plot $S_1(x)$ from (4.3.21) as a function of x for $V_0 = \gamma = \Delta = 1$ as before but with $V_1 = 0.1$, so that the Bixon-Jortner levels non-resonant with $|0\rangle$ are only weakly coupled.

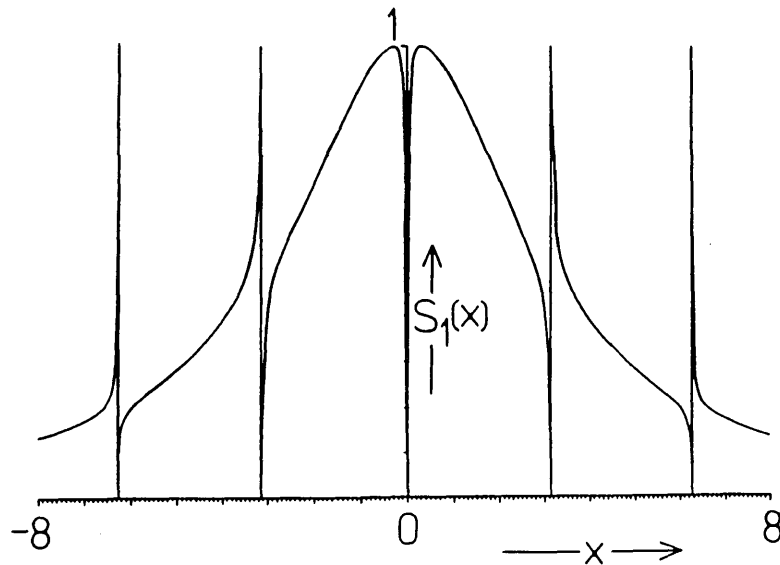


Figure 4.3. The spectrum $S_1(x)$ from equation (4.3.21) for

$$V_0 = \gamma = \Delta = 1, V_1 = 0.1 \text{ (Bixon-Jortner QC)}.$$

The spectrum has an underlying Lorentzian structure (a single state is strongly coupled to the true continuum) with a narrow hole at $x = 0$, as would be expected from the calculations of Knight [1979]; in

addition there are the zeros at the energy positions of the Bixon-Jortner levels and the approach to multiple confluences [Rzążewski & Eberly, 1981; *ibid*, 1983; Deng & Eberly, 1984b]. We note here that the peaks all have the same height for the spectrum $S_1(x)$ in (4.3.21) since they occur where $x \sin(x) = H \cos(x)$ and $S_1(x)$ then has value F/G ($= 1$ in Figures 4.2 & 4.3).

(ii) $c_o(0) = 0$, $c_{b=N}(0) = 1$, $c_{b \neq N}(0) = 0$ (so that $A = 0$, $B_N = 1$, $B_{b \neq N} = 0$.)

Here we begin with all the population in one of the Bixon-Jortner levels $b=N$, where $N = 0, \pm 1, \pm 2, \dots$. In this case

$$|a_f(\infty)|^2 = \frac{V_o^2 V_1^2}{(\Delta_{of} - N\Delta)^2 \left[\gamma^2 + \left[\Delta_{of} - \frac{\pi V_1^2}{\Delta} \cot \left[\frac{\pi \Delta_{of}}{\Delta} \right] \right]^2 \right]} \quad (4.3.22)$$

so that using the same notation as before, in (4.2.20),

$$S_2(x) = \frac{F H \sin^2 x}{(x - N\pi)^2 \left[(x \sin(x) - H \cos(x))^2 + G \sin^2 x \right]} \quad (4.3.23)$$

Note that the existence of population initially in level $|b = N\rangle$ of the QC generates a factor $(x - N\pi)^2$ which will cancel the corresponding zero (of the factor $\sin^2 x$ at $x = N\pi$) at the position of this Bixon-Jortner level in the same manner as at a confluence [Rzążewski & Eberly, 1981; *ibid*, 1983; Deng & Eberly, 1984b]. We shall describe this feature again in section 4.4. In Figure 4.4, we plot $S_2(x)$ against x for $V_o = V_1 = \gamma = \Delta = 1$ and $N = 0$.

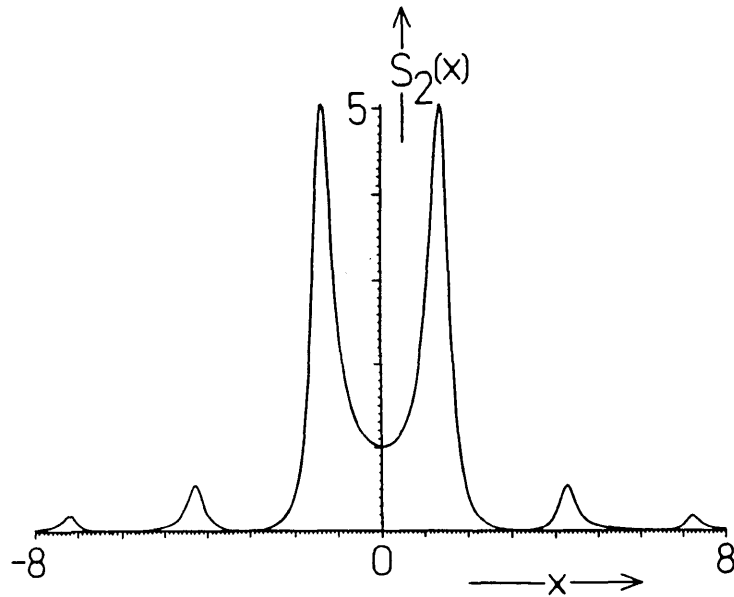


Figure 4.4. The spectrum $S_2(x)$ from equation (4.3.23) for $V_0 = V_1 = \gamma = \Delta = 1$, $N = 0$ (Bixon-Jortner QC).

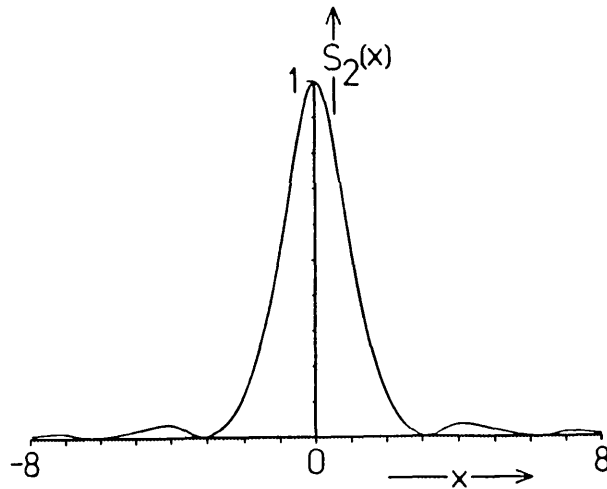


Figure 4.5. The spectrum $S_2(x)$ from equation (4.3.23) for $V_0 = V_1 = \Delta = 1$, $N = 1$ & $\gamma = 4$ (Bixon-Jortner QC).

The zero at $x = 0$ has been removed and the spectrum retains the pair of central peaks from Figure 4.2, arising from the strongly coupled states $|0\rangle$ and $|b=0\rangle$. If we decrease the coupling V_1 or increase γ , we should see the two peaks merge into a single central peak. To

illustrate the effect of large γ , we plot $S_2(x)$ against x for $V_0 = V_1 = \Delta = 1$, $N = 0$ and $\gamma = 4$ in Figure 4.5. A single peak is observed, but note that the other zeros persist. In Figure 4.6 we again choose $V_0 = V_1 = \Delta = 1$, but put $N = 1$ to show an asymmetric spectrum. Now the zero corresponding to $x = \pi$ at the energy position $|b=1\rangle$ has been removed.

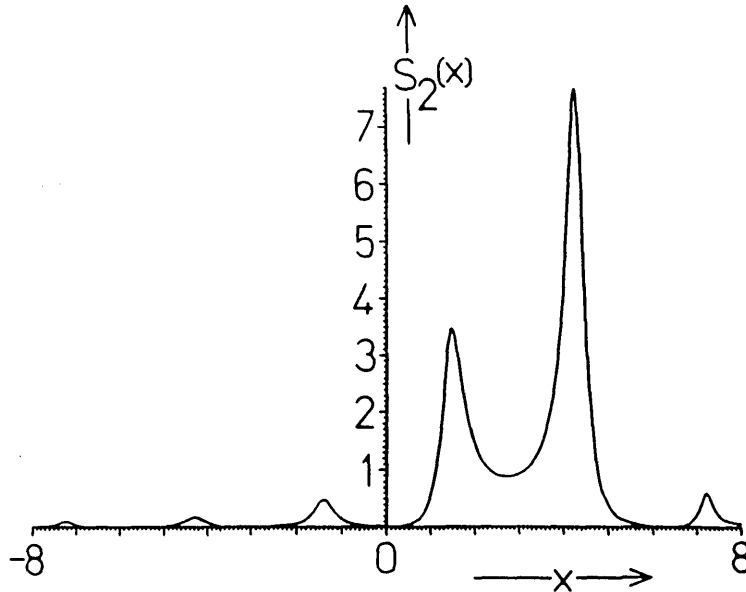


Figure 4.6. The spectrum $S_2(x)$ from equation (4.3.23) for $V_0 = V_1 = \Delta = \gamma = N = 1$ (Bixon-Jortner QC).

(b) Rydberg Series

We take $(|b\rangle)$ to be the levels of a Rydberg series $|n\rangle$ with the level $|n=N\rangle$ resonantly coupled to the discrete state $|0\rangle$. The detunings are

$$\Delta_{on} = D \left[1 - \frac{N^2}{n^2} \right] \quad (4.3.24)$$

and the initial conditions $c_o(0) = 1$, $c_n(0) = 0$ and $c_f(0) = 0$ to begin

with. Hence in (4.2.17), $A = 1$ and $B_b = 0$ and the spectrum is

$$S_1(y) = \frac{P}{Q + [\pi y - \theta(y)]^2} \quad (4.3.25)$$

where

$$P = \pi^2 V_o^2 / D^2, \quad Q = \pi^2 \gamma^2 / D^2, \quad y = \Delta_{of}/D \quad (4.3.26)$$

and

$$\theta(y) = \frac{\pi}{D^2} \sum_{n=1}^{\infty} \frac{V_n^2}{y - 1 + (N^2/n^2)} \quad (4.3.27)$$

Taking the matrix elements to be

$$V_n^2 = V^2/n^3 \quad (4.3.28)$$

we may write (4.3.27) as

$$\theta(y) = R \sum_{n=1}^{\infty} \frac{1}{n [n^2(y-1) + N^2]} \quad (4.3.29)$$

where

$$R = \pi V^2 / D^2 \quad (4.3.30)$$

The function $\theta(y)$ can be evaluated in closed form in terms of digamma functions [Abramowitz & Stegun, 1972]. We plot $S_1(y)$ from (4.3.25) against y in Figure 4.7 for $P = Q = R = N = 1$.

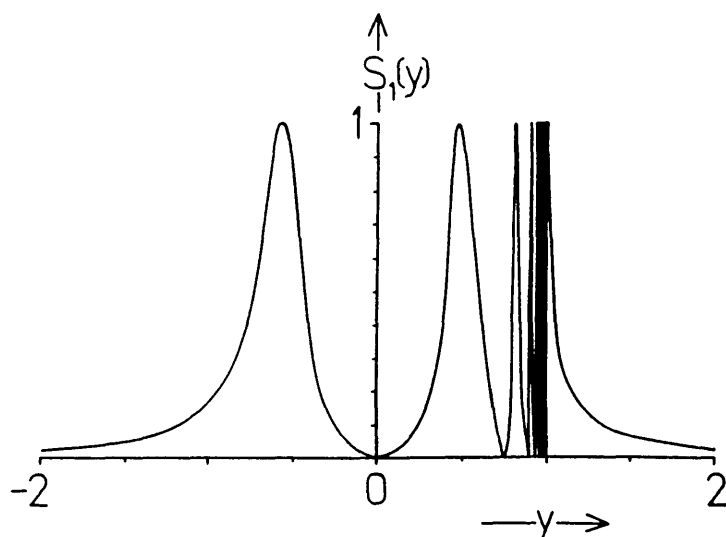


Figure 4.7. The spectrum $S_1(y)$ from equation (4.3.25) for $P = Q = R = N = 1$ (Rydberg QC).

Note that there is a zero in the spectrum at each position of a Rydberg level ($y = 1 - n^{-2} = 0, 3/4, 8/9, 15/16, \dots$). The zeros end at $y = 1$ which corresponds to the upper limit of the Rydberg series and crowd together as y tends to 1 from below as expected [Connerade et al., 1985; Connerade & Lane, 1987].

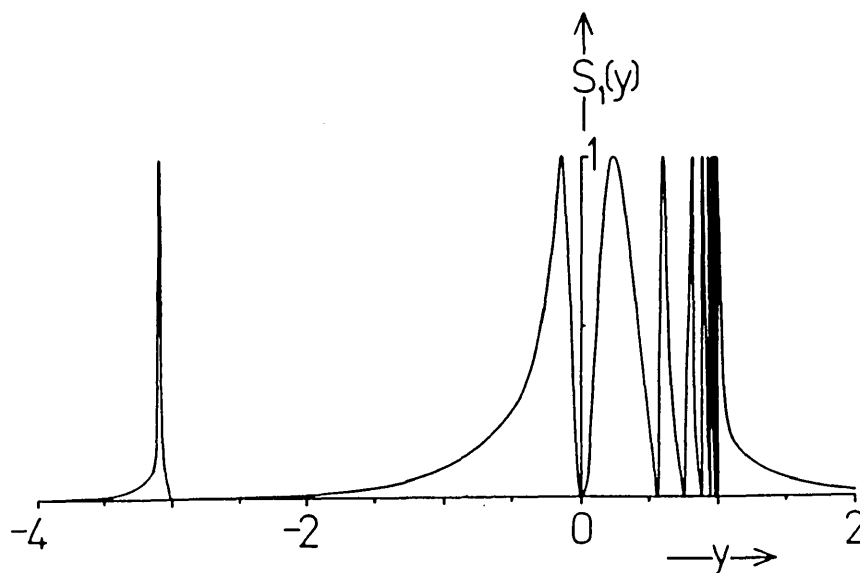


Figure 4.8. The spectrum $S_1(y)$ from equation (4.3.25) for $P = Q = R = 1, N = 2$ (Rydberg QC).

In Figure 4.8 we plot $S_1(y)$ against y with $P = Q = R = 1$ but choose $N = 2$ (and note that the zeros now occur at $y = 1 - (4n^{-2}) = -3, 0, 5/9, 3/4, 21/25, 8/9, \dots$).

The zeros of $S_1(y)$ in (4.2.25) originate from the divergences in $\theta(y)$ at the positions of the Rydberg levels. We can see from (4.2.17) that if initial conditions were chosen with all the population in one Rydberg level N ($A = 0, B_N = 1$), then the divergence in the denominator of (4.2.17) at that place is matched by that of the single term in the numerator. Hence the zero in the spectrum corresponding to the populated Rydberg level is removed and the y -dependence of the spectrum is for $N = 1$

$$S_2(y) \propto \left[y^2 \left[Q + \left[\pi y - \theta(y) \right]^2 \right] \right]^{-1} \quad (4.3.31)$$

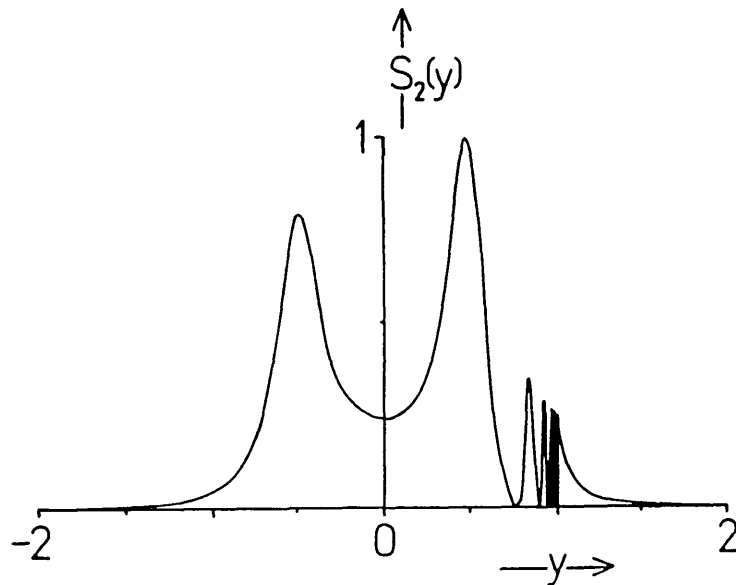


Figure 4.9. The spectrum $S_2(y)$ from equation (4.3.31) for $Q = R = N = 1$ normalised to unit height (Rydberg QC).

We illustrate this in Figure 4.9 by plotting this spectrum normalised to unit height with $Q = R = N = 1$. Note the absence of the zero at $y = 0$ corresponding to the $n = 1$ Rydberg level.

It is also instructive to consider a Rydberg-like series where the detunings are as above (4.3.24), but the matrix elements are taken to be

$$v_n^2 = v^2/n^2 \quad (4.3.32)$$

instead of (4.3.28). With this choice

$$\theta(y) = R \sum_{n=1}^{\infty} \frac{1}{n^2(y-1) + N^2} \quad (4.3.33)$$

This series can be summed analytically in terms of the coth function but we do not specifically need the expression here. With $\theta(y)$ as in (4.3.33), we plot $S_1(y)$ from (4.3.25) in Figure 4.10 with $P = Q = R = N = 1$ and compare this with Figure 4.7.

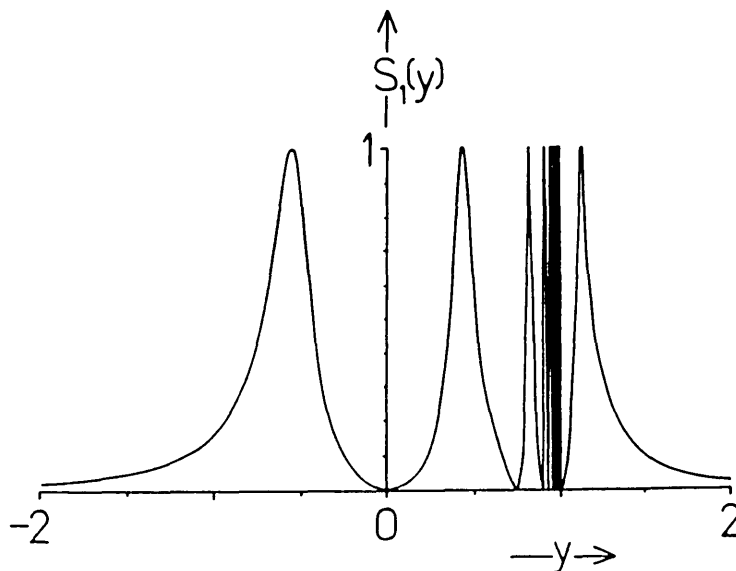


Figure 4.10. The spectrum $S_1(y)$ from equation (4.3.25) with $\theta(y)$ given by (4.3.33) and $P = Q = R = N = 1$ (Rydberg-like QC). This is to be compared with Figure 4.7.

The two spectra are very similar: the zeros occur at the same positions in both. The particular form of the matrix elements does not affect these zeros but the peaks differ slightly in position and shape in the two figures. Again, a particular zero can be removed by initially populating the corresponding QC level.

In the next section we discuss the dressed states for the total system with a general QC and explain the above features in the spectra.

4.4 Dressed States

We now discuss the dressed states for the whole system in Figure 4.1 in order to more fully account for the features in the spectra of section 4.3. With labels 0 and 1 to denote the fields driving the $|0\rangle$ to $|f\rangle$ and zero to $|b\rangle$ transitions respectively, with photon numbers n_0 and n_1 , we write

$$|i\rangle = |0, n_0, n_1\rangle \quad (4.4.34)$$

$$|k\rangle = |f, n_0-1, n_1\rangle \quad (4.4.35)$$

$$|l\rangle = |b, n_0, n_1-1\rangle \quad (4.4.36)$$

The states have energies, say, E_i , E_k , and E_l . We wish to find eigenstates of the total Hamiltonian

$$\hat{H} = \hat{H}_0 + \sum_l \hat{V}_{il} + \sum_k \hat{W}_{ik} \quad (4.4.37)$$

where $\hat{H}_0|i\rangle = E_i|i\rangle$, and similarly for $|k\rangle$ and $|l\rangle$. The sums represent the possible couplings between $|i\rangle$ and any of the states

$|1\rangle$, in the case of \hat{V}_{i1} , and between $|i\rangle$ and any of the states $|k\rangle$, in the case of \hat{W}_{ik} . We require $|\epsilon\rangle$ where $\hat{H} |\epsilon\rangle = \epsilon |\epsilon\rangle$, and expand $|\epsilon\rangle$ in terms of the basis states (4.4.34)-(4.4.36):

$$|\epsilon\rangle = P(\epsilon)|i\rangle + \sum_1 Q_1(\epsilon)|1\rangle + \int dk c_k(\epsilon) |k\rangle \quad (4.4.38)$$

The procedure is similar to that adopted by Fano and by Coleman et al. [Fano, 1961; Coleman & Knight, 1982; Coleman et al., 1982]: taking matrix elements of the eigenvalue equation for $|\epsilon\rangle$ with each of (4.4.34) to (4.4.36) in turn gives

$$(E_i - \epsilon)P(\epsilon) + \sum_1 Q_1(\epsilon)V_{i1} + \int dk c_k(\epsilon) W_{ik} = 0 \quad (4.4.39)$$

$$(E_1 - \epsilon) Q_1(\epsilon) + P(\epsilon) V_{i1} = 0 \quad (4.4.40)$$

$$(E_k - \epsilon) c_k(\epsilon) + P(\epsilon) W_{ik} = 0 \quad (4.4.41)$$

The sensitivity of the zeros in the spectra to initial conditions arises because of the existence of special dressed states, namely states which contain no contribution from $|i\rangle$, so that if all atomic population begins in $|i\rangle$, then these dressed states are initially unpopulated. We first find these states. For them to exist, there must be values of ϵ , $\bar{\epsilon}$ say, such that $P(\bar{\epsilon}) = 0$ (see (4.4.38)). Hence from (4.4.40) we have

$$(E_1 - \bar{\epsilon}) Q_1(\bar{\epsilon}) = 0 \quad (4.4.42)$$

Note that (4.4.42) is a set of equations, one for each l . Now not all the $Q_l(\bar{\epsilon})$ are zero (otherwise the dressed state contains no continuum states) so the only possibility is that $\bar{\epsilon}$ equals one particular E_l and that the corresponding $Q_l(\bar{\epsilon})$ is the only non-zero one. We therefore have a set of possible solutions for $\bar{\epsilon}$, namely any of the energies of the QC levels (the positions where the zeros appear in the spectra). We conclude that there are as many of these 'sparse' dressed states containing no contribution from $|i\rangle$ as there are QC levels and that their energies are those of QC levels. To find these states, we first use (4.4.40)

$$Q_l(\epsilon) = \frac{V_{il} P(\epsilon)}{\epsilon - E_l} \quad (4.4.43)$$

From (4.4.41), since E_k is a continuous variable [Fano, 1961; Coleman & Knight, 1982; Coleman et al., 1982],

$$c_k(\epsilon) = P(\epsilon) W_{ik} \left[\mathcal{P} \frac{1}{\epsilon - E_k} + R(\epsilon) \delta(\epsilon - E_k) \right] \quad (4.4.44)$$

where \mathcal{P} denotes the principal part and $R(\epsilon)$ must be found self-consistently. Substituting (4.4.43) and (4.4.44) into (4.4.39) gives

$$(E_i - \epsilon)P(\epsilon) + \sum_l \frac{V_{il}^2 P(\epsilon)}{\epsilon - E_l} + \int dk P(\epsilon) W_{ik}^2 \left[\mathcal{P} \frac{1}{\epsilon - E_k} + R(\epsilon) \delta(\epsilon - E_k) \right] = 0 \quad (4.4.45)$$

This must be true for all ϵ , so that cancelling $P(\epsilon)$ gives

$$E_i - \epsilon + \sum_1 \frac{V_{i1}^2}{\epsilon - E_1} + \mathcal{O} \int dk \frac{W_{ik}^2}{\epsilon - E_k} + R(\epsilon) W_{i\epsilon}^2 = 0 \quad (4.4.46)$$

where $W_{i\epsilon}$ means that value of W_{ik} such that E_k equals the chosen ϵ .

Hence

$$R(\epsilon) = \frac{1}{W_{i\epsilon}^2} \left[\epsilon - E_i - \sum_1 \frac{V_{i1'}^2}{\epsilon - E_{1'}} - \mathcal{O} \int dk \frac{W_{ik}^2}{\epsilon - E_k} \right] \quad (4.4.47)$$

From (4.4.44), we find that

$$c_k(\epsilon - E_1) = \lim_{\epsilon \rightarrow E_1} W_{ik} P(\epsilon) R(\epsilon) \delta(\epsilon - E_k) \quad (4.4.48)$$

Combining (4.4.47) and (4.4.48), we notice that as $\epsilon \rightarrow E_1$, $P(\epsilon)$ tends to zero whereas $R(\epsilon)$ diverges. The only term which contributes therefore is

$$c_k(\epsilon - E_1) = \frac{W_{ik} \delta(E_1 - E_k)}{W_{i1}^2} \lim_{\epsilon \rightarrow E_1} \left[-P(\epsilon) \sum_1 \frac{V_{i1'}^2}{\epsilon - E_{1'}} \right] \quad (4.4.49)$$

where W_{i1} means W_{ik} for that value of k such that $E_k = E_1$. Again only one term in the sum in (4.4.49) will contribute

$$c_k(\epsilon - E_1) = \frac{-W_{ik} \delta(E_1 - E_k)}{W_{i1}^2} \lim_{\epsilon \rightarrow E_1} \left[P(\epsilon) \frac{V_{i1}^2}{\epsilon - E_1} \right] \quad (4.4.50)$$

Substituting for $P(\epsilon)/(\epsilon - E_1)$ in (4.4.50) using (4.4.43), we find finally

$$c_k(\epsilon - E_1) = \frac{-W_{ik}}{W_{i1}^2} V_{i1} Q_1(\epsilon = E_1) \delta(E_1 - E_k) \quad (4.4.51)$$

The dressed state $|\epsilon = E_1\rangle$ is therefore, from (4.4.38),

$$\begin{aligned} |\epsilon = E_1\rangle = & Q_1(E_1) |1\rangle + \int dk c_k(\epsilon - E_1) |k\rangle \\ & - Q_1(E_1) \left[|1\rangle - \frac{V_{i1}}{W_{i1}} |s_1\rangle \right] \end{aligned} \quad (4.4.52)$$

where $|s_1\rangle$ means that continuum state $|k\rangle$ with energy equal to the chosen QC energy E_1 . We therefore have a set of sparse dressed states, as many as there are QC states, each of which contains contributions only from a particular QC state and the true continuum state that is two-photon resonant with that QC state. This is a similar situation to that encountered in other systems with two-photon resonance, for example three-level systems and other multi-level systems [Radmore & Knight, 1982; Radmore, 1982], where population trapping results. In the present system, if the population is initially in $|i\rangle$, then the sparse dressed states are unpopulated initially; zeros appear in the spectrum at places corresponding to the energies of these $|i\rangle$ -independent states. If however we populate one of these states initially then the corresponding zero is removed.

Hence we anticipate that the population in the true continuum states at the special positions should contain a non-vanishing term for long times that is proportional to the initial sparse dressed state population. We now show that this is the case.

The total wavefunction would be

$$|\Psi\rangle = \int A(\epsilon) e^{-i\epsilon t} |\epsilon\rangle d\epsilon \quad (4.4.53)$$

so that

$$\langle s_1 | \Psi \rangle = \int A(\epsilon) e^{-i\epsilon t} c_{s_1}(\epsilon) d\epsilon \quad (4.4.54)$$

Now

$$c_{s_1}(\epsilon) = P(\epsilon) W_{i1} \left[\mathcal{P} \frac{1}{\epsilon - E_1} + R(\epsilon) \delta(\epsilon - E_1) \right] \quad (4.4.55)$$

Using the expression for $R(\epsilon)$, (4.4.47) in (4.4.55),

$$c_{s_1}(\epsilon) = P(\epsilon) W_{i1} \mathcal{P} \frac{1}{\epsilon - E_1} + P(\epsilon) \frac{W_{i1}}{W_{i\epsilon}^2} \delta(\epsilon - E_1) \\ \times \left[\epsilon - E_i - \sum_{l'} \frac{V_{il'}^2}{\epsilon - E_{l'}} - \mathcal{P} \int dk \frac{W_{ik}^2}{\epsilon - E_k} \right] \quad (4.4.56)$$

Substituting (4.4.56) into (4.4.54) we find

$$\begin{aligned}
\langle s_1 | \Psi \rangle &= W_{i1} \mathcal{P} \int_{-\infty}^{\infty} \frac{P(\epsilon) A(\epsilon)}{\epsilon - E_1} e^{-i\epsilon t} d\epsilon \\
&= \frac{1}{W_{i1}} A(E_1) e^{-iE_1 t} V_{i1}^2 \lim_{\epsilon \rightarrow E_1} \frac{P(\epsilon)}{\epsilon - E_1} \quad (4.4.57)
\end{aligned}$$

Again using the expression for $P(E)/(\epsilon - E_1)$ from (4.4.40) in (4.4.57) and taking modulus squared, we have the population in the true continuum state $|s_1\rangle$ is

$$\begin{aligned}
|\langle s_1 | \Psi \rangle|^2 &= \left| A(E_1) Q_1(E_1) \frac{V_{i1}}{W_{i1}} \right. \\
&\quad \left. - \frac{W_{i1}}{V_{i1}} e^{iE_1 t} \int_{-\infty}^{\infty} Q_1(\epsilon) A(\epsilon) e^{-i\epsilon t} d\epsilon \right|^2 \quad (4.4.48)
\end{aligned}$$

If $|\Psi(t=0)\rangle = |i\rangle$ then $A(E_1) = 0$ and we know that $|\langle s_1 | \Psi \rangle|^2 \rightarrow 0$ as $t \rightarrow \infty$. If $|\Psi(t=0)\rangle = |l'\rangle$ then $A(E_1) \neq 0$ and the first term on the right-hand side of (4.4.58) is non-zero. At long times the expression tends to a constant and the zero in the spectrum is removed.

4.5 Conclusions

We have shown how sparse dressed states containing contributions from a limited number of continuum levels are responsible for the appearance of zeros in our model QC problem. The existence of the zeros is determined by the initial populations in these sparse dressed states. We stress that the treatment is valid for a general QC so that the positions of the zeros follow the distribution of QC levels.

In the Rydberg example, this results in a successively narrower gap between adjacent zeros as the Rydberg levels crowd together at the top of the series. The matrix elements in the case of the Rydberg-like series we considered do not therefore affect the positions of the zeros. Note that we assumed the continuum to have no threshold, so as a result there is no Stark shift to the ground state; (however an energy-varying continuum with no threshold does give a shift.) These calculations indicate how clear the features of certain resonantly coupled multi-level problems may become when a dressed treatment is adopted. The consideration of Rydberg-like series was instructive, because it gave a closed-form analytical solution, and highlighted the fact that the zeros are independent of the matrix elements so long as the relevant sum (eqn. (4.3.33)) converges.

CHAPTER FIVE

THE INVERTED HARMONIC OSCILLATOR:SOME STATISTICAL PROPERTIES.5.1 Introduction

There has been much recent interest in optical amplification. Early hopes of cloning photons by stimulated emission were confounded, when it was shown that the amplifier instead acts as a source of noise, statistically independent of the input field [Wootters & Zurek, 1983; Heidmann & Reynaud, 1984]. It was shown that both linear amplification and linear damping in a quantal system coexist with external noise fluctuations; (see [Caves, 1982; Stenholm, 1986a] and references therein.) Both coherence and correlation properties of the output light have been researched [Chyba & Abraham, 1985; Friberg & Mandel, 1983; Woger et al., 1986]. There have also been studies of minimum limits for the noise that accompanies amplification [Ley & Loudon, 1985], as well as many derivations [Hong et al., 1985; Stenholm, 1986b] of limits for squeezing-preserving intensity gains of squeezed output from linear light amplifiers, with subsequent attempts [Pegg & Vaccaro, 1987; Vaccaro & Pegg, 1987; Dupertuis et al., 1987] to overcome the latter bounds for atomic amplifiers. In particular, inverted oscillator light amplifiers have been the subject of much investigation, where such objects have been used to discuss fundamental problems in the quantum theory of measurement [Glauber,

1986], the short-time behaviour in superfluorescence [Glauber, 1978], and of a spin magnetic moment in a magnetic field [Glauber, 1985].

Below, we briefly outline some properties of the inverted harmonic oscillator which are analogues of important relations obeyed by the familiar 'upright' harmonic oscillator, in terms of which modes of the electromagnetic field are described. We adopt Glauber's model of an inverted oscillator [Glauber, 1986] for the quantum amplifier, which assumes the following Hamiltonian,

$$H = \frac{1}{2} \left[p^2 + \omega^2 q^2 \right] - \hbar \omega (c^+ c + 1/2)$$

so that the annihilation operator evolves as $c(t) = c(0) e^{i\omega t}$. The n^{th} stationary state $|n\rangle$ obeys

$$|n\rangle = \frac{c^+}{\sqrt{n!}} |0\rangle \quad c |n\rangle = \sqrt{n} |n-1\rangle$$

$$c^+ c |n\rangle = n |n\rangle \quad E_n = -\hbar \omega (n + 1/2)$$

We can obtain our inverted oscillator from the usual simple harmonic oscillator, described by operators a, a^+ by the substitutions $\omega \rightarrow -\omega$ and $a \rightarrow c^+$, as in Fig. 5.1. Important differences between the models of Figs. 5.2 and 5.3 have been found; see for example [Glauber, 1986] and ref. therein. Physically, Fig. 5.3 represents a collection of atoms (the inverted oscillator), losing their energy to a bath of cavity field modes; the atoms may have all their 'input' modes occupied, but only one mode is amplified.

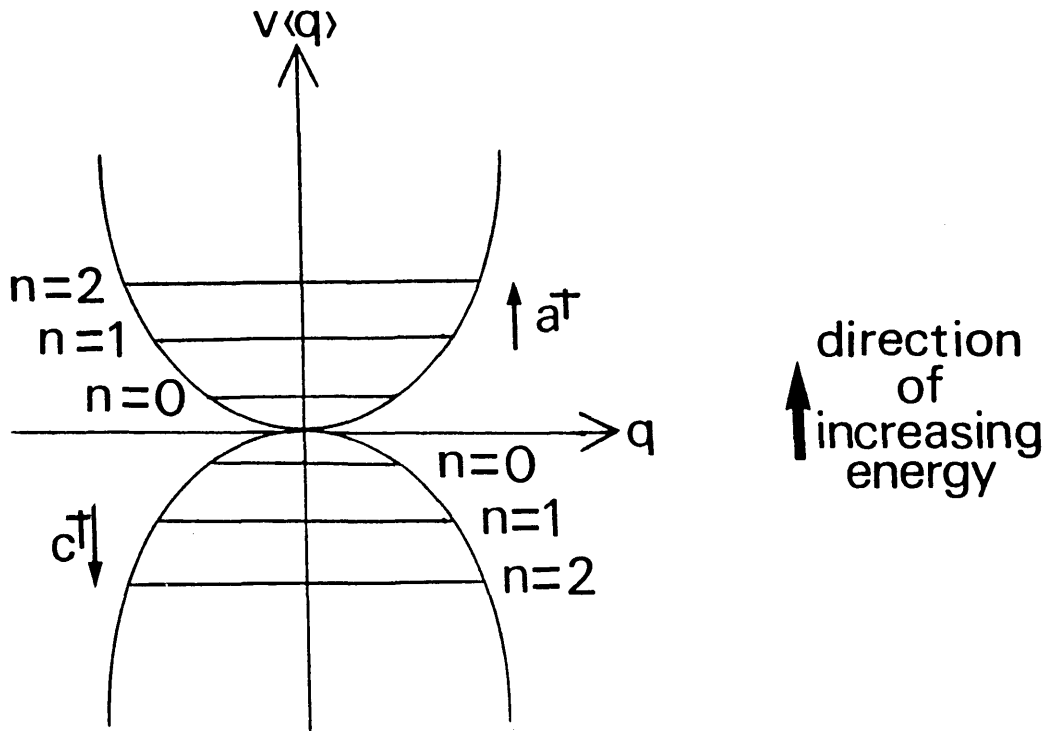


Figure 5.1. Harmonic & Inverted oscillator potentials and stationary states.

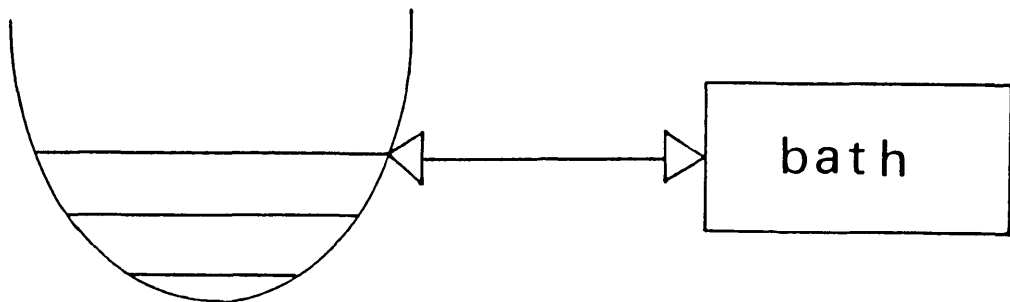


Figure 5.2. Harmonic oscillator coupled to a heat bath of oscillators.

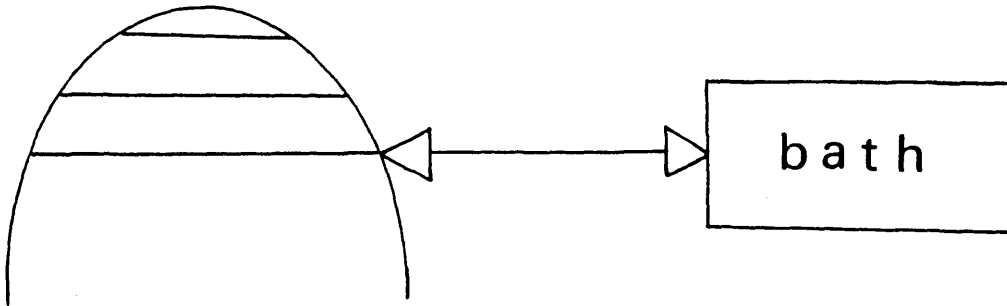


Figure 5.3. Inverted oscillator coupled to a heat bath of oscillators.

5.2 The Fluctuation Amplification Theorem

In this section, we derive a connection between amplification and quantum (vacuum) fluctuations for an inverted oscillator coupled to a heat bath of oscillators. We follow the method of Louisell [1973] who obtains the well-known Fluctuation-Dissipation Theorem for an 'upright' oscillator coupled to a reservoir. Let c and $\{b_j\}$ be the annihilation operators for the inverted oscillator and bath oscillator modes respectively. The oscillator-bath system is described by the Hamiltonian

$$H_I = -\hbar \omega_c (c^\dagger c + 1/2) + \hbar \sum_j \omega_j (b_j^\dagger b_j + 1/2) + H_I \quad (5.2.1a)$$

where H_I contains the linear couplings and is given by

$$H_I = \hbar (\kappa_j b_j c + \kappa_j^* c^\dagger b_j^\dagger) \quad (5.2.1b)$$

and $\{\kappa_j\}$ are a set of coupling constants. Henceforth, we omit the zero-point energies, and set $\hbar = 1$. Only in the limit as $j \rightarrow \infty$, can we strictly expect truly irreversible behaviour.

We proceed by deriving the Heisenberg equations of motion for the annihilation operator 'c', and in doing so adopt the Weisskopf-Wigner approximation to produce a true dissipative subsystem (the reservoir) and a Langevin approach whereby the fluctuations in the system arise from the inclusion of random forces as driving terms. These latter are chosen to have properties which ensure equal-time commutation relations are obeyed. This in turn ensures that the time-evolution preserves unitarity; probabilities relevant to the problem sum to unity. Working in the Heisenberg Picture, we find the following equations of motion:-

$$\dot{b}_j(t) = -i \omega_j b_j - i \kappa_j^* c^\dagger \quad (5.2.2)$$

$$\dot{c}(t) = i \omega_c c + \sum_j |\kappa_j|^2 \int_0^t c(t') e^{i \omega_j (t-t')} dt' + G_c \quad (5.2.3a)$$

where

$$G_c = -i \sum_j \kappa_j^* b_j^\dagger(0) e^{i \omega_j t} \quad (5.2.3b)$$

Note that $b_j(0)$ and $b_j^\dagger(0)$ are in the Schrodinger Picture.

We now transform to the Interaction Picture, by removing the freely-rotating high-frequency part of the evolution of c , by making the substitution

$$d(t) = c(t) e^{-i\omega_c t} \quad (5.2.4)$$

Then we find that

$$\dot{d}(t) = \sum_j |\kappa_j|^2 \int_0^t d(t') e^{i(\omega_j - \omega_c)(t-t')} dt' + G_d \quad (5.2.5a)$$

where

$$G_d = -i \sum_j \kappa_j^* b_j^+(0) e^{i(\omega_j - \omega_c)t} \quad (5.2.5b)$$

Now, we define the Laplace Transform of $f(t)$ by

$$\bar{f}(s) = \int_0^\infty e^{-st} f(t) dt.$$

Then, in Laplace Transform space, equation (5.2.5) becomes

$$\bar{d}(s) = \frac{c(0) + \bar{G}_d(s)}{s - \sum_j \frac{|\kappa_j|^2}{s - i(\omega_j - \omega_c)}} \quad (5.2.6a)$$

where

$$\bar{G}_d(s) = -i \sum_j \frac{\kappa_j^* b_j(0)}{s - i(\omega_j - \omega_c)} \quad (5.2.6b)$$

Under the Weisskopf-Wigner approximation, the system is only weakly perturbed so the pole in (5.2.6a) is close to zero, and we can make the approximation

$$\begin{aligned} & -i \sum_j \frac{|\kappa_j|^2}{-(\omega_j - \omega_c) - is} \\ & \longrightarrow \lim_{s \rightarrow 0^+} -i \int \frac{g(\omega_j) |\kappa(\omega_j)|^2}{-(\omega_j - \omega_c) - is} d\omega_j \\ & = \frac{\gamma}{2} - i \delta\omega \end{aligned} \quad (5.2.7)$$

where

$$\begin{aligned} \gamma &= 2\pi g(\omega_c) |\kappa(\omega_c)|^2 \\ \delta\omega &= - \int \frac{g(\omega_j) |\kappa(\omega_j)|^2}{\omega_j - \omega_c} d\omega_j. \end{aligned}$$

Here $g(\omega_j)$ is the density of states, γ is the amplification rate and $\delta\omega$ is a frequency shift. We have assumed that the heat-bath modes are numerous enough to form a continuum, with the central oscillator frequency embedded in it.

Substituting (5.2.6b) and (5.2.7) into (5.2.6a), and inverting the transformation $\bar{d}(s)$ over an appropriate Bromwich contour in the complex plane gives,

$$c(t) = u(t) c(0) + \sum_j v_j(t) b_j^+(0) \quad (5.2.8)$$

where

$$u(t) = \exp [(\gamma/2) + i(\omega_c - \delta\omega)]t \quad (5.2.8a)$$

and

$$v_j(t) = \frac{-\kappa_j^* [1 - e^{-i(\omega_j - \omega_c + \delta\omega)t} e^{\gamma t/2}] e^{i\omega_j t}}{(\omega_j - \omega_c) + \delta\omega + (i\gamma/2)} \quad (5.2.8b)$$

Hence, ignoring negligible frequency shifts, we have

$$\dot{d}(t) = \frac{\gamma}{2} d + G_d(t) \quad (5.2.9)$$

and

$$G_d(t) = -i \sum_j \kappa_j^* b_j^+(0) e^{+i(\omega_j - \omega_c)t} \quad (5.2.10)$$

Here, G_d is the quantum mechanical Langevin force, which is a random operator, acting as a noise source, adding fluctuations to the system. The term $(\gamma/2)d(t)$ signifies the mean drift motion. If the reservoir is initially in thermal equilibrium, at temperature T , then its density matrix is

$$\rho_o(R) = \frac{e^{-\beta H_R}}{\text{Tr}_R e^{-\beta H_R}},$$

where H_R is that part of the total Hamiltonian that describes the reservoir. Therefore, the Langevin force operator has zero expectation value

$$\langle G_d(t) \rangle_R = \text{Tr}_R \rho_o(R) G_d(t)$$

$$= 0$$

since we are tracing over the initial, or time independent states of the bath. For a bath with a large number of degrees of freedom, it takes little time for the bath correlations to decay and so the system can be assumed Markovian.

Thus, we obtain

$$\frac{d}{dt} \langle d(t) \rangle_R = \frac{\gamma}{2} \langle d(t) \rangle_R \quad (5.2.11)$$

so that,

$$\langle d(t) \rangle_R = e^{\gamma t/2} c(0) \quad (5.2.12)$$

By inspection of equation (5.2.12), we see that we can feel justified in calling ' γ ', the 'amplification constant.' Further, it follows that the autocorrelation function vanishes

$$K_{dd}(t_1 - t_2) = \langle G_d(t_1) G_d(t_2) \rangle_R$$

- 0.

Similar expectation values hold for $G_{d^+}(t)$ and $K_{d^+d^+}(t_1 - t_2)$.

The cross-correlation function is likewise given by

$$\begin{aligned}
 K_{d^+d} (t_1 - t_2) &= \langle G_{d^+}(t_1) G_d(t_2) \rangle_R \\
 &= \sum_{j,1} \kappa_1 \kappa_j^* \langle b_1(0) b_j^+(0) \rangle_R e^{i(\omega_j - \omega_c)t_2 - i(\omega_1 - \omega_c)t_1} \\
 &= \int_0^\infty g(\omega_j) |\kappa(\omega_j)|^2 (\bar{n}(\omega_j) + 1) \\
 &\quad e^{i(\omega_j - \omega_c)(t_2 - t_1)} d\omega_j \tag{5.2.13}
 \end{aligned}$$

where $\bar{n}(\omega_j) = \langle b_j^+(0) b_j(0) \rangle_R$ is the mean photon number in the j^{th} oscillator, and we have gone to the continuum limit, in j , the bath variables.

Also, we have that,

$$K_{d d^+}(t_1 - t_2) = \langle G_d(t_1) G_{d^+}(t_2) \rangle_R$$

$$= \int_0^{\infty} g(\omega_j) |\kappa(\omega_j)|^2 \bar{n}(\omega_j) e^{-i(\omega_j - \omega_c)(t_2 - t_1)} d\omega_j \quad (5.2.14)$$

Clearly, these functions depend only on time differences, and not on absolute values of time. Hence they describe stationary Markovian (random) processes. From Langevin theory [Haken, 1981], we know that as the time difference approaches infinity such expectation values approach zero, due to decorrelation of the Langevin forces $G_d(t)$.

We may associate with the dynamics, a correlation time τ_c , of the forces, which is a minimum time in which the Langevin force changes significantly. We choose a time interval Δt , such that

$$\tau_c \ll \Delta t \ll \gamma^{-1} \quad (5.2.15)$$

Next, we define the "Diffusion Coefficient", by

$$2 \langle D_{dd^+} \rangle_R = \frac{1}{\Delta t} \int_t^{t+\Delta t} dt_1 \int_t^{t+\Delta t} dt_2 \langle G_d(t_1) G_{d^+}(t_2) \rangle_R \quad (5.2.16)$$

We again assume that the integrand attains its peak value when $\omega_j = \omega_c$ enabling us to extend the lower limit to $-\infty$, so that we can perform the time integrals. The assumption that $g(\omega_j) |\kappa_j(\omega_j)|^2 \bar{n}(\omega_j)$ is a slowly varying function of ω_j enables us to perform the integration

over ω_j . Using this latter in (5.2.14) and (5.2.16) respectively yields

$$K_{dd^+}(t_1 - t_2) = \gamma \bar{n} \delta(t_1 - t_2) \quad (5.2.17)$$

and

$$2 \langle D_{dd^+} \rangle_R = \gamma \bar{n} \quad (5.2.18)$$

In correspondence with classical Brownian motion, the reservoir is assumed to become uncorrelated early in the evolution of the system, so that subsequent evolution is Markovian. Integration of both sides of (5.2.17) now gives

$$\gamma = \frac{1}{\bar{n}} \int_{-\infty}^{\infty} \langle G_d(\tau) G_{d^+}(0) \rangle_R d\tau. \quad (5.2.19)$$

This takes the form of a "Fluctuation-Amplification Theorem", wherein the system amplification rate γ and the reservoir fluctuating forces which introduce fluctuations into the system are inter-related.

An alternative, but equally valid expression is

$$\gamma = \frac{1}{(\bar{n} + 1)} \int_{-\infty}^{\infty} \langle G_{d^+}(\tau) G_d(0) \rangle_R d\tau \quad (5.2.20)$$

evaluated from

$$K_{d^+d}(t_1 - t_2) = \gamma (\bar{n} + 1) \delta(t_1 - t_2) \quad (5.2.20a)$$

$$2 \langle D_{d^+d} \rangle_R = \gamma (\bar{n} + 1) \quad (5.2.20b)$$

The vanishing of auto-correlation functions, and thus 'auto-diffusion coefficients' $\langle D_{dd} \rangle_R$ and $\langle D_{d^+d^+} \rangle_R$, is a sign of energy-conservation within the bath modes, at $t = 0$.

5.3 The Einstein Relation and Spectra

In similar fashion, we can derive a Langevin equation for the photon number in our inverted oscillator (see also [Stenholm, 1986a].)

We find, under the Markov approximation, that,

$$\frac{d}{dt} d^+d = \gamma d^+d + \gamma (\bar{n} + 1) + G_{d^+d} \quad (5.3.21)$$

where the relevant Langevin force is

$$G_{d^+d}(t) = d^+(t_c) G_d(t) + G_{d^+}(t) d(t_c) \quad (5.3.22)$$

and t_c is a time such that

$$0 < \tau_c \ll t - t_c \ll \gamma^{-1}.$$

It follows that

$$\frac{d}{dt} \langle d^+ d \rangle_R = \gamma \langle d^+(t) d(t) \rangle_R + \gamma (\bar{n} + 1) \quad (5.3.23)$$

requiring the property

$$\langle G_{d^+ d} (t) \rangle_R = 0.$$

From equations (5.2.9) and (5.3.21), and conditions (5.3.15), we may write,

$$\frac{\Delta d(t)}{\Delta t} = \frac{\gamma}{2} d(t) + \frac{1}{\Delta t} \int_t^{t+\Delta t} G_d(s) ds \quad (5.3.24a)$$

$$\frac{\Delta d^+ d(t)}{\Delta t} = \gamma d^+ d + \gamma (\bar{n} + 1) + \frac{1}{\Delta t} \int_t^{t+\Delta t} G_{d^+ d}(s') ds' \quad (5.3.24b)$$

where

$$\Delta d = d(t + \Delta t) - d(t) \quad (5.3.25a)$$

$$\Delta d^+ d = d^+(t + \Delta t) d(t + \Delta t) - d^+(t) d(t) \quad (5.3.25b)$$

Now,

$$\left\langle \frac{\Delta d^+ d}{\Delta t} \right\rangle_R = \left\langle d^+(t) \frac{\Delta d}{\Delta t} + \frac{\Delta d^+ d}{\Delta t} + \frac{\Delta d^+ \Delta d}{\Delta t} \right\rangle_R \quad (5.3.26)$$

To prevent the system from developing memory, we must ensure decorrelation of the system operators and reservoir Langevin forces over our working time interval $(s - t)$.

Further, on substituting (5.3.24) in (5.3.25) and in the limit $\Delta t \rightarrow 0$,

$$\frac{d}{dt} \langle d^+ d \rangle_R = \gamma \langle d^+ d \rangle_R + 2 \langle D_{d^+ d} \rangle_R \quad (5.3.27)$$

Finally, (5.2.9) and (5.2.20a) give

$$\begin{aligned} 2 \langle D_{d^+ d} \rangle_R &= \frac{d}{dt} \langle d^+ d \rangle_R - \frac{\gamma}{2} \langle d^+ d \rangle_R - \frac{\gamma}{2} \langle d^+ d \rangle_R \\ &= \frac{d}{dt} \langle d^+ d \rangle_R - \left\langle d^+ \left[\frac{d}{dt} d - G_d \right] \right\rangle_R \\ &= \left\langle \left[\frac{d}{dt} d^+ - G_d^+ \right] d \right\rangle_R \end{aligned} \quad (5.3.28)$$

which is the Einstein Relation for the diffusion coefficient.

For example, for our problem, using (5.2.9), (5.2.15) and (5.3.21),

$$2 \langle D_{d^+ d} \rangle_R = \gamma (\bar{n} + 1).$$

That is, the diffusion constant is given in terms of the drift terms, which determine the mean, underlying motion of a system. We can derive a Generalised Einstein Relation, using perturbation theory,

as in Sargent III [1974]. This has the same form as (5.3.28) but the drift terms can, for example, include spin-flip operators describing two-level atoms, or oscillators which obey Fermi-Dirac Statistics.

Next, we define the fluctuation, intensity and photon number spectra (unnormalised), for our example, respectively by

$$I_1 = \int_{-\infty}^{\infty} e^{-i\omega t} \langle c^+(t) c(0) \rangle dt \quad (5.3.29a)$$

$$I_2 = \int_{-\infty}^{\infty} e^{-i\omega t} \langle c^+(0) c^+(t) c(t) c(0) \rangle dt \quad (5.3.29b)$$

$$I_3 = \int_{-\infty}^{\infty} e^{-i\omega t} \langle c^+(t) c(t) c^+(0) c(0) \rangle dt \quad (5.3.29c)$$

Evaluating these equations using (5.2.9) and (5.3.21), we find that

$$I_1 = \frac{-\gamma \langle c^+(0) c(0) \rangle}{(\omega + \omega_c)^2 + (\gamma/2)^2} \quad (5.3.30a)$$

$$I_2 = \frac{-2\gamma}{\gamma^2 + \omega^2} \left[\langle c^{+2}(0) c^2(0) \rangle + (\bar{n}+1) \langle c^+(0) c(0) \rangle \right] \\ - 2\pi (\bar{n}+1) \langle c^+(0) c(0) \rangle \delta(\omega) \quad (5.3.30b)$$

$$I_3 = I_2 - \frac{2\gamma}{\gamma^2 + \omega^2} \langle c^+(0) c(0) \rangle \quad (5.3.30c)$$

The positivity of the spectra is born out, since c^+c represents a

de-excitation, that is a negative energy, on the absolute energy scale. This arises because of the even powers of operators in their definitions (5.3.29), so positive definiteness is assured. For comparison, the corresponding expression for I_1 for the model of Fig.5.2 is

$$I_1(a, a+) = \frac{\gamma \langle a^+(0) a(0) \rangle}{(\omega - \omega_c)^2 + (\gamma/2)^2}.$$

5.4 Relevance of the Quantum Regression

Theorem and the Kubo Formula

Because we have been dealing with a Markovian evolution, the Quantum Regression Theorem (Q. R. T.) will be of relevance. In our case, we can use it to find an expression for γ . A statement of the Q. R. T. is that if

$$\langle \hat{A}(t + \tau) \rangle = \sum_i \alpha_i(\tau) \langle \hat{A}_i(t) \rangle$$

then

$$\langle \hat{B}(t) \hat{A}(t + \tau) \hat{C}(t) \rangle = \sum_i \alpha_i(\tau) \langle \hat{B}(t) \hat{A}_i(t) \hat{C}(t) \rangle.$$

In other words, the theorem helps us to write two-time operator correlation functions in terms of one-time correlation functions. We need to evaluate the term $\langle G_d(\tau) G_d^+(0) \rangle_R$, which arises in the

expression for the fluctuation-amplification rate, of equation (5.2.19).

Now,

$$G_d(t) = -i \sum_j \kappa_j^* b_j^+(0) e^{i(\omega_j - \omega_c)t}.$$

Hence, by the Q. R. T.,

$$\langle G_d(t + \tau) \rangle = \sum_j \alpha_j(\tau) \langle G_d^{(j)}(t) \rangle \quad (5.4.31)$$

where $\alpha_j(\tau) = -i \kappa_j^* e^{i(\omega_j - \omega_c)(t + \tau)}$ and $G_d^{(j)}(t) = b_j^+(0)$.

Temporarily assuming γ to be time-dependent,

$$\begin{aligned} \gamma(t) &= \frac{1}{\bar{n}} \int_{-\infty}^{\infty} \langle G_d(t + \tau) G_d^+(t) \rangle_R d\tau \\ &= \frac{1}{\bar{n}} \sum_j \langle G_d^{(j)}(t) G_d^+(t) \rangle_R \int_{-\infty}^{\infty} \alpha_j(\tau) d\tau \\ &= \frac{1}{\bar{n}} \sum_j \langle b_j^+(0) \left[i \sum_l \kappa_l b_l(0) e^{-i(\omega_l - \omega_c)t} \right] \rangle_R \\ &\quad \times \int_{-\infty}^{\infty} -i \kappa_j^* e^{i(\omega_j - \omega_c)(t + \tau)} d\tau. \end{aligned} \quad (5.4.32)$$

If the reservoir is in thermal equilibrium, then $\langle b_j^+(0) b_l(0) \rangle_R =$

$\delta_{j1} \bar{n}_j$. After setting $t = 0$, we find that

$$\gamma = \frac{2\pi}{\bar{n}} \sum_j |\kappa_j|^2 \bar{n}_j \delta(\omega_j - \omega_c) \quad (5.4.33)$$

Further, if $|\kappa_j(\omega_j)|^2 \bar{n}_j$ is assumed to be a slowly varying function of ω_j , we can convert the sum to be an integral, to give as before,

$$\gamma = 2 \pi g(\omega_c) |\kappa(\omega_c)|^2, \quad (5.4.34)$$

where $g(\omega_c)$ is a density of states, about the most prominent frequency ω_c . The latter is densely surrounded by the frequencies of the other oscillators, which then effectively function as a heat bath. Therefore, we have reduced (5.2.19) to the usual dissipation or amplification rate, familiar from time-dependent first order perturbation Fermi Golden Rule Theory. It is interesting to note that (5.2.19) takes the form of a 'Kubo equation', [Ziman, 1980], giving the response of a system to an oscillating perturbation.

We now outline the connection, with a precis of Callen's derivation of the Kubo formula [Callen, 1962].

Imagine the relevant Hamiltonian takes the form

$$H = H_o + \sum_i F_i Q_i + H_{sg} \quad (5.4.35)$$

where H_o represents the driven system, H_{sg} represents the signal

generator (driving system) and $\sum_i F_i Q_i$ is the interaction term. The signal generator applies a set of forces $\{F_i\}$ to the driven system, creating fluctuations in the system. F_i and Q_i depend on the coordinates and the momenta of, respectively, the generator and the dissipative system. Since the signal generator has a few degrees of freedom and moreover is highly excited to large quantum numbers, we can take the functions $F_i(t) = f_i(t)$ to be classical. Hence,

$$H = H_o + \sum_i f_i(t) Q_i. \quad (5.4.36)$$

The response $\langle Q_i(t) \rangle$ to the applied 'forces' $f_i(t)$ is,

$$\langle Q_i(t) \rangle = \text{Tr } Q_i \rho(t) \quad (5.4.37)$$

where $\rho(t)$ is the requisite density matrix, obeying the Schrodinger Picture equation of motion $i\hbar \dot{\rho} = [H, \rho]$.

Using the equilibrium density matrix, this can be solved by iteration to find a first order approximation for ρ , which is linear in the applied forces. We find that

$$\langle Q_i(t) \rangle^{(1)} = \sum_i \int_{-\infty}^t f_i(t') \frac{1}{i\hbar} \langle [Q_i(t'), Q_j(t)] \rangle^{(0)} dt' \quad (5.4.38)$$

where $\langle \dots \rangle^{(0)}$ is an ensemble average for the system in equilibrium. Simply noting the following identifications,

$$H_{sg} = -\hbar\omega_c (c^\dagger c + 1/2),$$

$$H_o = \hbar \sum_i \omega_i (b_i^\dagger b_i + 1/2), \quad (5.4.39)$$

$$F_i = c, \quad (Q_i) = (b_i),$$

our problem clearly reduces to a special case of this general formalism.

We observe that the integrand of (5.4.38) has no classical analogue, a confirmation that the link between fluctuations and dissipative/amplificative behaviour is purely quantum mechanical.

To be more precise, although, for example, classical Brownian motion has an equivalent fluctuation-dissipation theorem associated with it [Haken, 1981], quantum phenomena require quantum Langevin theory in order to identify this theorem.

5.5 Discussion.

It is a general result in statistical mechanics, that all dissipative processes may be thought of as being induced by spontaneous fluctuations in the dissipative system. This general result is called Nyquist's Theorem [Callen, 1962; Callen & Welton, 1951; Jackson, 1952; Reif, 1985], and relates the generalised resistance (an irreversible process,) to the fluctuations of the generalised forces in linear dissipative systems.

Thus, spontaneous (i.e. vacuum stimulated) transitions may be considered as arising from the random fluctuations of the electromagnetic field in the vacuum state (the dissipative system,) acting as an excited atom [Milonni, 1984]. Nyquist relations correlate the fluctuations of a system in equilibrium with an irreversible process.

A physical explanation for the fluctuation-decay theorem, for a damped 'upright' harmonic oscillator may take the following form. The harmonic oscillator has a simple structure, and is excited to high energy-levels, with its large energy coherently associated with one or a very few degrees of freedom. The reservoir has a more complex structure. On coupling, the reservoir acts as a dissipative system, destroying the coherence of the oscillator. It is the random fluctuations generated by the dissipative system which creates a loss of energy and coherence within the harmonic oscillator, leaving the latter with only the random disordered thermal equilibrium energy. Nyquist fluctuations manifest themselves as macroscopic dissipations. The same mechanism can be used to explain the fluctuation-amplification theorem, however the energy loss is exponentially increasing.

Note that we do not necessarily require a reservoir within our system, in order to achieve amplification. A simpler model of a parametric amplifier (paramp) is an oscillator coupled to an inverted oscillator. As we move down the ladder of states in the latter, by creating quanta of 'negative' energy, positive energy is lost to the upright oscillator, whose mode is thus amplified, by creation of quanta, and movement up the ladder of energy levels. Our above model

comprises a field of modes being amplified. In addition, there is a stage where our analogy with the fluctuation-dissipation theorem breaks down. For whereas our dissipator decays to zero in the long-time limit, amplification proceeds ad infinitum, requiring an unrestricted energy source. This would explain why our amplification models do not occur in nature, but are as yet merely approximations to physical situations.

We conclude this section by noting the difference in structure of the Langevin equations of motion for harmonic and inverted oscillators respectively,

$$\frac{df}{dt}(t) = -\frac{\gamma}{2} f(t) + G_f(t)$$

$$G_f(t) = -i \sum_j \kappa_j b_j(0) e^{-i(\omega_j - \omega_c)t}$$

and

$$\frac{dd}{dt}(t) = \frac{\gamma}{2} f(t) + G_d(t)$$

$$G_d(t) = -i \sum_j \kappa_j^* b_j^+(0) e^{i(\omega_j - \omega_c)t}$$

where $f(t) = a(t) e^{i\omega t}$.

Nevertheless, the dissipation width

$$\gamma = \frac{1}{\bar{n}} \int_{-\infty}^{\infty} \langle G_{f^+}(\tau) G_f(0) \rangle_R d\tau$$

is identical with the fluctuation width of (5.2.19), as we have shown above using the Q. R. T., or as can be proved by direct substitution.

5.6 Conclusions

We have discussed the exponentially increasing energy loss of an inverted harmonic oscillator by its linear coupling to a collection of harmonic oscillators from a statistical viewpoint. It was found that, just as for the equivalent linear damping problem, the central oscillator lost its energy to the bath, which in turn returned part of that energy in a random fashion, back to the primary oscillator

The operation of a quantum linear amplifier adds Langevin noise to the emitted signal, thus degrading the efficiency of the output by decreasing the signal-to-noise ratio. In going from attenuator problems to the analogous amplifier problems with which we have dealt above, we have found that the replacements $\omega \rightarrow -\omega$ and $a \rightarrow c^+$ in the formalism have the same effect as the naive substitutions

$$-\gamma \rightarrow \gamma \quad \text{and} \quad \bar{n} \leftrightarrow \bar{n} + 1.$$

The first of these changes is perhaps to be expected; the factor of unity in the second is an intrinsic spontaneous emission term, essential for the elucidation of quantum amplification. The Langevin equation (5.3.21) for the photon number, is a good example of how both input photons and zero-point photons initially present are amplified.

Prudence is necessary in fashioning the time-evolution of physical systems comprising the inverted oscillator; for large enough times, the evolution becomes nonlinear and the model breaks down.

CHAPTER SIX

DISCUSSION & CONCLUSIONS

In this thesis, we have been primarily concerned with the dynamical evolution of population in two models. In chapter five, we looked at some quantum statistical properties of the inverted oscillator.

Firstly, in chapter two, we developed a theoretical analysis of the interaction of a closely-spaced manifold of energy levels, the quasicontinuum (QC), with a relatively isolated discrete level, which is in turn dissipating its population to a true continuum. The latter was treated through the Markov approximation, and for definiteness we assumed constant coupling to equally spaced levels comprising the QC. We named this scheme, the Extended Bixon-Jortner model.

We found that when all of the population was chosen to reside in the isolated state, there was initial decay as though to a true continuum. Then, 'kicks' were administered at integer values of normalised time, which created recurrence in ground-state population as discrete spectra was resolved. The long-time evolution became more complicated. The true continuum wins the competition for population in the steady-state limit, because loss to the QC is reversible, whereas that to the continuum is ^{ir-}reversible. The overall dynamics was a superposition of recurrence of initial-state probability and exponential decay.

Then followed a discussion of limiting and special cases including that of energy-level degeneracy.

Finally, we looked at the QC population dynamics, noting the possibilities of initial condition-dependent population trapping, in the long time limit.

In chapter three, we investigated an analytically soluble model, which we called the 'Structured Continuum', in which the dipole matrix elements between the ground-state and the continuum vary sinusoidally between zero and a maximum. The time-evolution of the ground-state population still exhibited the periodic disruption observed in the Bixon-Jortner model, although much reduced. We allowed the ground-state to be resonant with an arbitrary place in the continuum; population trapping was observed in the case of resonance with a zero in the continuum.

In chapter four, we dealt with dressed states and spectra in QC excitation for arbitrary quasicontinua. We found that, if the population was initially placed in $|0\rangle$, then at long times the true continuum spectrum exhibited zeros at the frequencies of the QC levels. Zeros could be removed by placing population initially in corresponding QC levels. In particular, these features were present when the QC levels were chosen to be equally spaced (the Bixon-Jortner model) or those of a Rydberg series, and we illustrated each of these.

In order to study these features, we investigated the dressed states for the total system. We proved the existence of dressed states $|s_1\rangle$, which contain no contribution from the ground state (plus appropriate photon numbers), regardless of the QC chosen. These dressed states are each formed from one QC level and an isolated state

of the true continuum having the same energy as the QC level. Calculating the populations at positions in the true continuum spectrum corresponding to the energies of the QC levels, we found both a constant term and a transient. The constant is proportional to the population initially in $|s_1\rangle$. If the states $|s_1\rangle$ were initially unpopulated, zeros in the spectrum were produced. Conversely, these could be removed by initially populating one or more of the $|s_1\rangle$.

The approximations made in our studies yielded analytically closed-form expressions for the time evolution, which have the advantage over numerical solutions of offering insight into our understanding of the processes involved.

Little has been said in this thesis about empirical verification of the models in real systems. Certainly, the region below dissociation threshold where molecular vibrational levels are dense but not continuous, is identified as a QC. Ultimately the justification for our juggling with idealisations, is that this is a thesis dealing with theoretical, as opposed to experimental Quantum Optics.

Moreover, with relatively simple models, we have succeeded in revealing many of the features that would normally only transpire from more complex treatments of similar systems; for example, the final-state spectra studies of our Structured Continuum displayed asymptotic confluences and q-reversals, which would normally show up only on utilizing the autoionisation theory of Fano.

We expect that this work will have important practical implications for multiphoton dissociation of polyatomic molecules.

In chapter five, perhaps the main message is that, for linear systems, dissipation and amplification can be regarded in a sense as different manifestations of the same phenomenon of response to within the approximations that we have employed. This conclusion is independently born out by the research of Dupertuis et al. [1987]. They go on to show that one can 'rig' the reservoir response, which for an attenuator can produce a squeezed output, irrespective of its input, and for an amplifier can provide a squeezed output for an arbitrary gain, thus beating the photon-cloning limit of two. Similar conclusions are reached by Vaccaro and Pegg [1987], using single-stage and multi-stage squeezed atomic light amplifiers instead of a suitably rigged reservoir.

We hope that this account may help to elucidate the role of the inverted oscillator as a potential amplifier.

Perhaps the most striking underlying feature of our work is the generality of the models presented. It is clearly to be expected that such themes will arise in other areas of physics, outside the strict domains of Multiphoton Physics or Quantum Optics. Some of these have been mentioned above for example, the study of time-reversal asymmetry, Landau levels or quantum measurement theory. Others undoubtedly exist, although specific features of our analysis will have to be altered to suit the idiosyncrasies of the problems of interest.

We hope that our models will serve as a stepping-stone toward understanding more physically interesting schemes.

APPENDIX I

In this appendix, we derive the general equation of motion which is used in the text. We write the time-dependent Schrödinger Equation as,

$$i \hbar \frac{\partial \Psi(\underline{r}, t)}{\partial t} = \hat{H} \Psi = (\hat{H}^{(0)} + \hat{H}') \Psi \quad (\text{I.1})$$

In the absence of \hat{H}' ,

$$i \hbar \frac{\partial \chi}{\partial t} = \hat{H}^{(0)} \chi$$

where the wavefunction χ can be written $\chi = \sum_n a_n \chi_n$, where the stationary states of an atom are $\chi_n = u_n e^{-iE_n t/\hbar}$, with $\hat{H}^{(0)} u_n = E_n u_n$ ($\chi = \chi(\underline{r}, t)$, $\chi_n = \chi_n(\underline{r}, t)$.)

When the field is weak, for example, obeys Beer's absorption law, then the interaction can be considered as a perturbation to the Hamiltonian H_0 , and the unperturbed atomic eigenstates still provide an adequate set of basis states under irradiation. Thus,

$$\begin{aligned} \Psi(\underline{r}, t) &= \sum_n a_n(t) \chi_n(\underline{r}, t) \\ &= \sum_n a_n(t) u_n(\underline{r}) e^{-iE_n t/\hbar}, \end{aligned}$$

and by the Superposition Principle, (a postulate of Quantum Mechanics), the general solution is a linear superposition of the particular solutions and the summation strictly includes integration over all continuum states. If the perturbation of the system is time-dependent, then the weighting functions $a_n(t)$ will be time dependent.

When $\Psi(\underline{r}, t)$ is normalised, then the $a_n(t) e^{-iE_n t/\hbar}$ can be interpreted as the probability amplitudes, whose modulus square is the probability of being in the state $|n\rangle$. The interaction between the 'atom' (through its dipole moment, \underline{d}), and the field (through the polarization $\underline{\epsilon}$), is given by $H = H_0 - \underline{d} \cdot \underline{E}$.

Substituting into equation I.1, gives,

$$\begin{aligned} i\hbar \sum_n \dot{a}_n(t) u_n e^{-iE_n t/\hbar} + \sum_n E_n a_n(t) u_n e^{-iE_n t/\hbar} \\ = (\hat{H}^{(0)} + \hat{H}') \sum_n a_n(t) u_n e^{-iE_n t/\hbar}. \end{aligned}$$

Hence,

$$i\hbar \sum_n \dot{a}_n(t) u_n e^{-iE_n t/\hbar} = \sum_n \hat{H}' a_n(t) u_n(\underline{r}) e^{-iE_n t/\hbar}.$$

Premultiplying both sides by u_k^* , integrating over all space, and using the orthonormality condition

$$\int u_n^*(\underline{r}) u_m(\underline{r}) d\underline{r} = \delta_{nm}$$

gives,

$$i\hbar \dot{a}_k(t) e^{-iE_k t/\hbar} = \sum_n a_n(t) \hat{H}'_{kn} e^{-iE_n t/\hbar},$$

where,

$$\hat{H}'_{kn} = \int u_k^* \hat{H}' u_n d\underline{r},$$

which is the matrix element of the matrix representing the quantum mechanical operator \hat{H}' . Generally, matrix elements of the form $H'_{kk}(t)$ are zero since the dipole moment is only non-zero between states of opposite parity.

Defining $\omega_{kn} = E_k - E_n$, we conclude that

$$i\hbar \dot{a}_k(t) = \sum_n \hat{H}'_{kn} a_n(t) e^{i\omega_{kn} t}. \quad (\text{I.2})$$

APPENDIX II

In this appendix, we evaluate the integral in equation (2.3.6),
($\hbar = 1$),

$$\begin{aligned} \dot{c}_0 &= \frac{-iV}{\hbar} \sum_n c_n(t) e^{-i\Delta_n t/\hbar} \\ &- \frac{1}{\hbar^2} \int d\omega_f |V_{of}|^2 \int_0^t dt' e^{-i\Delta_f(t-t')/\hbar} c_0(t') \end{aligned} \quad (\text{II.1})$$

treating the decay of the discrete state $|0\rangle$ to a continuum of final states, using the Markov approximation. We follow the treatment of Cohen-Tannoudji et al. [1977, p.1343 et seq.], and Radmore & Knight [1982, p.571].

\dot{c}_0 here is non-Markovian, being dependent on the past history of c_0 , due to the integral term. We now make our approximation. If $|V_{of}|^2$ is a sufficiently broad function of f , then for large $t-t'$, the exponential, whose period with respect to ω_f is $2\pi\hbar/(t-t')$, undergoes many cycles of oscillation as f is varied and consequently averages to zero.

More precisely, if the values of t and t' are chosen such that this period is very much smaller than the width of $|V_{of}|^2$ say $\hbar\delta$, (the latter being interpreted as the range which covers most of the variation of V_{of}), then the product $|V_{of}|^2 e^{-i\Delta_f(t-t')/\hbar}$ undergoes numerous oscillations when ω_f is varied and its integral over ω_f is negligible. So the modulus of this latter integral is large for $t-t' \approx 0$, & becomes negligible as soon as $t-t' \gg 1/\delta$. This property means that the only values of $c_0(t')$ to enter significantly into the right-hand side of II.1 are those which correspond to t' very close to t ($t-t' \ll 1/\delta$.) So the presence of the integral over ω_f practically eliminates the contribution of $c_0(t')$ as soon as $t-t' \gg 1/\delta$.

For any value of t , then, $\dot{c}_0(t)$ depends only on the values of c_0 at times immediately before t . This property enables us to transform the integro-differential equation II.1, into a differential equation.

If $c_0(t)$ varies little over a time interval of the order of $1/\delta$, we take $t-t' \approx 0$, so to within a small error, $c_0(t') \approx c_0(t)$.

Now note that [Cohen-Tannoudji, 1977, p.1470]

$$\lim_{t \rightarrow \infty} \int_0^t e^{-i\Delta_f \tau / \hbar} d\tau = \hbar \left[\pi \delta(\Delta_f) - i \mathcal{P} \left[\frac{1}{\Delta_f} \right] \right].$$

The limiting procedure is not essential; it suffices that $\hbar/t \ll \hbar\delta$, that is, $t \gg 1/\delta$.

Hence, given this validity condition, we have that

$$\begin{aligned} \Gamma &= \int d\omega_f \frac{|V_{of}|^2}{\hbar} \left[\pi \delta(\Delta_f) - i \mathcal{P} \left[\frac{1}{\Delta_f} \right] \right] \\ &\equiv \gamma + i\Delta\omega_0, \end{aligned}$$

and the result in equation (2.3.7).

γ here is half of the first order perturbation theory, Fermi Golden Rule decay rate. (γ^{-1} is the decay lifetime of the 'atom' from its excited state.)

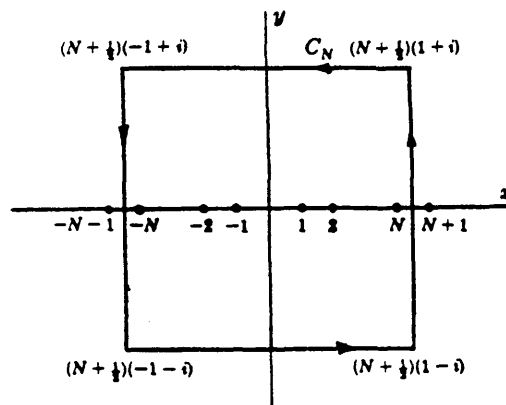
The δ -function ensures energy conservation, as required by the emission of real photons, whereas it is virtual photons that shift the energy level, since energy conservation is not called for.

The Principal Part ensures a non-divergent result if $\Delta_f = 0$. We recognize this second order in V quantity from stationary perturbation theory. $\Delta\omega_0$ is then simply the sum of the shifts due to the various continuum states.

Note that to the order to which we are working, the Markov and Weisskopf-Wigner approximations are equivalent.

APPENDIX III

Here, we present a proof of equation (2.3.15), by application of a theorem of Residue Calculus [Spiegel, 1972, p.188]



Theorem:-

Let $f(z)$ be a function of a complex variable such that along the path c_N , $|f(z)| \leq \frac{M}{|z|^l}$, where $l > 1$ and M are constants independent of N ; (see figure above). Then,

$$\sum_{n=-\infty}^{\infty} f(n) = - \sum_{n=-\infty}^m \text{Res}(\pi \cot(\pi z) f(z), a_k),$$

where a_k ($k = 1, \dots, m$) are poles of $f(z)$. We assume that none of the

finite poles of f is integer, i.e. the poles of $\pi \operatorname{Cot}(\pi z)$ and $f(z)$ do not coincide.

For our example,

$$\sum_{n=-\infty}^{\infty} \frac{1}{s + in\Delta} = \frac{1}{i\Delta} \sum_{n=-\infty}^{\infty} \frac{1}{n + (s/i\Delta)}.$$

Take $a = (s/i\Delta)$ ($a \in \mathbb{C}$, and non-integer by assumption.)

Then $f(z) = (z + a)^{-1}$ has a simple pole at $z = -a$, and a residue at $'-a'$ of $\operatorname{Res}(-a) = 1$.

Therefore,

$$\sum \operatorname{Residues} = -1 \cdot \pi \cdot \operatorname{Cot}(\pi z) \Big|_{z=-a}$$

$$= -\pi \operatorname{Cot}(-\pi a)$$

$$= i \pi \operatorname{Coth}(\pi s / \Delta)$$

Therefore,

$$\sum_{n=-\infty}^{\infty} (s + in\Delta)^{-1} = \frac{\pi}{\Delta} \operatorname{Coth} \left[\frac{\pi s}{\Delta} \right] \quad \text{QED.}$$

APPENDIX IV

Here, we evaluate equation (2.5.4) for $c_p(t)$.

Now,

$$\begin{aligned}
c_p(t) = & -i v_{po} \int_0^t e^{-\Gamma t} e^{(i\Delta_p - \Gamma - r^2)r} dr \\
& + i v_{po} e^{-\Gamma t} \sum_{n=1}^{\infty} \frac{2r^2}{n} \left[\int_0^t r_n e^{(i\Delta_p - \Gamma - r^2)r} L_{n-1}^{(1)}[2r^2 r_n] \right. \\
& \left. e^{-in\Delta_o 2g} \theta(\tau_n) dr \right] e^{(\Gamma + r^2)2ng} \quad (V.1)
\end{aligned}$$

where $\tau_n = \tau - 2ng$. By definition of Generalised Laguerre Polynomial

$$L_j^{(\alpha)}(x) = \sum_{k=0}^j \begin{bmatrix} j + \alpha \\ j - k \end{bmatrix} \frac{(-x)^k}{k!}.$$

We concentrate on solving the second integral above, using

$$\delta(x) = \frac{d}{dx} \theta(x), \text{ or with } x = \tau - 2ng, \delta(\tau_n) = \frac{d}{d\tau} \theta(\tau_n).$$

Therefore this term becomes, on integration by parts,

$$\begin{aligned}
& \left[\int_0^t (\tau_n)^{k+1} e^{(i\Delta_n - \Gamma - r^2)r} dr \right] \theta(\tau_n) \Big|_0^t \\
& - \int \frac{d\theta(\tau_n)}{d\tau} dr \left[\int_0^t (\tau_n)^{k+1} e^{(i\Delta_n - \Gamma - r^2)r} dr \right] \quad (V.2)
\end{aligned}$$

Also,

$$\begin{aligned}
\int^x (y-\delta)^\beta e^{\gamma y} dy &= \frac{(x-\delta)^\beta e^{\gamma x}}{\gamma} - \frac{\beta}{\gamma} \int (y-\delta)^{\beta-1} e^{\gamma y} dy \\
&= \frac{(x-\delta)^\beta e^{\gamma x}}{\gamma} - \frac{\beta}{\gamma} \left[\left[\frac{(x-\delta)^{\beta-1} e^{\gamma x}}{\gamma} \right] \right. \\
&\quad \left. - \frac{(\beta-1)}{\gamma} \int (y-\delta)^{\beta-2} e^{\gamma y} dy \right] \\
&= \frac{(x-\delta)^\beta e^{\gamma x}}{\gamma} - \frac{\beta (x-\delta)^{\beta-1} e^{\gamma x}}{\gamma^2} \\
&\quad + \frac{\beta (\beta-1)}{\gamma} \int (y-\delta)^{\beta-2} e^{\gamma y} dy \\
&= \frac{(x-\delta)^\beta e^{\gamma x}}{\gamma} - \frac{\beta (x-\delta)^{\beta-1} e^{\gamma x}}{\gamma^2} + \frac{\beta(\beta-1) (x-\delta)^{\beta-2} e^{\gamma x}}{\gamma^3} \\
&\quad - \dots + \frac{\beta(\beta-1)(\beta-2)\dots 1 (x-\delta)^{\beta-\beta}}{\gamma^{\beta+1}} \int (y-\delta)^{\beta-\beta} e^{\gamma y} dy \\
&= e^{\gamma x} \sum_{q=0}^{\beta} \frac{(x-\delta)^{\beta-q} (-1)^q \beta!}{\gamma^{q+1} (\beta-q)!}
\end{aligned}$$

Therefore, $\int_0^t (\tau_n)^{k+1} e^{(i\Delta_n - \Gamma - r^2)t} \theta(\tau_n) d\tau$ with $\gamma = i\Delta_n - \Gamma - r^2$

$x = \tau$, $\delta = 2ng$, $\beta = k+1$ becomes,

$$e^{(i\Delta_n - \Gamma - r^2)t} \sum_{q=0}^{k+1} \frac{(\tau_n)^{k+1-q} (-1)^q (k+1)!}{(i\Delta_n - \Gamma - r^2)^{q+1} (k+1-q)!}.$$

From $\frac{d}{d\tau} \theta(\tau_n) = \delta(\tau_n)$, we see that the integral part of (V.2) vanishes. We can evaluate the integrated part of (V.2) by using the sum from the recurrence relation. So we have,

$$\begin{aligned} & \int_0^t (\tau_n)^{k+1} e^{(i\Delta_n - \Gamma - r^2)\tau} \theta(\tau_n) d\tau \\ &= \left[\left[\int (\tau_n)^{k+1} e^{(i\Delta_n - \Gamma - r^2)\tau} \right] \theta(\tau_n) \right]_0^t. \end{aligned}$$

Then, with $\gamma = i\Delta_n - \Gamma - r^2$, $x = \tau$, $\delta = 2ng$, $\beta = k + 1$, this becomes,

$$\begin{aligned} & \theta(\tau_n) e^{(i\Delta_n - \Gamma - r^2)\tau} \sum_{q=0}^{k+1} \frac{(\tau_n)^{k+1-q} (-1)^q (k+1)!}{(i\Delta_n - \Gamma - r^2)^{q+1} (k+1-q)!} \Bigg|_0^t \\ &= e^{(i\Delta_n - \Gamma - r^2)t} \sum_{q=0}^{k+1} \frac{(\tau_n)^{k+1-q} (-1)^q (k+1)!}{(i\Delta_n - \Gamma - r^2)^{q+1} (k+1-q)!} \theta(\tau_n) \quad (V.3) \end{aligned}$$

because if $t = 0$, then $-2ng < 0$ and so $\theta(\tau_n) = 0$.

The first integral in V.1 is,

$$\int_0^t e^{(i\Delta_n - \Gamma - r^2)r} dr = \frac{e^{(i\Delta_n - \Gamma - r^2)t} - 1}{(i\Delta_n - \Gamma - r)^2}. \quad (\text{V.4})$$

Substituting (V.3) and (V.4), into (V.1) gives the result (2.5.5).

APPENDIX V

Below we elaborate on some of the terms used within the text of the thesis.

Bloch Sphere [Allen & Eberly, 1975].

We can parameterize the interaction of a two-level atom in a steady field using three variables. The inversion 'w' or single atom population difference, which is proportional to the expectation of the atom's unperturbed energy, $\hbar \omega_0 w / 2$ is one such variable (with ω_0 being the level spacing.) The other two are the components of the atomic dipole moment in-phase and in-quadrature with the field, 'u' and '-v' respectively. The absorptive component of the dipole moment, v, is the component effective in coupling to the field to produce energy changes, while u is the dispersive component. Now, these three vector components are the result of a coordinate transformation of the expectation values of the original Pauli spin operators which defined the evolution. Because this transformation is merely a rotation,

lengths of vectors are reserved. Hence conservation of probability requires that

$$u^2(t) + v^2(t) + w^2(t) = 1.$$

This equation indicates that the dynamics of the interaction is plotted-out on a 'Bloch Sphere,' formed by the Bloch pseudo-vector components u , v and w .

Autler - Townes doublet splitting

The state vector $\Psi(t)$ for a two-level atom (TLA) may be described in terms of two states $|1\rangle$ and $|2\rangle$ which define the two levels. If the two levels are coupled via an atom-electromagnetic field interaction the system oscillates between $|1\rangle$ & $|2\rangle$, and so these states are no longer stationary states and are not eigenstates of the total Hamiltonian H . It is possible to find new eigenstates $|+\rangle$ and $|-\rangle$ with eigenvalues E_+ , E_- by diagonalising H . These two sets of states ($|1\rangle$, $|2\rangle$) and ($|+\rangle$, $|-\rangle$) may be thought of as two different sets of basis states in terms of which $\Psi(t)$ can be expanded

$$\Psi(t) = a_1(t) e^{-iE_1 t} |1\rangle + a_2(t) e^{-iE_2 t} |2\rangle$$

or

$$\Psi(t) = \lambda_+ e^{-iE_+ t} |+\rangle + \lambda_- e^{-iE_- t} |-\rangle$$

The states ($|+\rangle$, $|-\rangle$) are linked to the states ($|1\rangle$, $|2\rangle$) by a transformation matrix. The expansion coefficients $a_1(t)$ & $a_2(t)$ have been made time dependent because of the oscillation of the system between states $|1\rangle$ & $|2\rangle$. The expansion coefficients λ_+ and λ_- are

time independent because $|+\rangle$ and $|-\rangle$ are stationary states and there is no coupling between them. Because the probabilities $|\lambda_+|^2$ and $|\lambda_-|^2$ are time independent, the basis set ($|+\rangle$, $|-\rangle$) is a convenient basis to work with.

The actual state of the system $\Psi(t)$ and the expectation value of the energy $\langle \Psi(t) | H | \Psi(t) \rangle$ are independent of the choice of basis, and depend only on the initial conditions.

Now assume the atom is in a field with a single highly occupied field mode. If the energy of the total system (atom and field) is taken into account, the Hamiltonian is not time-dependent as in the semi-classical case. The energy levels of the total system are accordingly $|n,1\rangle$ and $|n-1,2\rangle$, separated by the detuning between the laser frequency and the resonance frequency of the atom. These states are termed undressed states. The eigenstates of the diagonalised Hamiltonian which are superpositions of $|1,n\rangle$ and $|2,n-1\rangle$ are termed dressed states because the atom is surrounded by and interacting with the photons, i.e. 'dressed' by the photons.

The energy spectrum of the total atom-single field mode system may be represented either by the undressed states (basis states in which the quantum of energy is either with the atom-excited atom, or in the field-mode excitation) or by the dressed states (basis states which are linear superpositions of states in which the quantum of energy is with and not with the atom.) Whereas in the undressed state representation the system is constantly oscillating between the two undressed states for a given field mode occupation number, n , in the dressed state representation, the system is in a state that is a linear superposition of the two dressed states. It has finite,

unchanging (equal for zero detuning, Δ) probabilities of being in the dressed states.

The process of alternate stimulated absorption and stimulated emission between $|1,n\rangle$ and $|2,n-1\rangle$ is called Rabi oscillation. The Rabi frequency of oscillation is also the dressed state separation, and for mode occupation number n is given by

$$\Omega_n = (\Delta^2 + 4|V_{12}|^2 n)^{1/2}$$

For a highly occupied field mode i.e. large n we take the dressed state separations for different mode occupation numbers to be approximately equal i.e. $\Omega_n \approx \Omega_{n-1} \approx \Omega_{n-2}$ etc.

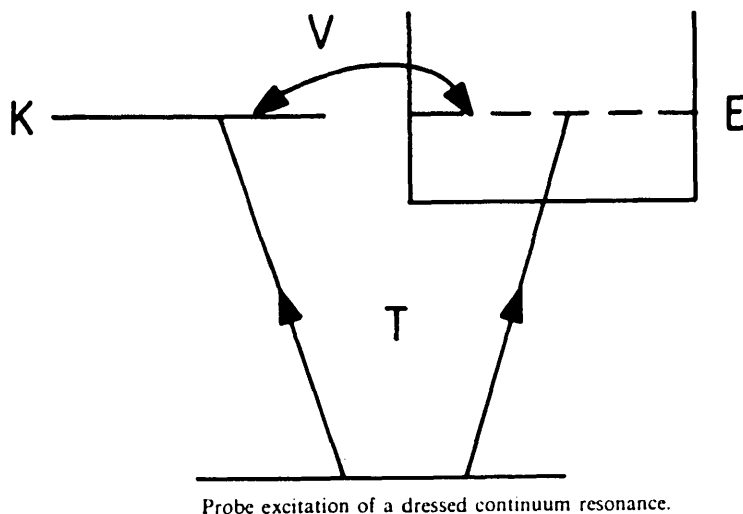
The Autler - Townes doublet splitting is a manifestation of the doublet nature of the dressed states in the dressed state energy spectrum. In order to observe this directly we introduce a third level into the system. The atom now has three levels, two of which are strongly coupled with Rabi oscillations between them. A weak laser probe field couples the third level to one of the other levels. As the probe frequency is varied, the absorption from the probe beam is greatest (as is the population of level $|3\rangle$), when the probe frequency equals the resonance frequency between one of the dressed states and $|3\rangle$. Therefore we expect to see a doublet structure corresponding to the two dressed states in the absorption spectrum of the probe. Alternatively we may monitor the fluorescence from level $|3\rangle$ as a function of probe frequency. The fluorescence detected is a measure of the population of $|3\rangle$, $P_3(t)$ and the fluorescence spectrum will have two peaks associated with the peaks in population. The

peaks are separated by the frequency separation between the two dressed states i.e. the Rabi frequency. The doublet structure will only be symmetrical if there is zero detuning for the first transition because the dressed states are equally populated only when this condition is satisfied. At the resonances, $P_3(t)$ peaks whilst there is a depletion in the $|2, n-1\rangle$ population.

A third level $|3'\rangle$ may be reached by spontaneous emission from one of the strongly coupled levels. The fluorescence spectrum that is obtained again has two peaks at the resonance frequencies between the dressed states and $|3'\rangle$.

Confluence [Rzazewski & Eberly, 1981 and 1983].

To illustrate a 'confluence', we consider the following model, [Knight, 1984].



Autoionisation is caused by the embedding of a discrete state of one configuration in a continuum of another configuration via a

Coulombic time-independent atomic perturbation, 'V'. This discrete state $|K\rangle$ (say describing both atom and field) is strongly mixed to the flat continuum E by V to produce a modified or dressed discrete state $|\varphi\rangle$

$$|\varphi\rangle = |K\rangle + \int_0^\infty \frac{V_{k\epsilon} |E\rangle}{\epsilon - E} dE.$$

The Fano wavefunction $|F(\epsilon)\rangle$ of the close-coupled $k - E$ system of energy ϵ is the stationary state which characterizes the structured continuum. If H is the total Hamiltonian and ϵ the energy of the dressed (interacting) system, then

$$H |F(\epsilon)\rangle = \epsilon |F(\epsilon)\rangle.$$

As the resonance condition $\epsilon - E \rightarrow 0$ is approached, the mixing of the embedded state and the original continuum becomes pronounced, and the modified discrete state becomes dominant. The Fano q parameter represents the ratio of the transition amplitude to the dressed discrete state $|\varphi\rangle$ to that of the old continuum $|\epsilon\rangle$.

The modification of the probe excitation of the continuum from j induced by the dressing is

$$R = \frac{|\langle F(\epsilon) | T | j \rangle|^2}{|\langle \epsilon | T | j \rangle|^2} = \frac{(q + e)^2}{(1 + e)^2},$$

where e is the detuning of the probe interaction, that is the energy mismatch between discrete and continuum states. If q is large, the

channel via the discrete state dominates and a more-or-less symmetric resonance in R (versus e) is produced. If q is small, the direct channel to the continuum dominates and an asymmetric enhancement as a function of detuning is produced with a zero at $q = -e$, where the decay channel closes down. Here the two transition dipoles to the continuum cancel. When the probe field is increased in intensity, the distinction between dressing and probe lasers become artificial. Two-photon dressed states can become decoupled from the continuum, immune to photoionisation, giving the possibility of autoionising states.

Rabi population oscillations are the quantum beats in the evolution of the dressed states. One can argue heuristically that the autoionisation mechanism provides a channel by which electrons originally in level $|j\rangle$ can reach the continuum, and thus autoionisation acts as a probe of the Autler-Townes effect. However, with increasing laser power, as the Autler-Townes peak moves into the Fano minimum, the effectiveness of the radiative matrix element decreases, reducing the throughput of the autoionisation channel. As the channel closes, the lifetime of the bound state increases dramatically, explaining the sharp narrowing in linewidth seen in the photoelectron spectrum (versus detuning.) Hence one of the dressed states couples to the continuum in a diminishing way, the other in an increasing way. At the critical "confluence point of coherences," one dressed state becomes stable and the Rabi oscillation quantum beats are altered (and disappear from the ion probability

$P_{\text{ION}}(t) = 1 - P_j(t) - P_k(t)$ where P_j , P_k are the discrete state probabilities.) Ionisation time dependences reflect the trapping in

the persistence of an un-ionised bound state population as $t \rightarrow \infty$. Hence, whenever a confluence occurs, the spectral peak is infinitely high and narrow, the lifetime of one excitation channel is infinite, and a definite fraction of the atomic electrons is trapped in $|j\rangle$. The exact conditions for confluence are easily derived by requiring that the zero in the numerator of the expression for the photoelectron spectrum be counteracted by an identical zero in the denominator. The zero in Fano's original model indicates that quantum interference may, for an appropriate choice of detuning, shut off the ground state from both its ionisation channels (direct and indirect.) The confluence line narrowing shows that, regardless of the detuning, an appropriate choice of laser power leads to a conspiracy of interferences with the same effect: the ground state cannot be completely ionised.

q - reversal

The interaction between a Rydberg series of weakly autoionising states and an extra level with a large decay width has been studied by Connerade et al. [1985; 1987]. They modelled what they called the 'q - reversal' effect, whereby there is a reversal of the symmetry of the Fano profiles as the series passes through the point of maximum coupling with the broad level. The q - reversal is the result of a reversal in the sign of 'q', caused by the very broad interloping resonance, and occurs on either side of the maximum of the broad feature, between adjacent members of the Rydberg series. The sharper the interloper level, the more pronounced the q - reversals. q - reversal is the hallmark of weak mixing; all q - reversals

disappear at large mixing strength. Thus q - reversal plays a fundamental role in assessing coupling strength from experimental data.

REFERENCES

- Abramowitz M. and Stegun I. A. (1972); "Handbook of Mathematical Functions". (Dover Publications, New York.)
- Ackerhalt J. R., Knight P. L., and Eberly J. H. (1973); Phys. Rev. Lett.30, 456.
- Ackerhalt J. R. and Milonni P. W. (1986); Phys. Rev.A34, 1211 .
- Agassi D. and Eberly J. H. (1986); Phys. Rev.A34, 2843.
- Allen L. and Eberly J. H. (1975); "Optical Resonance and Two-Level Atoms". (John Wiley and Sons, Inc.)
- Bixon M. and Jortner J. (1968); J. Chem. Phys.48, 715.
- Bixon M. and Jortner J. (1969a); J. Chem. Phys.50, 3284.
- Bixon M., Jortner J. and Dothan Y. (1969b); Molecular Physics 17, 109.
- Blakemore J. S. (1974); "Solid State Physics" (Saunders, New York.)
- Bloch F. and Siegert A. J. F. (1940); Phys. Rev. 57, 522.
- Bocchieri P. P. and Loinger A. (1957); Phys. Rev.107, 337.
- Callen H. B. (1962); in "Fluctuations, Relaxation and Resonance in Magnetic Systems" edited by D. Ter Haar (Oliver and Boyd, London.)
- Callen H. B. and Welton T. A. (1951); Phys. Rev. 83, 34.
- Casati G., Chirikov B. V., Israilev F. M. and Ford J. (1979); in "Stochastic Behaviour in Classical and Quantum Systems"

- edited by G. Casati and J. Ford, Lecture Notes in Physics 93
(Springer, New York.)
- Caves C. M. (1982); Phys. Rev.D23, 1817.
- Gerdeira H. A. and Huberman B. A. (1987); Phys. Rev.A36, 1382.
- Chyba T. H. and Abraham N. B. (1985); J. Opt. Soc. Am.B2, 377.
- Cohen-Tannoudji C., Diu B. and Laloe F. (1977); "Quantum Mechanics" (John Wiley, New York.)
- Coleman P. E. and Knight P. L. (1982); J. Phys.B15, L235.
- Coleman P. E., Knight P. L. and Burnett K. (1982); Opt. Comm.42, 171.
- Connerade J. P., Lane A. M., and Baig M. A. (1985); J. Phys. B18, 3507.
- Connerade J. P. and Lane A. M. (1987); J. Phys.B20, 1757.
- Davies P. C. W. (1977); "The Physics of Time Assymetry" (University of California Press.)
- Deng Z. and Eberly J. H. (1984a); Phys. Rev. Lett.53, 1810.
- Deng Z. and Eberly J. H. (1984b); J. Opt. Soc. Am.B1, 102.
- Deng Z. and Eberly J. H. (1985a); J. Opt. Soc. Am.B2, 486.
- Deng Z. and Eberly J. H. (1985b); J. Phys.B18, L287.
- Deng Z. and Eberly J. H. (1986); Phys. Rev.34, 2492.
- Dupertuis M-A and Stenholm S. (1987); J. Opt. Soc. Am.B4, 1094.
- Dupertuis M-A, Barnett S. M. and Stenholm S. (1987); J. Opt. Soc. Am.B4, 1102 and 1124.
- Eberly J. H., Yeh J. J. and Bowden C. M. (1982); Chem. Phys. Lett.86, 76.
- Fano U. (1961); Phys. Rev.124, 1866.

- Fonda L. and Ghirardi G. C. (1972); Nuovo Cimento 7A, 180
and 10A, 850.
- Friberg S. and Mandel L. (1983); Optics Comm.46, 141.
- Galbraith H. W., Ackerhalt J. R., and Milonni P. W. (1983); J.
Chem. Phys.78, 790.
- Gibbs J. W. (1960); "Elementary Principles in Statistical
Mechanics" (Dover, New York), pp. 139-151.
- Glauber R. J. (1978); Phys. Lett.68A, 29.
- Glauber R. J. (1986); "Frontiers in Quantum Optics " edited by
E. R. Pike & S. Sarkar (Hilger, London), p. 534.
- Glauber R. J. (1985); "Group Theoretical Methods in Physics "
edited by M. A. Markov, V. I. Man'ko and A. E. Shabad, Vol.I
(Harwood Academic, New York), p. 137.
- Grepel D. R., Prange R. E. and Fishman S. (1984); Phys.
Rev.A29, 1639.
- Haken H. (1981); "Light" Vol.I (North-Holland, Amsterdam.)
- Heidmann A. and Reynaud S. (1984); J. Physique 45, 873.
- Hogg T. and Huberman B. A. (1983); Phys. Rev.A28, 22.
- Hong C. K., Friberg S. and Mandel L. (1985); J. Opt. Soc.
Am.B2, 494.
- Jackson J. L. (1952); Phys. Rev.87, 471.
- Javanainen J. and Kyrola E. (1985); Opt. Comm.56, 17.
- Jolley L. B. W. (1925); "Summation of Series" (Chapman and
Hall Ltd.)
- Knight P. L. (1979); J. Phys.B12, 3297.
- Knight P. L. and Milonni P. W. (1980); Phys. Rep.66, 21.
- Knight P. L. (1984); Comm. At. Mol. Phys.15, 193.

- Kyrola E. (1984); J. Opt. Soc. Am.B1, 737.
- Kyrola E. (1986a); J. Opt. Soc. Am.B3, 453.
- Kyrola E. (1986b); J. Phys.B19, 1437.
- Kyrola E. and Eberly J. H. (1985); J. Chem. Phys.82, 1841.
- Kyrola E. and Lindberg M. (1987); Phys. Rev. A 35, 4207.
- Lefebvre and Savolainen J. (1974); J. Chem. Phys.60, 2509.
- Leonski W., Tanas R. and Kielich S. (1987); J. Opt. Soc.B4, 72
- Ley M. and Loudon R. (1985); Optics Comm.54, 317.
- Loudon R. (1985); "The Quantum Theory of Light" (Clarendon Press, Oxford.)
- Louisell W. H. (1973); "Quantum Statistical Properties of Radiation" (Wiley, New York.)
- Magnus W. and Oberhettinger F. (1949); "Functions of Mathematical Physics" (Chelsea Publishing Co., New York), p 131.
- Makarov A. A. , Platonenko V. T. and Tyakht V. V. (1978),
Soviet Phys. JETP 48, 1044.
- Milonni P. W. (1984); Am. J. Phys.52, 340.
- Milonni P. W. and Knight P. L. (1976); Am. J. Phys.44, 741.
- Milonni P. W., Ackerhalt J. R., Goggin M. E. (1987); Phys. Rev.A35, 1714.
- Milonni P. W., Ackerhalt J. R., Galbraith H. W., Mei-Li Shih (1982) Phys. Rev.A28, 32.
- Pegg D. T. and Vaccaro J. A. (1987); Optics Comm.61, 317.
- Peres A. (1982); Phys. Rev. Lett.49, 1118.
- Pietenpol J. L. (1967); Phys. Rev.162, 1301.
- Pomeau Y., Dorizzi B., and Grammaticos B. (1986); Phys. Rev. Lett.56, 681.

- Radmore P. M. (1982); Phys. Rev.A26, 2252.
- Radmore P. M. and Knight P. L. (1982); J. Phys.B15, 561.
- Radmore P. M. and Tarzi S. (1987); J. Mod. Opt.34,1409.
- Radmore P. M., Tarzi S. and Knight P. L. (1987); J. Mod Opt.34, 587.
- Reif F. (1985); "Fundamentals of Statistical & Thermal Physics" (McGraw-Hill, New York.)
- Rice O. K. (1933); J. Chem. Phys.1, 375.
- Robiscoe R. T. and Hermanson J. C. (1972); Am. J. Phys.40, 1443; (1973), Ibid. 41, 414.
- Rothenberg J. E. and Grischkowsky D. (1985); Opt. Lett.10, 22.
- Rzȃżewski K. and Eberly J. H. (1981); Phys. Rev. Lett.47, 408.
- Rzȃżewski K. and Eberly J. H. (1983); Phys. Rev.A27, 2026.
- Sargent III M., Scully M. O. and Lamb Jr. W. E. (1974); "Laser Physics" (Addison-Wesley, Reading, Mass.)
- Shore B. W. (1983); Chem. Phys. Lett.99, 240.
- Spiegel M. R. (1972); "Complex Variables" (Schaum's Outline Series, McGraw Hill), p.188.
- Stenholm S. (1986a); Physica Scripta T12, 56.
- Stenholm S. (1986b); Optics Comm.58, 177.
- Stey G. C. and Gibberd R. W. (1972); Physica 60, 1.
- Tarzi S. (1988); J. Phys. A, (to be published.)
- Tarzi S. and Radmore P. M. (1988); Phys. Rev.A, (to be published.)
- Vaccaro J. A. and Pegg D. T. (1987); J. Mod. Opt.34, 855.
- Wax M. (1954) (ed.); "Selected Papers on Noise and Stochastic Processes" (Dover Publications, New York.)

- Winter R. G. (1979); "Quantum Mechanics" (Wadsworth Publication Co., Belmont, California.)
- Woger W., King H., Glauber R. J. and Haus J. W. (1986); Phys. Rev.A34, 4859.
- Wootters W. K. and Zurek W. H. (1983); Nature 304, 188.
- Yeh J. J., Bowden C. H. and Eberly J. H. (1982); J. Chem. Phys.76, 5936.
- Zewail A. H. and Lethokov (Nov., 1980); Physics Today, pp.27-41.
- Ziman J. M. (1972); "Principles of the Theory of Solids" (Cambridge University Press, Cambridge.)
- Ziman J. M. (1980); "Elements of Advanced Field Theory." (Cambridge University Press, Cambridge.)

ACKNOWLEDGMENTS

I would like to thank Dr. P. L. Knight for his ideas and guidance throughout the course of this research.

I would also like to thank Dr. P. M. Radmore, many of whose suggestions provided creative ground for this work.

I am also grateful to my family, and to my colleagues in research, in particular A. Greenfield, S. C. Lee, B. Piraux and B. C. Sanders, for their friendly support, and for uplifting me when my spirits were at their lowest. I must also thank F. A. M. de Oliveira for his valuable help with the word-processing of this thesis.

Finally, I would like to thank the S. E. R. C. for the award of a research studentship, allowing me to undertake this research.